Case Study Guides for Select NMDID Cases

These guides were developed with support from the National Institute of Justice and RTI International and was funded through a cooperative agreement from the National Institute of Justice (2016-MU- BX-K110), Office of Justice Programs, U.S. Department of Justice. The opinions and recommendations expressed in this guide are solely those of the authors and do not necessarily reflect the views of RTI or the National Institute of Justice.

About the NMDID Case Study Guides

The New Mexico Decedent Image Database (nmdid.unm.edu) provides access to whole body postmortem computed tomography (PMCT) images of more than 15,000 decedents, and a rich body of associated metadata, in support of research and education.

The PMCT scanning was conducted in the course of death investigation and research at the Office of the Medical Investigator (OMI) at the University of New Mexico, from 2010 to 2017.

These study guides each feature one or two cases from the NMDID. The study guides include a case description and summary of notable imaging, pathology, and/or anthropology findings, with examples of findings shown in a few selected CT images. For many cases, corresponding autopsy or anthropology photos are also shown. Literature references and/or suggested articles for further reading are also included.

To get the most benefit from each case study guide, the user can request a user account for NMDID (nmdid.unm.edu/how-to-use), which enables searching of the database. The full image data for a given case can then be requested from NMDID and (after the request is approved) downloaded to the user's computer, allowing the user to scroll through full image sets using a DICOM viewer installed on the user's local computer. Viewing the full image dataset will allow the user to get a better idea of the PMCT appearance of the findings featured in the guide and will also enable the user to view many other findings that are mentioned (but not illustrated/discussed) in the guide.

(Detailed instructions for accessing NMDID and downloading and viewing images are provided in the New Mexico Decedent Image Database Webinar Series, archived here: https://forensiccoe.org/nmdid-webinar-series/.)

There are four Case Study Guides that feature anthropology cases, and four devoted to the topic of decomposition/post-mortem change at different stages. The remainder of the guides are medical examiner cases representing a variety of case types (homicide, suicide, accident, and natural) with a wide variety of findings, many commonly encountered in the medical examiner setting, and some unusual findings.

For forensic pathologists, radiologists, anthropologists, and other forensic practitioners who are interested in learning more about the use of PMCT in death investigation and anthropological analysis, we hope these guides will provide a starting point for learning about the way PMCT may be used for various case types and the PMCT appearance of some common and some unusual findings.

The following individuals contributed to these study guides: Dr. Yi-Li (Grace) Wong, M.D. (forensic radiologist), Kethery Haber, MHA RT(R)(CT)(M)(MR) (radiologic technologist), Roberto Maselli, M.D. (forensic pathologist), Heather J. H. Edgar, Ph.D. (forensic anthropologist), Phoebe Nichols (medical student), Nicollette Appel (anthropology Ph.D. candidate), Paige Lynch (anthropology Ph.D. candidate), and Natalie L. Adolphi, Ph.D. (medical physicist).

Natalie L. Adolphi, PhD
Director, Center for Forensic Imaging
New Mexico Office of the Medical Investigator
2022

Contents

NMDID 151981 Hypothermia with lung cancer pleural effusion emphysema [Accident]

NMDID 152372 Acute pancreatitis [Natural]

NMDID 153141 Drug overdose with postmortem pulmonary edema [Accident]

NMDID 155040 Ruptured abdominal aortic aneurysm [Natural]

NMDID 158501 Multiple GSW of neck and leg [Homicide]

NMDID 164164 Hepatic cirrhosis and carcinoma with hepatitis C [Natural]

NMDID 169628 Drug overdose with distended urinary bladder [Accident]

NMDID 176154 Drug overdose with high densities in stomach [Accident]

NMDID 181912 Ruptured thoracic aneurysm with methamphetamine use [Accident]

NMDID 185843 MVA with vertebral metastasis [Accident]

NMDID 188757 MVA diaphragmatic rupture long bone fractures [Accident]

NMDID 188922 Multiple GSW of torso with organ procurement [Homicide]

NMDID 193393 GSW of head [Suicide]

NMDID 198518 Fall from height with skull cervical thoracic trauma [Accident]

NMDID 199470 Drug overdose with remote projectile [Accident]

NMDID 100017, 100035

Anthropological analysis of a homicide with animal predation

Case Description: Two decedents, one male and one female, were found in a home.

The male decedent (NMDID 100017) was on top of the female decedent, supine, fully dressed, between the wall and a wood stove. There were multiple, small lacerations on the chest and abdomen of the male. The fingers and hands were in the early stages of mummification. The lower abdomen was in the early stages of decomposition.

The female decedent (NMDID 100035) was supine, under the male decedent. The body of the female was intact and fresh from the torso down. The upper torso was torn away with multiple bone fragments near the body, and the cranium was near the stove. The skull was clean with no soft tissue present. Dog feces were collected from the scene due to the impression that the dog had eaten some of the remains.

Autopsy Findings: The pathological diagnosis for the male decedent is suicide by gunshot wound to the head. The pathologic diagnosis for the female decedent is homicide by unspecified means.

There was significant animal predation to the female's remains, specifically to the upper half of the thorax and neck. There was blunt force trauma to the head with focal contusion and subarachnoid hemorrhage of the left temporal lobe.

Anthropology Findings: Anthropological trauma analysis was performed on the cranium, C1, C2, and additional bone fragments of NMDID 100035. This analysis determined that there was no observable evidence of skeletal trauma to these elements around the time of death.

Imaging Findings: PMCT was performed to examine dog feces, recovered from the home, in search of additional bone fragments or other possible evidence, such as bullet fragments. After review of the images, feces suspected of containing human skeletal remains were retained.

Figure 1. Scout image from PMCT of dog feces. Bone fragments and feces recovered from the scene are on the left; additional bags of feces received from animal control are on the right.

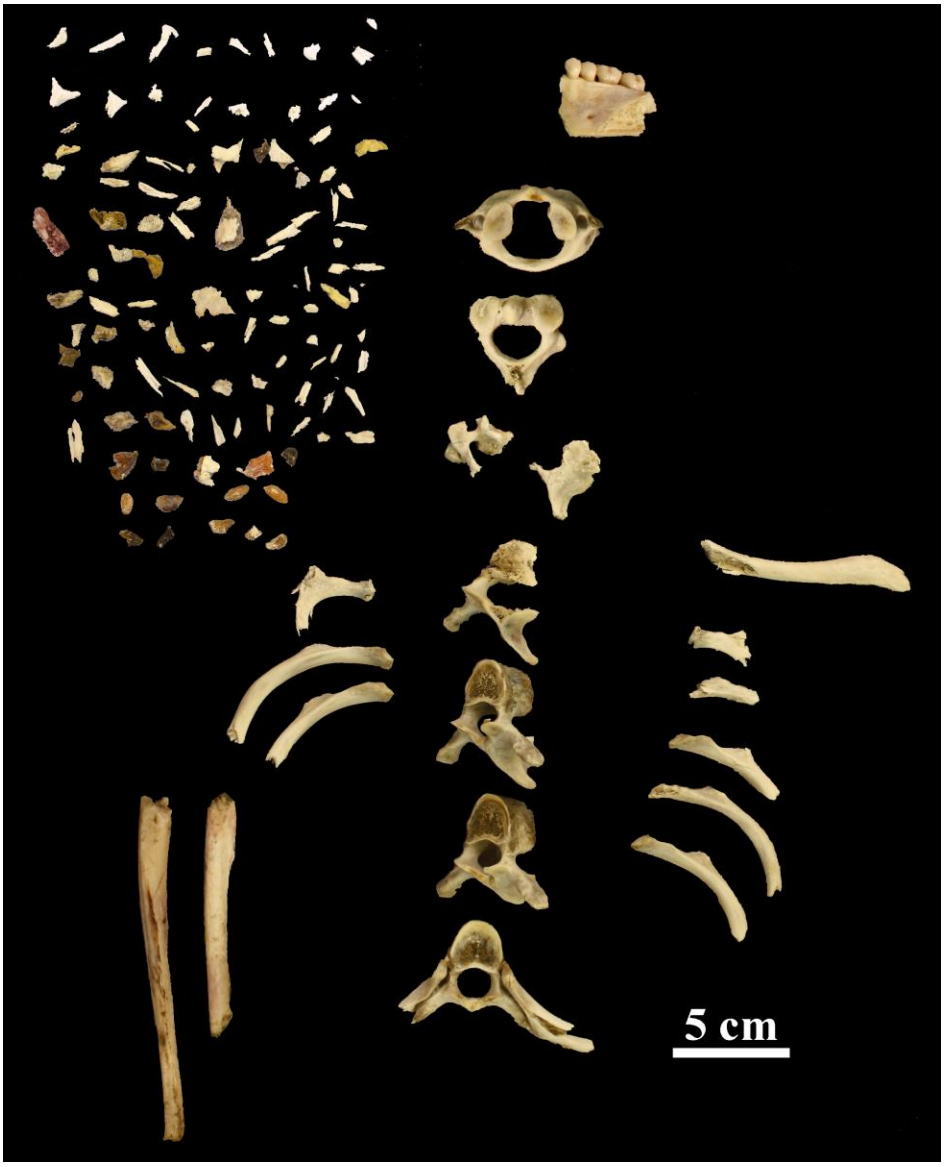

Summary: In this unique case, imaging allowed the anthropologists to expedite the screening process so that time was not wasted searching through fecal material that contained no skeletal elements or metallic fragments. Due to the quantity of fecal material collected, it would have been tedious and time-consuming to screen through all of it. The imaging allowed the anthropologists to prioritize screening only the material that appeared to have remnants of skeletal remains.

Figure 2. Skeletal remains from the female decedent.

Contributors: Nicollette Appel, Heather Edgar, Kethery Haber, and Natalie L. Adolphi

NMDID 100107

Skeletal remains: an unusual case of bilateral fractured fibulae without tibial injury

Case description: A male decedent was found partially buried and wrapped in a blanket. The area was excavated, and soil was screened as part of the process of collecting the remains. The body within the blanket was in a flexed position with the legs not completely in the blanket.

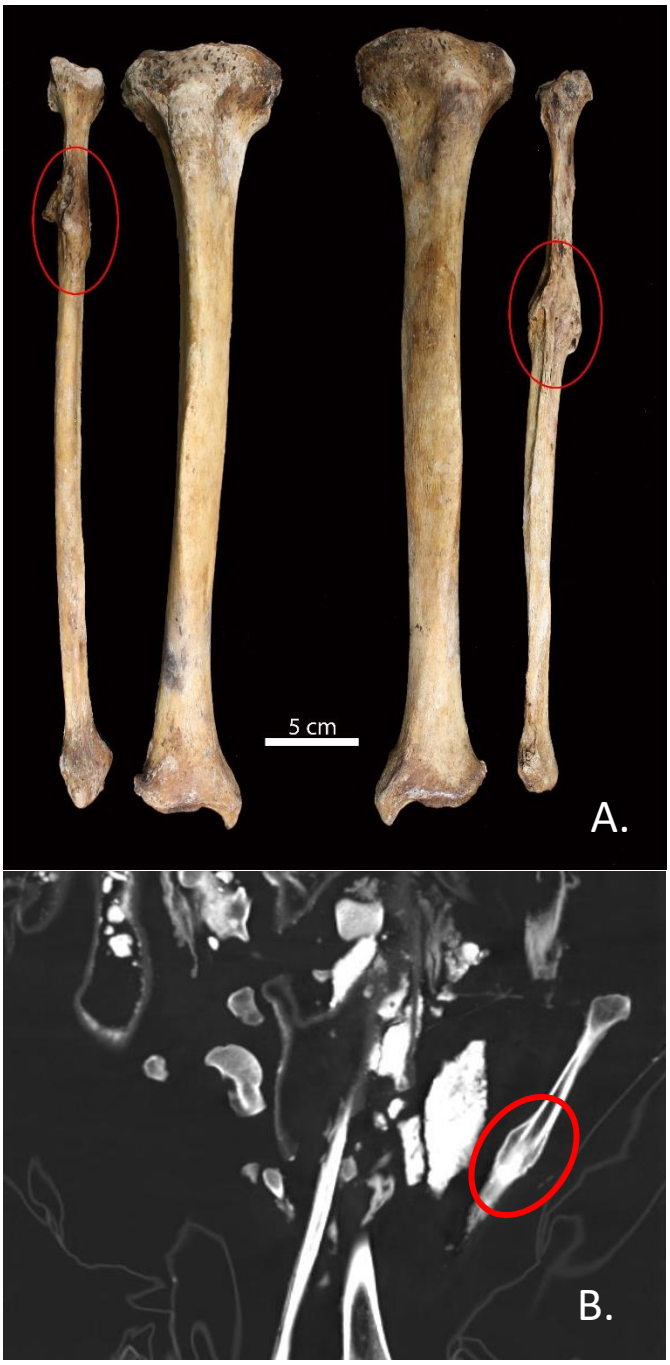

Figure. A. Red circles indicate regions of healed/healing fractures on the right and left fibulae. B. Thick-slab coronal multi-planar reformat of the PMCT imaging shows the presence of a bony callus and incomplete healing of a fibular fracture.

Anthropology Findings: No autopsy was performed due to the extent of decomposition and skeletonization of remains. Anthropological analysis was performed for biological profile and trauma. The individual was estimated to be male, 36-80 years old, 65.5-73.3 inches, and Hispanic or Native American. There was evidence of perimortem trauma to the cranium. There was evidence of antemortem trauma to the left and right fibulae. There were healed fractures on the proximal portions of the diaphysis. It appeared that the fractures occurred at the same time and at least six weeks prior to death, based on the amount of healing. There were no associated signs of trauma to either the left or right tibiae. The cause and manner of death remain undetermined.

Imaging Findings: PMCT was used to try to better understand and interpret the healed fractures of the fibulae. Questions to address included how long antemortem did these fractures occur, did they happen at the same time, are there any signs of infection, and what was the direction of force? Based on the CT scans it was confirmed that the fractures occurred at least six weeks prior to death. However, the bilateral involvement and lack of tibial fractures make this case atypical. The lack of tibial fractures indicate that the direction of force was lateral. Additionally, there were no signs of infection.

Comments: The antemortem trauma present in this case was quite puzzling due to the trauma to the fibulae being bilateral, likely simultaneous, and with no tibial involvement. Typically, when fractures are seen in the lower leg, the tibia and fibula will have associated trauma or only the tibia will be involved, because of how the elements are anatomically positioned and because the tibia is larger. If and when the fibula is fractured with no tibial involvement, it is likely due to the force coming from a lateral direction causing the fibula to be in contact with the force first, and the force not being great enough to also damage the tibia. Here, since both fibulae are involved, at approximately the same location, and have the same amount of healing, the anthropologists were interested to see if any further information could be gathered using CT imaging. The bony callus that surrounds a fracture during the process of healing in turn obscures the original fracture. The CT images allowed the anthropologists to see the original fracture lines on both the right and left fibulae. Although this did not ultimately

provide any additional information on the cause of these fractures, it did confirm our previous assumptions on the timing of the fractures.

Contributors: Nicollette Appel, Heather Edgar, and Natalie L. Adolphi

NMDID 100202

Skeletonized remains with possible tumor

Case Description: A forensic anthropological analysis was performed on human skeletal remains discovered in eastern Arizona. The investigator reported that a skull, vertebrae, hip, and ribs were found on a property that had not been occupied in more than two years. The skull was found in the roadway going to the residence. Approximately 15 feet from the roadway was a shallow grave about 18-24 inches deep. The remains were sealed in a box and transported to the Office of the Medical Investigator. Additional remains were located 8 months later. The purposes of the anthropological analysis were to estimate a biological profile of the individual and describe any evidence of trauma to the skeleton.

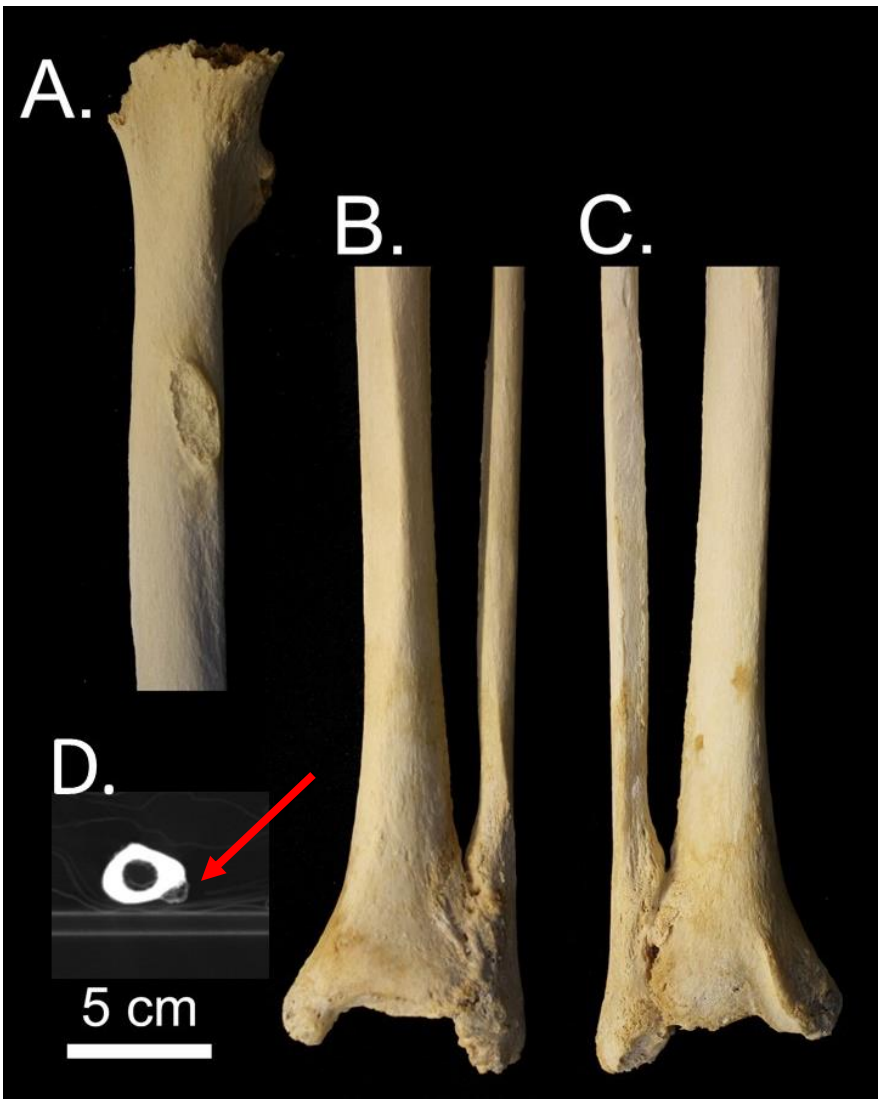

Figure: Pathological features of the lower limbs. A. Anterior surface of the right femur, showing evidence of a possible tumor; B. Anterior view of the fused right tibia and fibula; C. Posterior view of the fused right tibia and fibula. D. CT slice showing possible tumor on femur highlighted by the red arrow. Note disruption of the cortex and lobulated bone in area of expansion. Scale does not apply to CT slice.

Scientific Findings:

Decedent

The items retrieved from the first scene response included human hair, three human cervical vertebrae, one partial human manual phalanx, and several other small fragments of human bone. Additional items included non-human bone. No human cranium, mandible, or components of the pelvis were present in the initial analysis. The remains located later included the skull, mandible, ossa coxae, sacrum, right femur, left tibia, right and left fibulae. The remains were partially skeletonized, and therefore did have some soft tissue present that required removal.

Findings

The decedent was estimated to be a male, probably Hispanic American or Native American, between 24-60 years old. He was edentulous, and had skeletal fusion of his spine, pelvis, and left ankle. There was evidence suggesting that the decedent may have had a tumor in the shaft of his right femur and carnivore scavenging, such as gnawing and puncture marks, on the ossa coxae, femur, and tibia. There was no skeletal evidence of perimortem trauma.

Imaging:

A disruption to the cortex of the right femur in the proximal third, on the anterior surface, may have been related to a bony tumor (see Figure). The skeletal element shows only an ovoid area of cancellous bone that appears superimposed to the cortical surface. However, the PMCT, obtained prior to processing the bones, shows an area of bony expansion with lobulated (rings and arcs) interior and possible disruption of the cortex.

Comments: The PMCT allowed for a deeper understanding of what was occurring pathologically underneath the surface of the bone that otherwise would not have visible through visual examination of the physical specimen after processing.

Contributors: Paige Lynch, Heather Edgar, and Natalie L. Adolphi

NMDID 100271, 100609

Human remains (dismembered, charred, encased in concrete) recovered from two sites

Case Description: A forensic anthropological analysis of human skeletal remains was performed. The Office of the Medical Investigator (OMI) was contacted by law enforcement regarding the location of human remains, which had been disclosed by a defendant in another case. Based on this information, this set of remains, NMDID 100271, was suspected to be related to a prior case, NMDID 100609, which had included burned skeletal elements that had not been identified. In the earlier case, NMDID 100609, the OMI was initially contacted after an unnamed source provided the location of the remains to law enforcement. The first set of remains was located in a rural area, buried on a hillside near a forest access road. The field investigator noted that the remains appeared dismembered and that there was a strong smell of a flammable liquid in the remains, and that only 5-7% of the complete skeleton was recovered. The second set of remains (NMDID 100271) was located some years later, in a different location, roughly 300 yards from a rural, single lane highway, in a forested area near a river. At the second site, law enforcement officials had excavated a hole two to three feet deep and uncovered a plastic, wheeled tool box, tied with wire. Cement was visible inside the tool box through some cracks. The box was brought in, as-recovered, from the scene. The anthropological analysis was conducted to recover elements that might be useful in radiographic comparison for identification, to determine whether NMDID 100271 represented the same individual as NMDID 100609, and to describe evidence of trauma and taphonomic treatment that occurred as the remains were disposed.

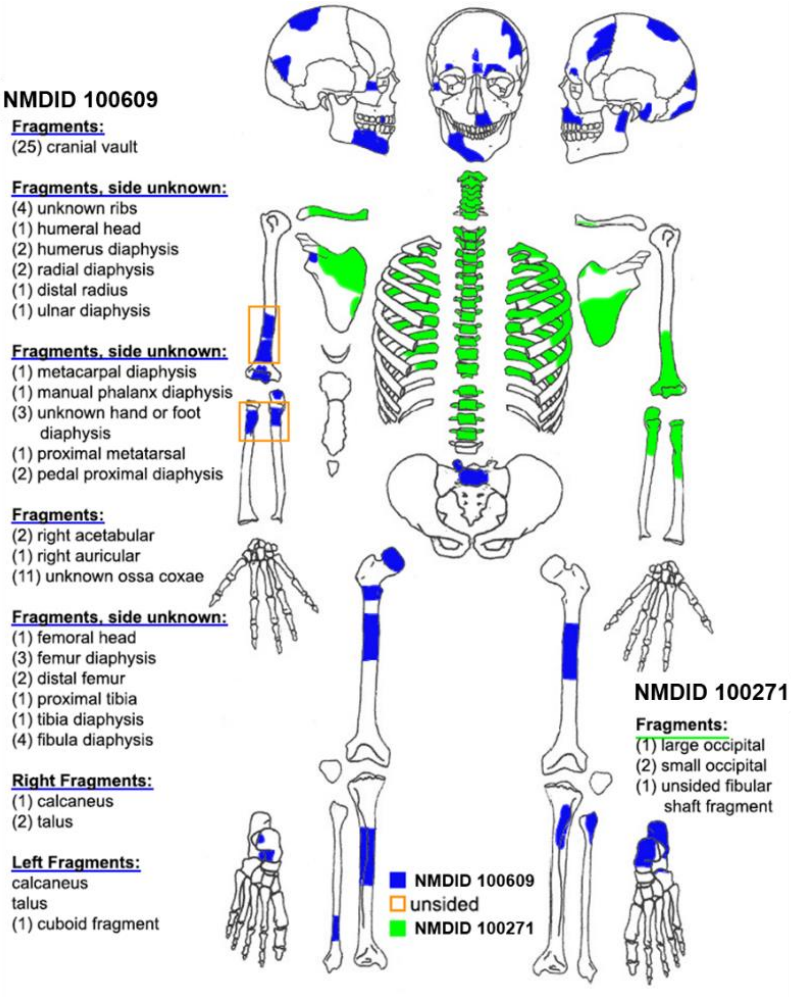

Figure 1. Skeletal elements present are in blue and green; the elements absent are in white. Bones marked by the orange boxes were described as left in the original report.

Scientific Findings:

Decedent

The skeletal elements recovered are described in Figure 1. The remains from NMDID 100609 have evidence of thermal alteration, with a majority of the remains exhibiting charring or calcination. The majority of the remains corresponding to NMDID 100271, except for a few fragments, do not have evidence of thermal alteration. The remains from these two cases were confirmed to be the same individual based on there being no duplication of skeletal elements.

Findings

The decedent was positively identified as a 42-year-old missing female. There was evidence of thermal damage and perimortem fracture of the right scapula.

Imaging:

The decedent was positively identified via radiographic comparison. The cervical vertebrae were analyzed by comparing the detailed morphology from antemortem X-ray images, taken at a local hospital, to correctly-oriented views of the vertebrae obtained from the PMCT scans.

The CT scans of a chunk of concrete removed from the tool box (NMDID 100271) was examined to identify areas of the concrete mass that included voids and unusual shapes,

including a ring shape, in a single portion of the concrete (Figure 2). The CT image data was used to map where these shapes were located within the concrete mass. Upon further physical examination of this portion of concrete, a single fibula fragment was found, as well as several objects that accounted for the unusual shapes seen on the CT scans, including an aluminum grommet in a tarp (which accounted for the ring-shape) and a wrapped cord with adhering gravel.

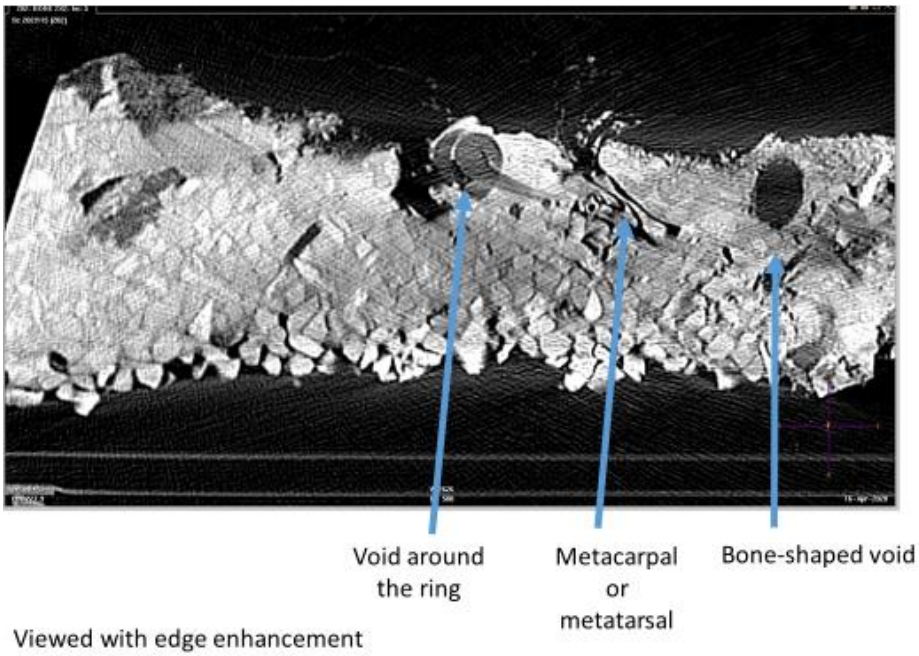

In addition, PMCT scans were performed on a single bone (the right scapula) with concrete adhered to it, which also came from the tool box of NMDID 100271. That CT scan (not shown) indicated the presence of a round metallic object in the concrete, possibly a projectile, adhered to the posterior surface of the bone. The pathologists and the anthropologist further broke up the concrete, using a hammer and chisel, to enable the smaller fragments to be x-rayed and scanned again using PMCT (not shown). The smaller concrete fragments that appeared to contain metal fragments by imaging were transferred as evidence.

Figure 2. A CT scan of the concrete mass highlighting voids, including a ring shape, metacarpal or metatarsal, and an unidentified bone shape.

Comments: When human remains are fragmented, they may also be mixed with, or encased in, other materials, e.g., soil, rocks, concrete, broken glass, metal, plant materials, cloth, plastic, or even feces (in cases involving animal predation of remains). PMCT can be helpful in these cases by providing a means to document the remains and other materials gathered from the scene in their "as-received" state, and imaging can help guide the process of physically searching through large quantities of mixed debris, a process which may be destructive. In this case, the large amount of concrete in the toolbox was particularly challenging, due to the size, and weight, requiring the tool box to be emptied prior to scanning the contents. Using CT to screen the large concrete chunks, and determine where objects of potential interest were located within, was helpful in reducing the time and physical labor involved in recovering remains and evidence from this difficult material. Even after breaking select regions of the concrete chunks into even smaller pieces, all of the fragments were still coated with mortar, and imaging proved useful for differentiating mortar-coated metal fragments from rock, as they could not be distinguished visually.

We note that the CT reconstructions were performed with the extended Hounsfield Unit (HU) option selected. This option extends the CT gray scale up to a maximum value of 32,000, rather than the conventional maximum of 3000. The extended HU scale, combined with using a higher than normal window level setting in the image viewer, were utilized to improve the image contrast between the densest materials, in this case bone, concrete, rocks, and metal fragments.[1]

Reference:

1. Paulis LE, Kroll J, Heijnens L, Huijnen M, Gerretsen R, Backes WH, Hofman PAM. Is CT bulletproof? On the use of CT for characterization of bullets in forensic radiology. Int J Legal Med. 2019 Nov;133(6):1869-1877. doi: 10.1007/s00414-019-02033-0. Epub 2019 Mar 26. PMID: 30911839; PMCID: PMC6811383.

Contributors: Paige Lynch, Heather Edgar, and Natalie L. Adolphi

NMDID 193948

Progression of decomposition on PMCT Part 1: No decomposition (fresh)

Case Description: A 30-year-old male with a known past medical history of illicit drug abuse was found lying face-down on a bed in a motel. A possible injection site on the left antecubital fossa with no other external signs of trauma were noted.

Imaging Findings: Livor mortis shown on PMCT as areas of higher attenuation (bright). High attenuation present due to increased hemoconcentration in the aortic wall and major vessels of the heart. High attenuation present in the superior sagittal sinus and transverse sinus. Thickening and increased attenuation of the dependent skin and subcutaneous fat. No other postmortem changes noted.

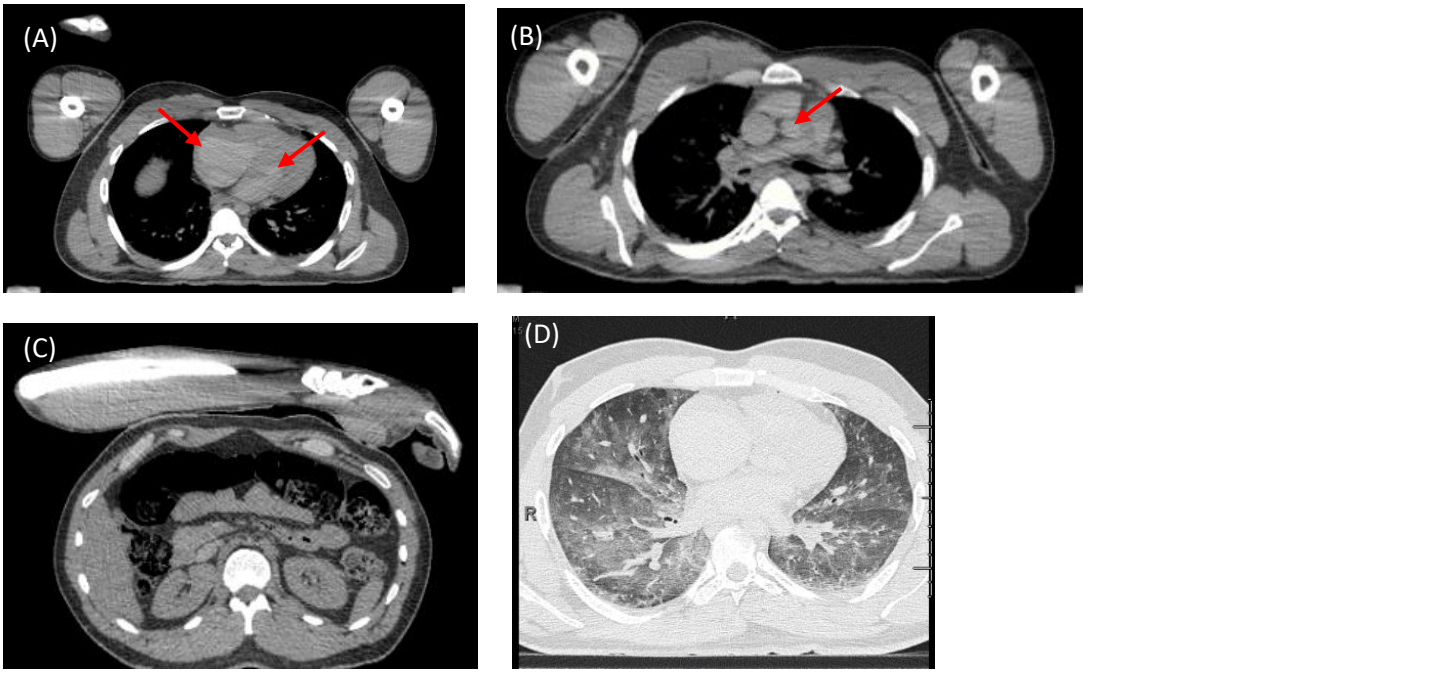

CT Figures: (A) and (B) High attenuation due to fluid settling (arrows) in the heart and large caliber venous system. (C) Abdomen has not yet distended from putrefaction, showing no decompositional changes. (D) Lungs and heart are in place with no signs of decompositional changes. (E) High attenuation present in the superior sagittal sinus (red arrow) and transverse sinus (blue arrow); ventricles of the brain visible (green arrow). (F) Abdominal organs and tissues in place, with no signs of decompositional change.

Pathology Findings: Autopsy revealed the body of a male with no signs of decompositional changes save for Tardieu spots on the neck, upper chest, and upper arms. Rigor mortis was receding with fixed purple livor mortis extending over the anterior and posterior aspects of the body except for areas exposed to pressure. No injuries or significant natural disease were noted, but there was a recent needle puncture wound of the left antecubital fossa with a surrounding ½ inch contusion noted that corresponded to the history of illicit drug abuse. Toxicology of the blood showed the metabolic products of heroin and cocaine.

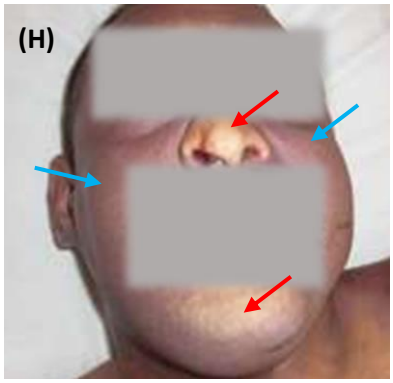

Autopsy Figures: (G) and (H) Fixed purple livor mortis extending over anterior portions of the face, neck, chest, and abdomen (blue arrows) with areas of blanching (red arrows) due to pressure. (I) Tardieu spots present on the upper right chest (red arrow)

Comments: In just minutes after death, the body begins the process of decomposition, the gradual breakdown of the body via various mechanisms, such as autolysis, putrefaction, insect activity, and animal predation. Rigor mortis (stiffening of skeletal muscles) and algor mortis (equilibration of the body's temperature with the ambient temperature) are not evident on PMCT, but they can help interpret time of death. Livor mortis, the settling of blood in gravity-dependent portions of the body, is the earliest postmortem change that occurs throughout the entire body, including the tissues and organs, appearing as reddish-purple cutaneous patches that become fixed and unmovable over time. Distribution of livor mortis is dependent upon positioning of the body, and the patches blanch with pressure. On PMCT, livor mortis appears as areas of increased attenuation (bright) in organs, vasculature, and tissues due to differences in hemoconcentration as blood separates into serum and erythrocytic components through the hematocrit effect. This attenuation, and potential fluid-fluid level, are easily observed in gravity-dependent portions of large caliber arteries/veins, the cardiac chambers, the posterior dural sinuses, and the lungs. The dependent subcutaneous fat and dermis also show increased attenuation as well as thickening. In autopsy, the color, fixation, and distribution of livor mortis can help determine if the body was repositioned after death, and coloration should always be differentiated from bruising or hemorrhage. Livor mortis may be mistaken for thrombosis in the vasculature or as pulmonary consolidation in the lungs, so evaluation of supportive findings and abnormalities from autopsy and CT scans, which help visualize anatomic structures, injury patterns, and foreign bodies, will be helpful to differentiate pathologic processes from livor mortis.

Further Reading/Reference:

Levy AD, Harcke HT, Mallak CT. Postmortem imaging: MDCT features of postmortem change and decomposition. Am J Forensic Med Pathol. 2010 Mar;31(1):12-7. doi: 10.1097/PAF.0b013e3181c65e1a. PMID: 20010292.

Contributors: Phoebe Nichols, Yi-Li Grace Wong, Roberto Maselli, and Natalie L. Adolphi

NMDID 174675 (Case A) and 119043 (Case B)

Progression of decomposition on PMCT Part 2: Early Decomposition (bloat)

Case Description A: A 31-year-old male paralyzed from the waist down from a past car accident was found cold and unresponsive in bed with his hands above his head and bloody purge coming from his mouth and nose. He had been hospitalized approximately 1 month prior for a possible bowel obstruction. Oxycodone, marijuana, and alcohol were present in his room. The decedent was last known alive 9 hours prior.

Imaging Findings Case A: PMCT displays early signs of decomposition. Evidence of cerebral autolysis present with gas present in the vasculature, a decrease in the grey-white matter junction, and a decrease in cerebral attenuation (bright). Putrefactive gas present in the intestines and intestinal walls with abdominal distension is noted. Intravascular gas is noted in the heart and systemic vasculature.

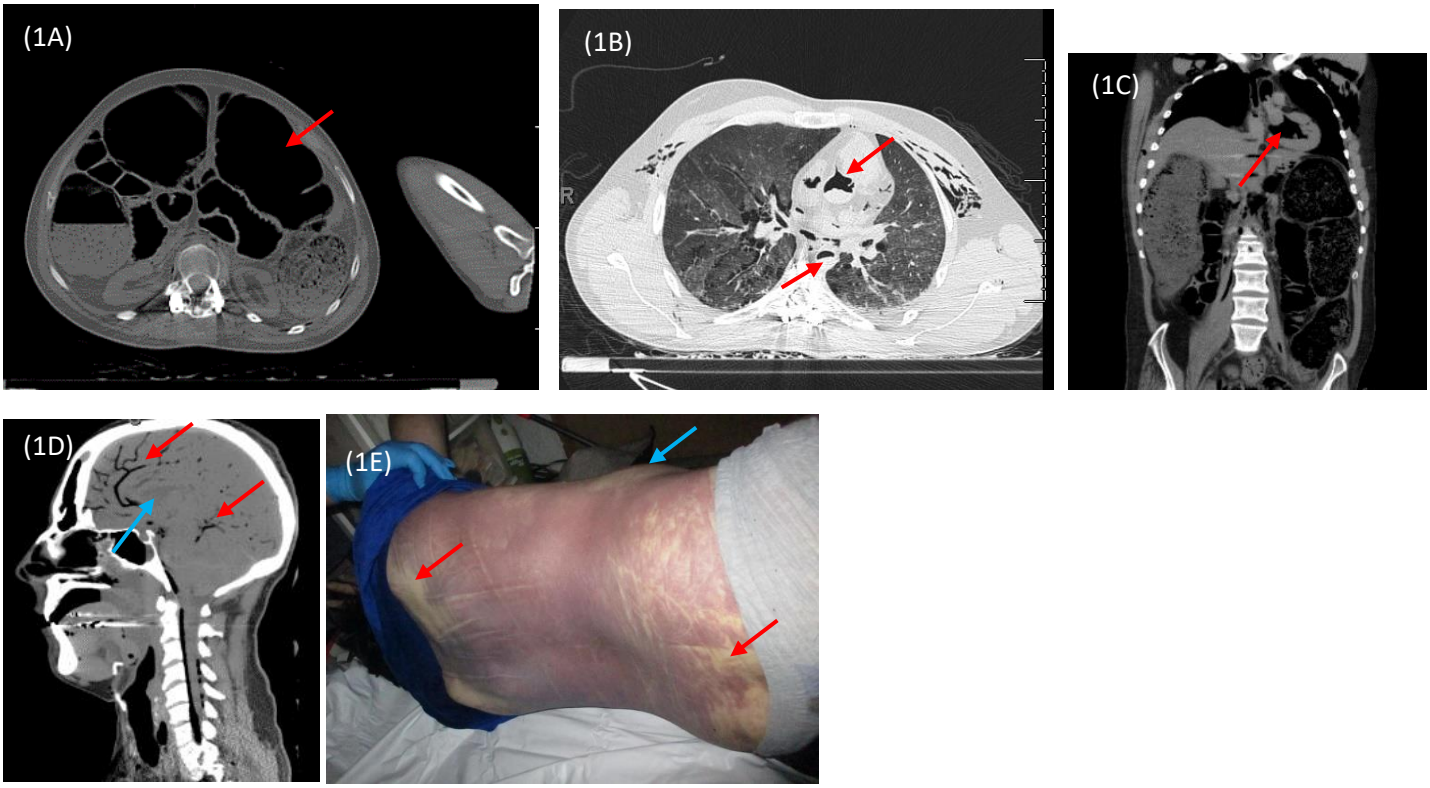

Fig. 1 (Case A): (1A) Distension of intestines and intestinal walls due to putrefactive gas (red arrow). (1B) Intravascular gas present in the systemic vasculature (red arrows). (1C) Gas present in the heart chambers (red arrow). (1D) Cerebral autolysis with putrefactive gas present in the vasculature (red arrows), decrease in cerebral attenuation (blue arrow). (1E) Purple livor mortis present over the back with areas of blanching due to pressure (red arrows). Abdomen is distended due to putrefactive gas present in the intestines (blue arrow).

Pathology Findings Case A: Autopsy revealed the body of a male in a mild state of decomposition with fixed rigor mortis. Purple liver mortis was present, but no major decompositional changes were noted to the body or organs save for abdominal and genital distension. Mild fatty infiltrations of the liver were noted, and postmortem toxicology studies revealed a toxic to lethal concentration of oxycodone along with moderate concentrations of caffeine, diazepam with its metabolites, and marijuana.

Case Description B: A 30-year-old male with a past medical history of Hepatitis C, obesity, and illicit drug use was found face-down in his bedroom. He was found on his knees with his face and upper chest pressed into the floor. Decedent was released from jail approximately 2 weeks before death and was last known alive approximately 1 day prior. Drug paraphernalia was found at the scene.

Imaging Findings Case B: PMCT displays putrefactive gas present in the intestines and intestinal walls with abdominal distension noted. Diffuse intravascular gas noted in the portal venous system and systemic vasculature.

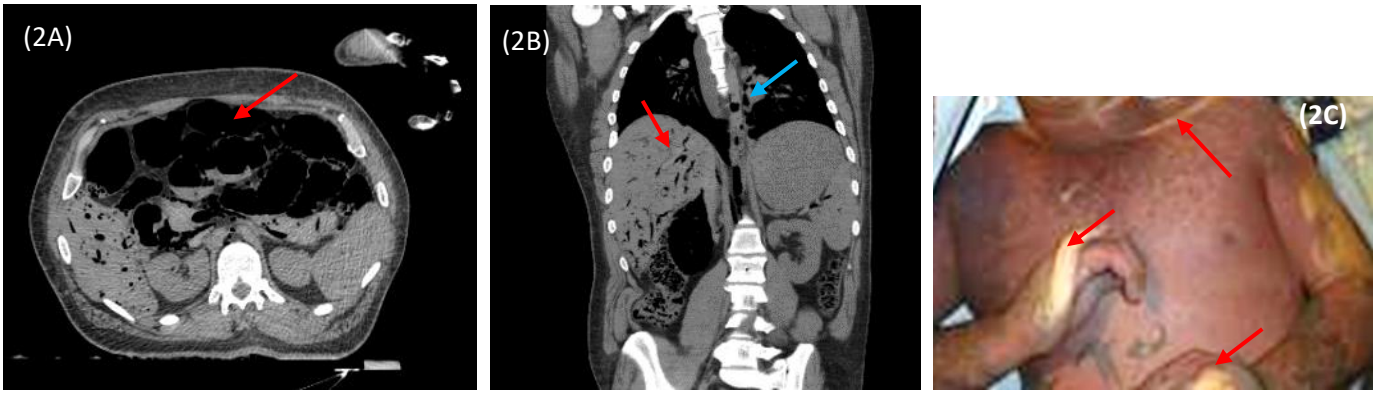

Fig. 2 (Case B): (2A) Distension of intestines and intestinal walls due to presence of putrefactive gas (arrow). (2B) Intravascular gas noted in the portal venous system (red arrow) and systemic vasculature (blue arrow). (2C) Purple-pink livor mortis extending over the chest, arms, and abdomen, with areas of blanching due to pressure (arrows).

Pathology Findings Case B: Autopsy revealed the body of a male in a mild state of decomposition with rigor mortis present. Fixed purple-pink livor mortis was noted to extend over the anterior surfaces of the body except in areas exposed to pressure. Evidence of splenomegaly, chronic hepatitis C, pulmonary edema/congestion, scarring over veins of the left arm, and a recent needle puncture mark of the left hand correspond to the history of acute/chronic injection drug use. Cardiomegaly, hypertension, and obesity were also noted. No decompositional changes were noted to the body or organs. Toxicology of the femoral blood showed the presence of morphine and ethanol.

Comments: In the early stages after death, the body begins to undergo its first structural changes that are visible on CT with correlates in autopsy. The first sign of decompositional change is usually cerebral autolysis (the progressive self-destruction of the brain) which begins within 24-48 hours after death. On CT, cerebral autolysis appears as an overall decrease in attenuation of the brain with blurring/loss of definition of the grey-white matter junction and effacement of the sulci and ventricles; in autopsy, this change is correlated with brain tissue that is soft but macroscopically normal upon examination. As the body continues to decompose, the intestinal bacteria begin to break down the intestines, leading to putrefactive gas accumulation in the tissues and vasculature. On CT, this gas is observed first in the intestinal wall (intramural gas) and the portal venous systems (intravascular gas), which can be identified on CT images as areas of lucency (dark; decreased attenuation) in normally attenuated areas. In autopsy, the accumulation of this putrefactive gas within the intestines is often grossly visible in the abdomen and is correlated to focal changes in the color of the skin. Putrefactive gas may be mistaken for pathologic gas collections, such as air embolisms or pneumothorax. While asymmetric/focal gas collections correlate to pathology, injury, or focal/asymmetric decomposition, putrefactive gas is correlated to symmetrical gas accumulation throughout the entire body. Focal areas of accelerated or decelerated decomposition are not uncommon as the rate of decomposition is affected by many variables, including body size, ambient temperature, trauma, location of the body, clothing, and insect activity or animal predation, so careful analysis of the CT scans, investigative reports, and autopsy findings will help to differentiate between normal decompositional changes and pathological changes.

Further Reading/References:

Levy AD, Harcke HT, Mallak CT. Postmortem imaging: MDCT features of postmortem change and decomposition. Am J Forensic Med Pathol. 2010 Mar;31(1):12-7. doi: 10.1097/PAF.0b013e3181c65e1a. PMID: 20010292.

Contributors: Phoebe Nichols, Yi-Li Grace Wong, Roberto Maselli, and Natalie L. Adolphi.

NMDID 107508

Progression of decomposition on PMCT Part 3: Moderate Decomposition (active decay)

Case Description: A 30-year-old male in a state of moderate decomposition found prone in the bathroom with one leg on either side of the toilet and bloody purge present. A note was found, but no past medical history of depression or thoughts of suicide were noted. He was identified using dental records as he was not able to be visually identified due to discoloration, bloating, and skin slippage.

Imaging Findings: PMCT displays cerebral settling to the dependent portion of the calvarium with diffuse putrefactive gas present in the non-dependent calvarium and vasculature. Gaseous distension of the facial soft tissues is noted. Visceral and subcutaneous gas is present through all tissue planes, vasculature, and visceral organs. Small amounts of cavity fluid and gas are present. The lungs and heart have partially collapsed into the gravity-dependent portions of the chest.

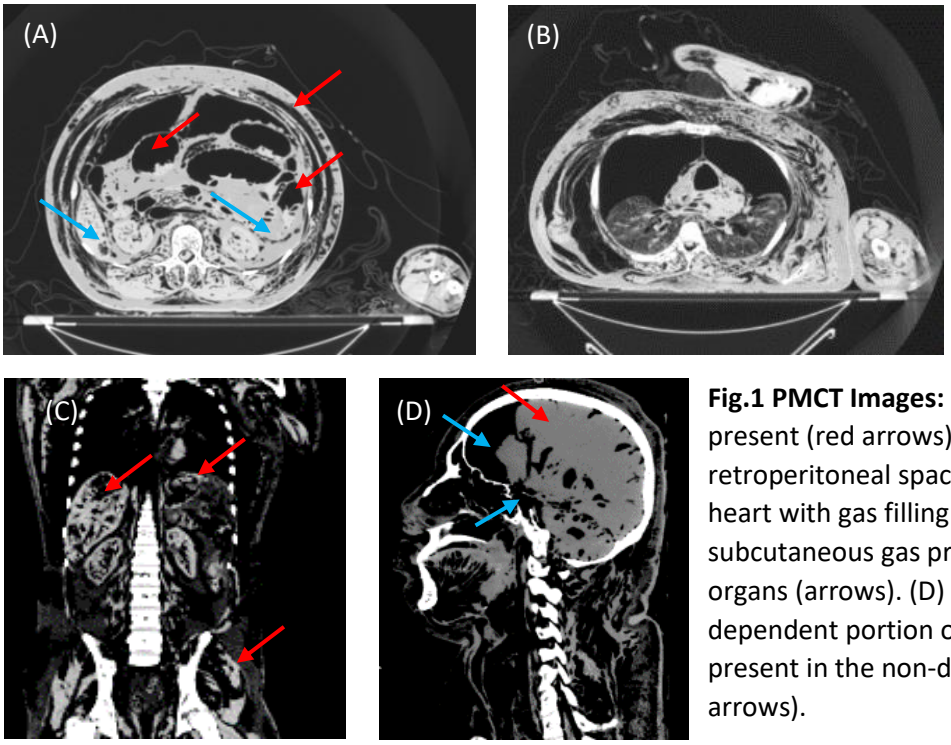

Fig.1 PMCT Images: (A) Visceral and subcutaneous gas present (red arrows) with a small amount of gas/fluid in retroperitoneal spaces (blue arrows). (B) Collapsed lungs and heart with gas filling the chest cavity. (C) Visceral and subcutaneous gas present in all tissue planes and visceral organs (arrows). (D) Cerebral settling (red arrow) in the dependent portion of the calvarium and putrefactive gas present in the non-dependent portions of calvarium (blue arrows).

Pathology Findings: Autopsy revealed the body of a male in a moderate state of decomposition with no rigor mortis present. Livor mortis was dark red in color and fixed to the anterior surfaces of the body. Evidence of moderate decomposition changes includes bloating of the face, torso, and genitalia; green/purple discoloration of the skin with focal skin slippage, and malodorous purge present in the mouth and nose. The abdomen was notably distended due to intestinal gas buildup. Organs were noted to be soft and partially autolyzed with decompositional changes noted to all organs. No injuries or significant natural disease were noted, and toxicology of the liver revealed no ethanol or drugs of abuse.

Fig. 2: (E) Bloating of the face with green-purple discoloration (red arrow) of the skin and focal skin slippage (blue arrow). (F) Livor mortis present to the distal fingers and palm with discoloration of the hand. (G) Bloating of the torso (green arrow) with focal skin slippage (red arrows) and marbling of the skin of the left arm (blue arrows).

Comments: In the moderate stages of decomposition, the body begins to display signs of decomposition throughout the tissues and organs, and due to external changes, the decedent becomes harder to visually identify. As cerebral autolysis continues, the softening brain begins to settle into the gravity-dependent portion of the calvarium while the non-dependent portions fill with gas. On CT, the brain will display decreased attenuation, the grey-white matter junction is no longer visible, and the sulci and ventricles have become further effaced. In autopsy, the brain will be soft and partially autolyzed, and will often display visual discoloration. As putrefactive decomposition continues, gas will enter all vascular structures, anatomic spaces, and body cavities, and body cavities may also contain small amounts of putrefactive fluid or liquefied fat. Subcutaneous and visceral gas becomes more prominent as time after death increases. On CT, the gas accumulations are normally symmetrically distributed throughout the body and are identified as areas of lucency (dark) in normally attenuating (light) areas. In autopsy, all organs will be soft and partially autolyzed, but the visceral organs will be recognizable as they will be normal in shape and contour. Externally the decedent will have become harder to visually identify due to decompositional changes such as bloating of the face, torso, and genitalia; skin slippage; discoloration of the skin (usually green and/or purple in coloration); and cutaneous marbling (greenish-blue discoloration of the skin due to the putrefaction of erythrocytes in the superficial vasculature). Focal areas of accelerated or decelerated decomposition are not uncommon as the rate of decomposition is affected by many variables, including body size, ambient temperature, trauma, location and positioning of the body, clothing, and insect activity or animal predation; therefore, careful analysis of the CT scans, investigative reports, and autopsy findings will help to differentiate between normal decompositional changes and pathological changes. In addition, decomposition can obscure relevant soft tissue findings, such as wounds or injuries from trauma, limiting the utility of CT scans for assessing these findings.

Further Reading/References:

Levy AD, Harcke HT, Mallak CT. Postmortem imaging: MDCT features of postmortem change and decomposition. Am J Forensic Med Pathol. 2010 Mar;31(1):12-7. doi: 10.1097/PAF.0b013e3181c65e1a. PMID: 20010292.

Contributors: Phoebe Nichols, Yi-Li Grace Wong, Roberto Maselli, Natalie L. Adolphi

NMDID 158907

Progression of decomposition on PMCT Part 4: Advanced Decomposition (skeletonization)

Case Description: A 28-year-old male was found in an advanced state of decomposition lying face-down on a dirt road in the desert. His clothing was found scattered around the area, and he was unable to be visually identified due to advanced decomposition.

Imaging Findings: PMCT displays cerebral liquefication with a fluid level and putrefactive gas filling the non-dependent space of the calvarium. Gas present through all tissue planes. Diffuse subcutaneous, mediastinal, and visceral gas noted with visible organ collapse present in the chest and abdomen. Fluid and gas noted in the dependent recesses of the peritoneum with gas in all peritoneal and retroperitoneal organs and tissues. Partial skeletonization noted to the right face.

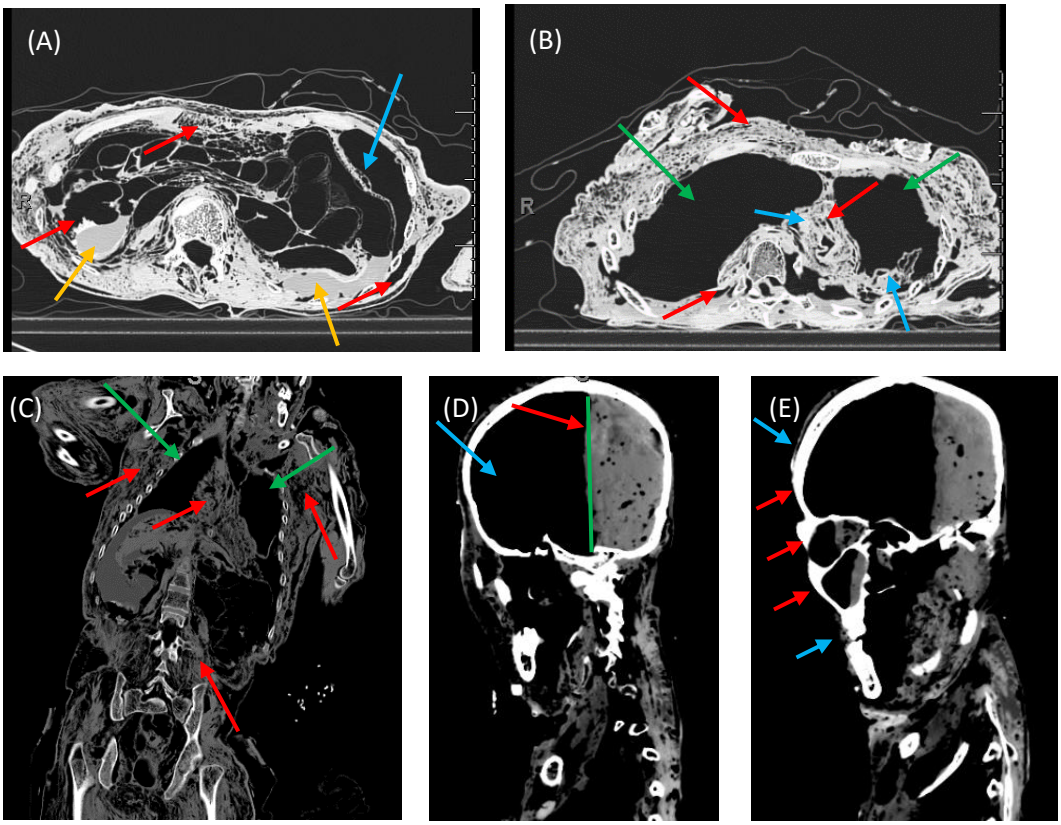

Fig. 1: PMCT Images (A), (B), and (C) Diffuse subcutaneous, mediastinal, and visceral gas (red arrows) throughout all tissue planes with visible organ collapse in the chest and abdomen (blue arrows). (A) Fluid and gas in the retroperitoneum (yellow arrows). (B) and (C) Gas filled chest cavity (green arrow). (D) Cerebral liquefaction and settling to the dependent portion of the calvarium (red arrow) to create a fluid-level (green line) with gas filling the non-dependent portions of the calvarium (blue arrow). (E) Loss of soft tissue to the right face (red arrows) with decomposing tissue attenuation (blue arrows).

Pathology Findings: Autopsy revealed the body of a male in an advanced state of decomposition with partial mummification of the left face, body, and extremities, and skeletonization of the right face. The skin of the anterior portion of the upper legs, chest, and abdomen displayed a white-green, waxy appearance while the anterior right upper arm, hand, and left forearm displayed maceration. Multiple smooth defects ranging from 1/4 to 4-1/2 inches were present in the tissue of the left upper arm that exposed the underlying humerus. Maggots and beetles were present with evidence of increased activity in the tissue of the neck, anterior right shoulder, left abdomen, left hand, anterior lower legs, and scalp. Visceral organs able to be identified showed extensive decomposition and postmortem change, most having lost significant mass and attained a paste-like consistency; the eyes are missing due to postmortem change.

Toxicology testing of the femoral blood showed no evidence of drug use, but a low ethanol level was detected. No evidence of significant natural disease or injuries was present to explain death.

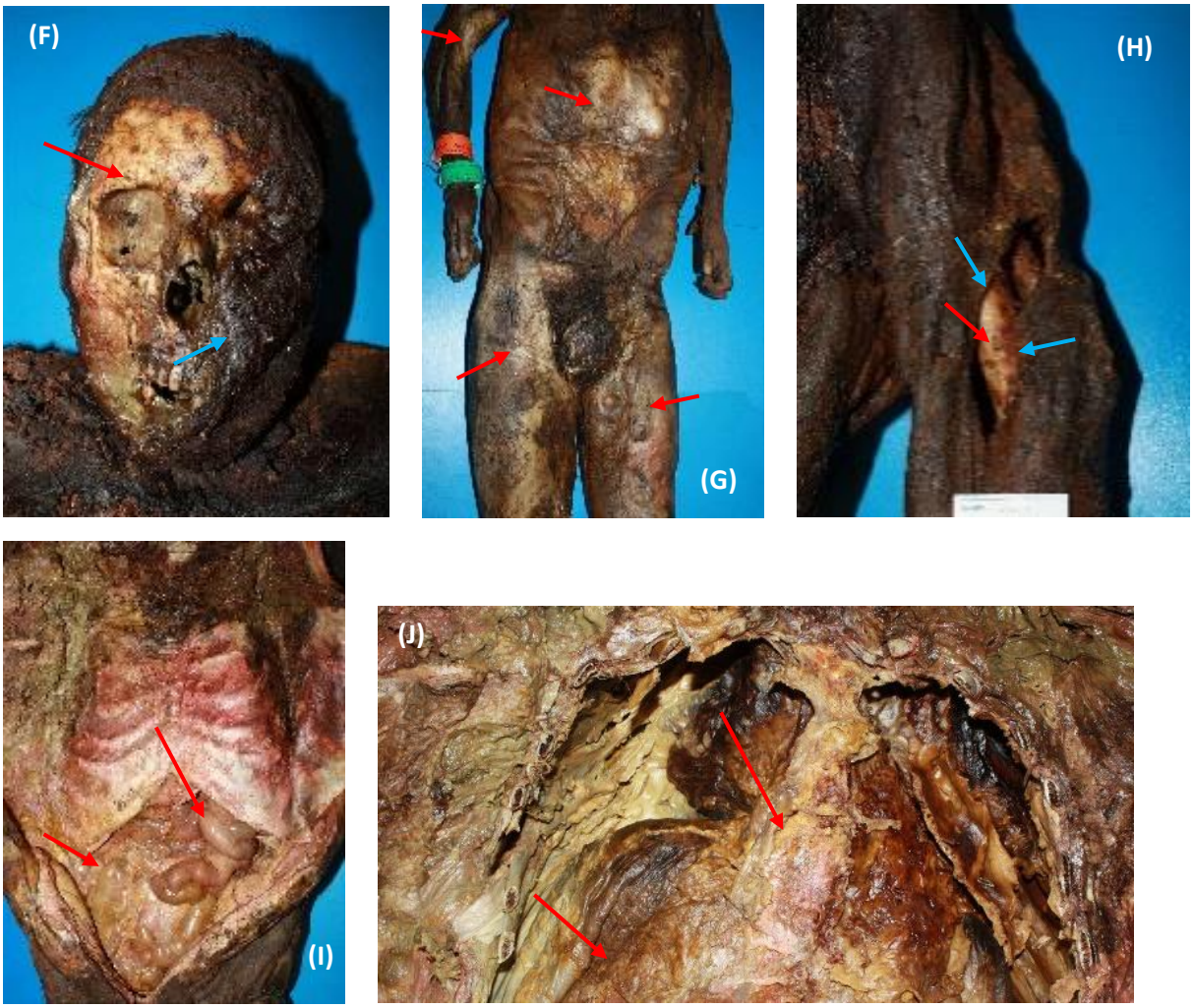

Figure 2: Autopsy Photos (F) Skeletonization of the right face (red arrow) and partial mummification of the left face (blue arrow). (G) Partial mummification of the torso and extremities (red arrows). (H) Exposure of the left humerus (red arrow) due to smooth defects (blue arrows). (I) and (J) Decomposed visceral organs of the abdomen and chest cavities (red arrows).

Comments: In the advanced stages of decomposition, the body displays signs of decomposition throughout the entire body, and visual identification is nearly impossible due to significant external changes, such as skeletonization. At an advanced stage of cerebral putrefaction, the brain reaches complete cerebral liquefaction, creating a fluid-level within the calvarium. On CT, the brain will display a fluid-level in the gravity-dependent portions of the calvarium with attenuation (bright) like that of water, and the rest of the calvarium will be filled with putrefactive gas. In autopsy, the brain will be completely liquefied with no recognizable anatomical features and has gained a paste-like consistency. Putrefactive gas is present throughout all tissue planes as connective tissues and organs collapse. The abdominal and chest cavities fill with gas as the organs lose their recognizable shapes and appearances, collapsing and liquefying in the gravity-dependent portions of the body, and putrefactive fluid is often seen in the dependent portions of the body. On CT, the gas accumulations are symmetrical throughout the body and are identified as areas of lucency (dark) in normally attenuated areas. In autopsy, the collapse of the organs makes them difficult to identify, and the breakdown of tissue can obscure soft tissue findings, such as wounds or injuries from trauma that may have contributed to the cause of death, limiting the diagnostic utility of CT scans for visualizing anatomic structures, injury patterns, and foreign bodies.

Insect activity and animal predation can provide further information about the location of the body at death, if the body has been moved after death, and narrow down time of death, but these external changes can be easily mistaken for

pathology or injury when interpreting CT scans. Maggots are attracted to moist areas of decomposing bodies, such as mucous membranes, and on CT they are visualized as linear/curvilinear soft tissue or surface irregularities. They are often found in the face or head of decomposing bodies, or in open wounds where they can obscure injury patterns. Animal predation can cause increased postmortem injuries to the body and obscure antemortem injury patterns, but animal predation makes identification especially challenging in cases where the body has become skeletonized due to increased scattering of the remains. Complete and partial skeletonization is common in most bodies, and this can further obscure injuries or evidence for cause of death as well as limit identification as the tissue disappears. On CT, skeletonization is identified by areas of bone without surrounding attenuation due to advanced tissue decomposition, and in autopsy the skeletonized areas will have bone open to the air and can have some desiccating tissue present. Rather than undergoing decomposition/skeletonization, in dry environments mummification (drying and preservation of the skin) can occur due to decreased bacterial growth. In moist environments, including graves, vaults, and crypts, a body may undergo adipocere formation (fat in the body coalesces into a waxy substance that preserves subcutaneous tissues and portions of internal organs) rather than decomposing and becoming skeletonized. On CT, adipocere has low attenuation and often coexists with normal putrefactive decomposition, so scans can show partial or fully decomposed organs surrounded by adipocere. In autopsy, adipocere is often grey-white in color and has a waxy appearance, often occurring in the subcutaneous fat of the body, but it can be seen in other fat deposits. Mummification and adipocere formation can preserve injuries due to preservation of the soft tissues, but as mummification, adipocere formation, and skeletonization are not uniform, these changes may also make interpretation of CT scans and autopsy findings more difficult.

Further Reading/References:

Levy AD, Harcke HT, Mallak CT. Postmortem imaging: MDCT features of postmortem change and decomposition. Am J Forensic Med Pathol. 2010 Mar;31(1):12-7. doi: 10.1097/PAF.0b013e3181c65e1a. PMID: 20010292.

Contributors: Phoebe Nichols, Yi-Li Grace Wong, Roberto Maselli, and Natalie L. Adolphi

NMDID 100467

Sigmoid malignancy on PMCT

Case description: An 88-year-old female with multiple comorbidities (hypertension, hyperlipidemia, atherosclerotic cardiovascular disease, end stage renal disease, anemia, and remote cervical cancer) had a fall resulting in left chest hematoma and hip fracture, the latter surgically repaired. She was discharged to a rehabilitation facility but developed joint infection and lower extremity deep vein thrombosis treated with anticoagulants. After initiation of treatment, her left chest swelling became acutely worse, and she developed abdominal discomfort. She was later found unresponsive in her hospital bed.

Imaging Findings: A short segment, eccentric sigmoid colon wall thickening up to 1.2 cm with intraluminal narrowing was seen with surrounding pericolonic fat stranding, representing either inflammation or infiltration. There were no enlarged regional pericolonic nodes seen in this study. Other findings included a left chest wall hematoma, cerebral atrophy, coronary, aortic and major branch calcifications, renal cysts, bilateral pleural collections, and an IVC filter.

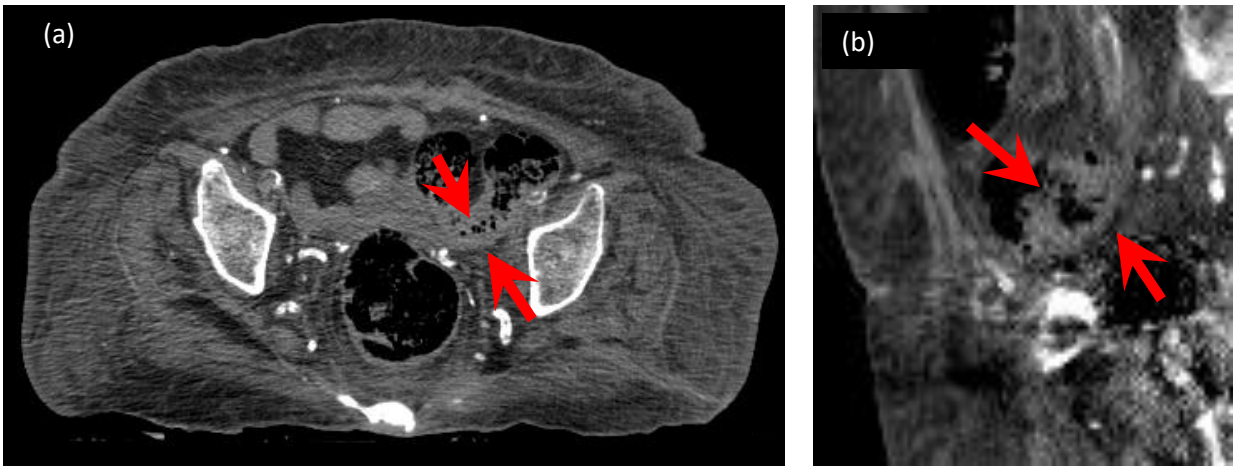

Fig 1: PMCT images in (a) axial and (b) sagittal planes showing short segment, sigmoid colon wall thickening corresponding to the sigmoid adenocarcinoma found at autopsy.

Fig 2: Autopsy shows abundant frank blood and melena and an ulcerated mass with surrounding induration in the sigmoid colon

Pathology Findings: In addition to a large left chest wall hematoma and natural disease concurring with her medical history, there was also evidence of significant gastrointestinal blood loss from numerous ulcers and advanced stage colon carcinoma. A 2 x 1.5 cm ulcerated mass with surrounding induration in the sigmoid colon with abundant intraluminal frank red blood and melena were present. Approximately 1 L of blood intestinal contents were found in the small and large intestine combined. Microscopic examination confirmed invasive adenocarcinoma with chronic inflammation and desmoplastic stromal response within the bowel wall. The cause of death was combined effects of chest wall hematoma and acute gastrointestinal hemorrhage, and the manner of death categorized as accident.

Comments: In clinical radiology, CT and MRI are used for staging of colon carcinoma. In this case, the sigmoid tumor is shown as a short segment irregular sigmoid bowel wall thickening causing luminal narrowing which corresponded to autopsy findings. However due to limited soft tissue contrast, the intraluminal hemorrhage was not well visualized on PMCT. The lack of

distension of bowel can also cause these tumors to be overlooked. Pericolonic fat stranding can either represent adjacent edema, inflammation, or extramural extension with an accuracy range between 60-80%. Regional nodal evaluation may not be as reliable on PMCT as compared to PMMR.

Further Reading:

Liu LH, Lv H, Wang ZC, Rao SX, Zeng MS. Performance comparison between MRI and CT for local staging of sigmoid and descending colon cancer. Eur J Radiol. 2019 Dec;121:108741. doi: 10.1016/j.ejrad.2019.108741. Epub 2019 Nov 10. PMID: 31743882.

Contributors: Yi-Li Grace Wong, Kethery Haber, Roberto Maselli, and Natalie Adolphi

NMDID 101358

Perforating Gunshot Wound of the Head on PMCT

Case description: A 21-year-old male was found dead in a motor home with a large pool of blood on and around the body and a handgun found under his body. There was a note expressing suicidal intent on a table inside the motor home.

Imaging Findings (Fig 1):

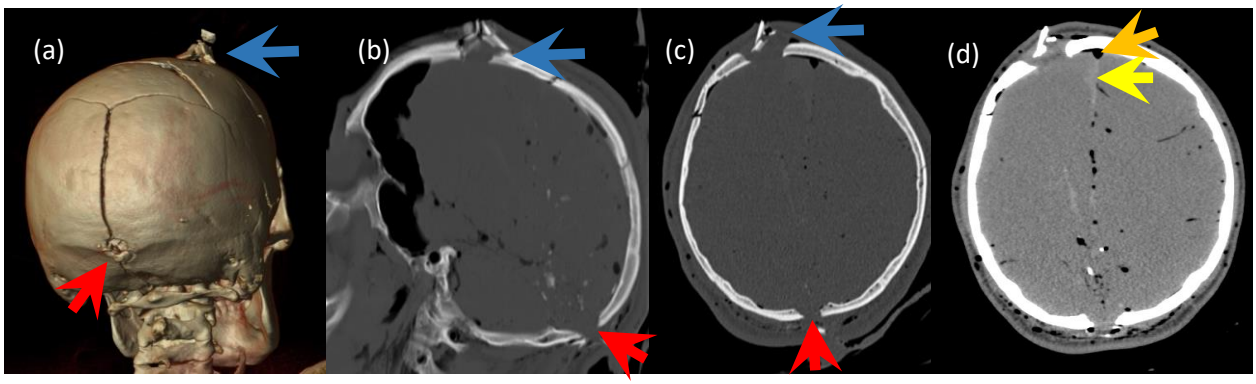

Fig 1: PMCT (a) 3D-volumetric reconstruction, (b) Sagittal view, bone reconstruction, (c) Axial view, bone reconstruction, demonstrating the entrance wound with internal beveling (red arrows) and exit wound (blue arrows) with external beveling and skull fragments displaced externally. (d) Axial view, brain window shows associated injuries of the gunshot wound, i.e. pneumocranium (orange) and hyperdense subarachnoid hemorrhages (yellow arrow). The trajectory of the bullet track can be inferred by following the linear path of air pockets and intracranial bone fragments back to front, slightly upwards and slightly towards the right.

Pathology Findings (Fig 2): A contact range gunshot wound with entrance at the midline occipital scalp, consisted of a 1/4-inch round defect with a circumferential, 1/8-inch, dark red marginal abrasion and radiating lacerations extending from the 2 o'clock (1/2 inch), 8 o'clock (1/2 inch), 9 o'clock (1/4 inch), and 10 o'clock (1/2 inch) positions. The underlying skull showed internal beveling. The exit was on the right frontal scalp, centered approximately 3/4 inches below the top of the head and 1 inch right of anterior midline, with a 1x1 inch stellate laceration without marginal abrasion. The underlying skull showed external beveling, and 3 irregular skull fragments laid within the laceration. Associated injuries included radiating skull fractures extending from the entrance and exit defects and lacerated brain matter. The wound track travelled from back to front, left to right, and upward. There was a small amount of fine blood spatter on the dorsal aspect of the right hand. Cause of death was a perforating gunshot wound of the head. Manner of death was classified as suicide.

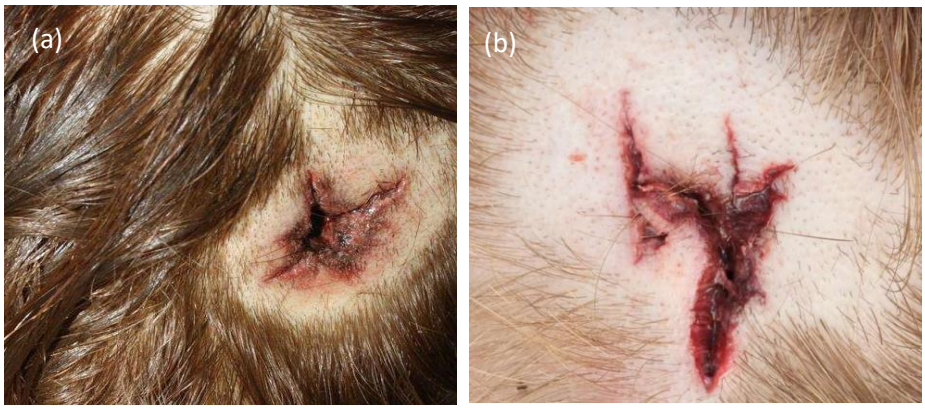

Fig 2: Autopsy photos showing the (a) entrance wound & the (b) exit wound.

Comments: PMCT complements autopsy findings with documentation of salient findings of gunshot wounds such as the identifications of entry and exit wounds, bullet pathways, bullet/fragments clouds, and associated fractures and injuries. Entry and exit sites are particularly identifiable in gunshot wounds of the head, characterized by internal and external

beveling of bones respectively; however, superficial findings and range of fire are best assessed through physical external examination. Three-dimensional techniques further enhance the ability of imaging to reconstruct the likely mechanism of death, which may influence the determination of the manner of death, e.g., homicide vs. suicide. Note, however, that large retained metallic projectiles can cause streak artifacts on PMCT, obscuring assessment of surrounding soft tissues.

Further reading:

1. Peschel O, Szeimies U, Vollmar C, Kirchhoff S. Postmortem 3-D reconstruction of skull gunshot injuries. Forensic Sci Int. 2013 Dec 10;233(1-3):45-50. doi: 10.1016/j.forsciint.2013.08.012. Epub 2013 Aug 18. PMID: 24314500.
2. Kirchhoff SM, Scaparra EF, Grimm J, Scherr M, Graw M, Reiser MF, Peschel O. Postmortem computed tomography (PMCT) and autopsy in deadly gunshot wounds--a comparative study. Int J Legal Med. 2016 May;130(3):819-26. doi: 10.1007/s00414-015-1225-z. Epub 2015 Jul 9. PMID: 26156451.

Contributors: Yi-Li Grace Wong, Kethery Haber, Roberto Maselli, and Natalie Adolphi

NMDID 101843

Traumatic hemothorax, hemopericardium, and hemoperitoneum on PMCT

Case description: An 82-year-old male with unknown medical history was involved in a high-speed motor vehicle accident. Upon arrival to emergency department, he was in an agitated state, sedated and resuscitated, but decompensated with cardiac arrest and died 1 hour after the accident. The PMCT was performed 15 hours after death.

Imaging Findings: Other than bilateral anterolateral displaced rib fractures, possibly due to resuscitation efforts, no other fractures were seen. PMCT revealed hemopericardium causing cardiac tamponade, bilateral hemothoraces, and hemoperitoneum at the perihepatic and perisplenic regions and pelvis. There was evidence of natural disease with generalized brain atrophy, atherosclerotic calcifications along large- and medium-sized arteries, and perinephric fat stranding with renal cysts.

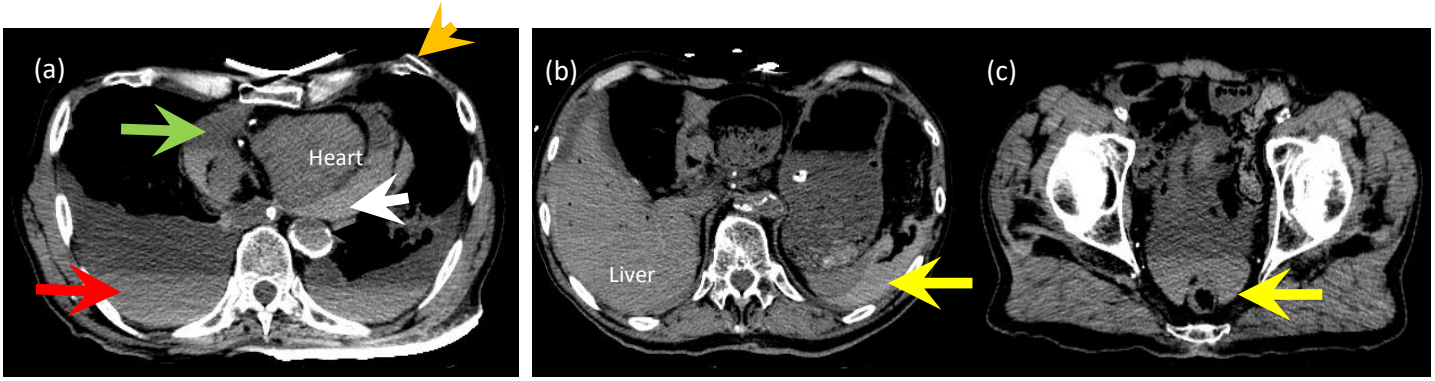

Axial slices of the (a) Lung bases showing hemopericardium (green arrow), bilateral hemothoraces (red arrow) and anterolateral rib fracture (orange arrow); Postmortem intravascular layering is also noted in the larger vessels, such as the descending thoracic aorta in this image (b) Hemoperitoneum at perihepatic and perisplenic regions and (c) Hemoperitoneum at the pelvis with hypodense layering at the non-dependent areas and hyperdense layering at the dependent areas.

Pathology Findings: External examination revealed abrasions and contusions of the face, trunk, and extremities. There was evidence of resuscitation. Livor and rigor mortis were fully fixed. There were no signs of decomposition otherwise. The cause of death was blunt trauma, and the manner of death was accident.

Comments: Hypodense and hyperdense fluid layering are seen in both antemortem and postmortem cases and represent serum (at non-dependent areas) and denser cellular elements of blood (at dependent areas) respectively. In living patients, this is described as the "hematocrit effect" which is often associated with coagulopathy or anticoagulation therapy. Layering can also be interpreted as re-bleeding into an older bleed in certain cases, such as in brain subdural hemorrhages, but does not fit the history, timeline and the pattern of blood collections in this case, i.e. pericardial, thoracic and peritoneal cavities with evidence of external injuries at these areas. Resuscitation efforts likely caused the anterolateral rib fractures. In postmortem CT, intravascular layering can often be found as a result of post mortem sedimentation due to gravity dependent hemoconcentration when circulation stops, most prominent in larger vessels such as the pulmonary arteries and aorta. Loss of osmotic pressure support within the vascular system causes serum and and electrolytes to leak out into extravascular spaces with increased hematocrit at dependent areas.

Further reading:

1. Hematocrit effect:*https://radiopaedia.org/articles/haematocrit-effect?lang=us*
2. Lubner M, Menias C, Rucker C, Bhalla S, Peterson CM, Wang L, Gratz B. Blood in the belly: CT findings of hemoperitoneum. Radiographics. 2007 Jan-Feb;27(1):109-25. doi: 10.1148/rg.271065042. PMID: 17235002.
3. Cox M, Bisangwa S, Herpich F, Crudele A, Pineda C. Fluid levels in the bleeding brain: a marker for coagulopathy and hematoma expansion. Intern Emerg Med. 2017 Oct;12(7):1071-1073. doi: 10.1007/s11739-017-1604-1. Epub 2017 Jan 13. PMID: 28091838.

4. Jackowski C, Thali M, Aghayev E, Yen K, Sonnenschein M, Zwygart K, Dirnhofer R, Vock P. Postmortem imaging of blood and its characteristics using MSCT and MRI. Int J Legal Med. 2006 Jul;120(4):233-40. doi: 10.1007/s00414-005-0023-4. Epub 2005 Nov 19. PMID: 16328426.

Contributors: Yi-Li Grace Wong, Kethery Haber, Roberto Maselli, Natalie L. Adolphi

NMDID 104091

Dilated ventricles: Cerebral atrophy v. normal pressure hydrocephalus (NPH)

Case description: A 61-year-old female with a past medical history of diabetes mellitus was found unresponsive on the floor of her residence with potted plants knocked over. No foul play was suspected.

Imaging Findings: Coronary artery, aorta, and mitral valve calcifications were seen. In the brain, there were prominent ventricles proportionate to sulcal prominence. No large segmental infarcts, intracranial bleed, skull nor facial bone fractures were seen. There was a healed left posterolateral 10th rib fracture, but otherwise no acute bone fractures.

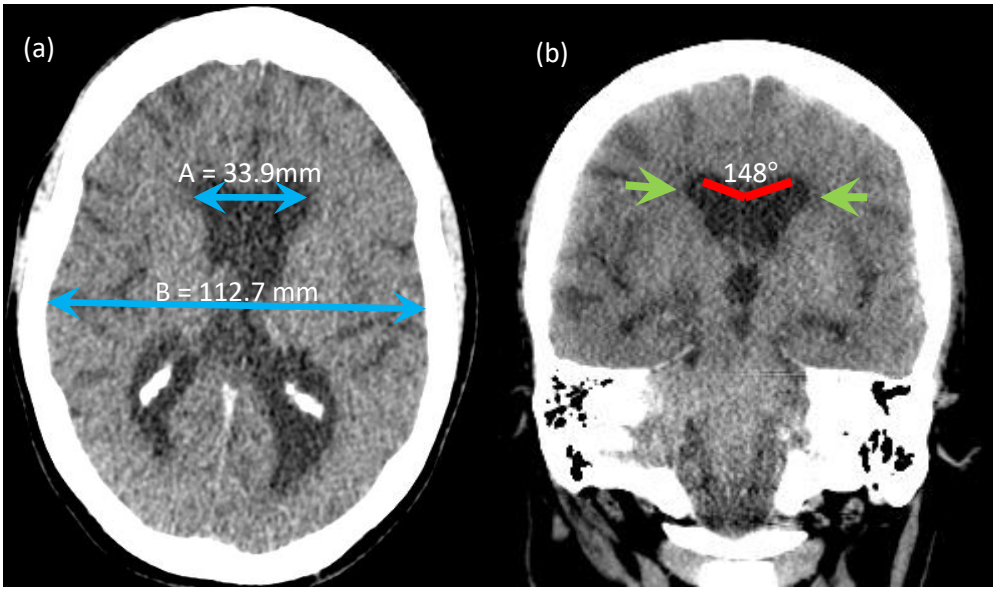

PMCT Brain (a) Axial and (b) Coronal - views demonstrated symmetrically dilated bilateral lateral ventricles proportionate to sulci prominence. Evan's Index (A/B) was 0.32 (blue arrows), callosal angle was 148° (red lines) and there was minimal periventricular hypoattenuation (green arrows).

Pathology Findings: External examination revealed an obese woman with body mass index of 31 kg/m^2, few minor abrasions and contusions at the left cheek, forehead, and lower extremities. Correlating scene investigations, medical history, PMCT and external examination findings, the cause of death was certified as atherosclerotic cardiovascular disease and the manner of death, natural.

Comments: Cerebral atrophy is commonly seen in asymptomatic elderly people, Alzheimer's disease or the sequelae of brain insults, e.g., stroke or traumatic injuries. Compensatory dilatation of ventricles (also termed hydrocephalus ex-vacuo) occurs due to loss of brain volume, but intracranial pressure and cerebrospinal fluid (CSF) flow are constantly normal. Normal pressure hydrocephalus (NPH) is characterized by the clinical triad of gait disturbance, dementia, and urinary incontinence. NPH is a misnomer because there are intermittent increases in CSF in the ventricular system due to flow impairment distal to the 4th ventricle[1]. 50% are idiopathic but other causes include meningitis, subarachnoid hemorrhages and cranial trauma. If left untreated, NPH can progressively worsen and directly or indirectly cause death. Deaths due to cerebrovascular disease or dementia are more common in NPH patients compared to controls[2]. Mortality in operated NPH patients was found to be 1.8 times higher compared to general population[2]. Imaging features of NPH that differentiate it from cerebral atrophy include ventricular enlargement *disproportionate* to cerebral atrophy (Evan's index > 0.3 cm), callosal angle between 40-90^O, enlarged Sylvian fissures and basal cisterns, and ballooning of frontal horns[1]. In this case, Evan's index was slightly above the normal cut-off value, but the callosal angle was still normal. Ventricular prominence was proportionate to sulci prominence, and there was not significant periventricular hypodensity,

i.e., acute CSF, seen in this case. Hence, this case was more likely to be compensatory ventricular dilation due to cerebral atrophy. To note, MRI more accurately defines the extent of periventricular CSF compared to CT, in addition to demonstrating other detailed features of NPH, such as corpus callosal thickening and elevation, hippocampal atrophy, and aqueductal/4th ventricular flow void.

Further reading and references:

1. Damasceno BP. Neuroimaging in normal pressure hydrocephalus. Dement Neuropsychol. 2015 Oct-Dec;9(4):350-355. doi: 10.1590/1980-57642015DN94000350. PMID: 29213984; PMCID: PMC5619317.
2. Andrén K, Wikkelsø C, Sundström N, Israelsson H, Agerskov S, Laurell K, Hellström P, Tullberg M. Survival in treated idiopathic normal pressure hydrocephalus. J Neurol. 2020 Mar;267(3):640-648. doi: 10.1007/s00415-019-09598-1. Epub 2019 Nov 11. PMID: 31713102; PMCID: PMC7035239.

Contributors: Yi-Li Grace Wong, Kethery Haber, Roberto Maselli, Natalie L. Adolphi

NMDID 112978

Large intraparenchymal, intraventricular, and subarachnoid hemorrhages

Case description: A 59-year-old male with history of hypertension and dysphagia did not show up at work and was found dead on the floor of his residence.

Imaging Findings: PMCT demonstrated a large left intraparenchymal hemorrhage with the epicenter at the left basal ganglia [size: 10.4 x 4.4 x 6.5 cm (anteroposterior x width x craniocaudal length) extending to frontal, parietal, and temporal lobes, with intraventricular and subarachnoid extensions]. There were surrounding perilesional edema and mass effect as evidenced by midline shift of 1.2 cm to the right, and effacement of left lateral ventricles and surrounding sulci. The 3rd ventricle was also compressed causing right lateral ventricle dilatations with hemorrhage within. There were no PMCT signs of head trauma nor fractures elsewhere. Additional natural findings included abundant calcifications of the aorta, coronary arteries, and Circle of Willis.

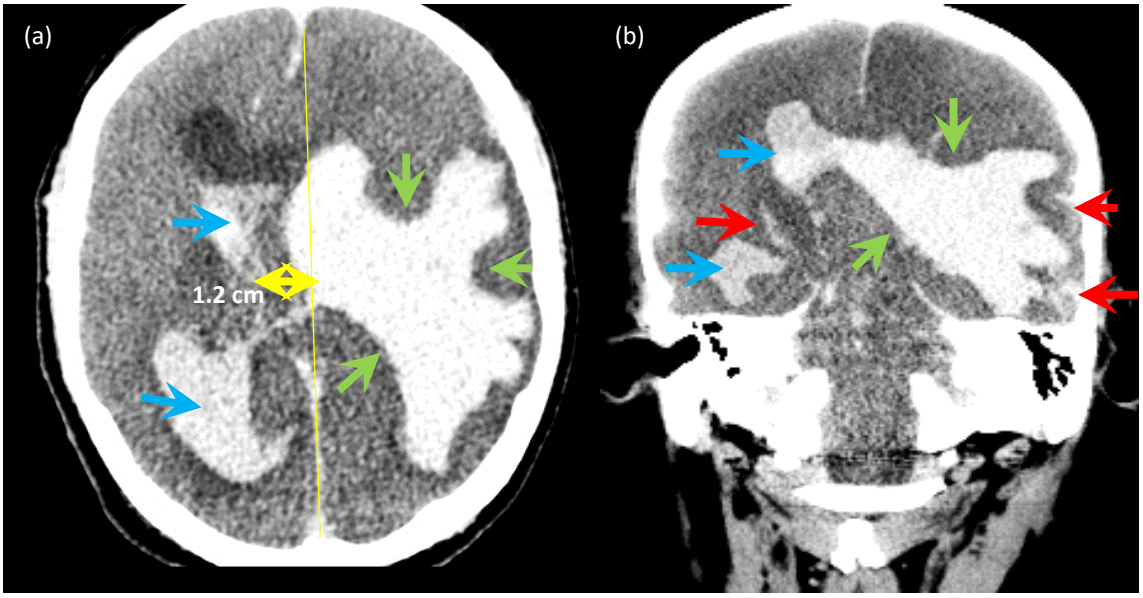

PMCT Brain in (a) Axial and (b) Coronal views demonstrated a large left basal ganglia intraparenchymal hemorrhage (green arrows) with intraventricular (blue arrows) and subarachnoid (red arrows) extensions of bleed, diffuse cerebral edema and mass effect with midline shift to the right (yellow arrows), compression of third and left lateral ventricles causing dilatation of the right ventricles with blood product (blue arrows) within.

Pathologist Findings: External examination showed no traumatic injuries that contributed to death. The cause of death was certified as hypertensive intracerebral hemorrhage. The manner of death was classified as natural.

Comments: PMCT clearly demonstrated the location, size/volume, extension, and mass effect of the large intraparenchymal hemorrhage (IPH) as a direct cause of death. There were no subgaleal hematomas or skull vault fractures that indicated trauma. Other conditions to consider in intraparenchymal hemorrhages include bleeding disorders, cerebral amyloid angiopathy, anticoagulant medications and chronic alcoholism[1]. Classical locations for hypertensive bleeds include the basal ganglia, thalamus, pons, and cerebellum. There was also subarachnoid hemorrhage characterized by hyperdensities along the sulci on PMCT in close vicinity to the IPH; caused by bleeding between the pia and the arachnoid membranes, as well as intraventricular hemorrhage, both of which can be associated with aneurysmal (often at perimesencephalic location) or arteriovenous malformation ruptures, more common in non-hypertensive and/or younger patients [2-3]. When these are highly suspected, PMCTA (angiography) can be considered to enable visualization of intracranial vessels.

Further reading and references:

1. Ritter MA, Droste DW, Hegedüs K, Szepesi R, Nabavi DG, Csiba L, Ringelstein EB. Role of cerebral amyloid angiopathy in intracerebral hemorrhage in hypertensive patients. Neurology. 2005 Apr 12;64(7):1233-7. doi: 10.1212/01.WNL.0000156522.93403.C3. PMID: 15824353.
2. Naidech AM. Intracranial hemorrhage. Am J Respir Crit Care Med. 2011 Nov 1;184(9):998-1006. doi: 10.1164/rccm.201103-0475CI. PMID: 22167847; PMCID: PMC3361326.
3. Herbstein DJ, Schaumburg HH. Hypertensive Intracerebral Hematoma: An Investigation of the Initial Hemorrhage and Rebleeding Using Chromium Cr 51-Labeled Erythrocytes. *Arch Neurol.* 1974;30(5):412–414. doi:10.1001/archneur.1974.00490350070013

Contributors: Grace Yi-Li Wong, Kethery Haber, Roberto Maselli, and Natalie Adolphi

NMDID 113505

Ingested magnets causing streak artifacts on PMCT

Case description: A 38-year-old male, last seen 2 days prior with no complaints, was found dead, face down on his kitchen floor. He had no known medical comorbidities and no primary care physician, preferring to treat any illnesses with "homeopathic remedies." Numerous herbal supplements were found in his house. Empty anti-freeze containers were seen in the trash.

Imaging Findings: A large volume of high-density material (mean attenuation value of 2975 HU) was visualized within the stomach causing significant streak artifact, suggestive of metallic content. There were no PMCT signs of viscus perforation or surrounding mesenteric fat inflammation or fluid to suggest acute peritonitis. There were also no signs of trauma or significant natural disease.

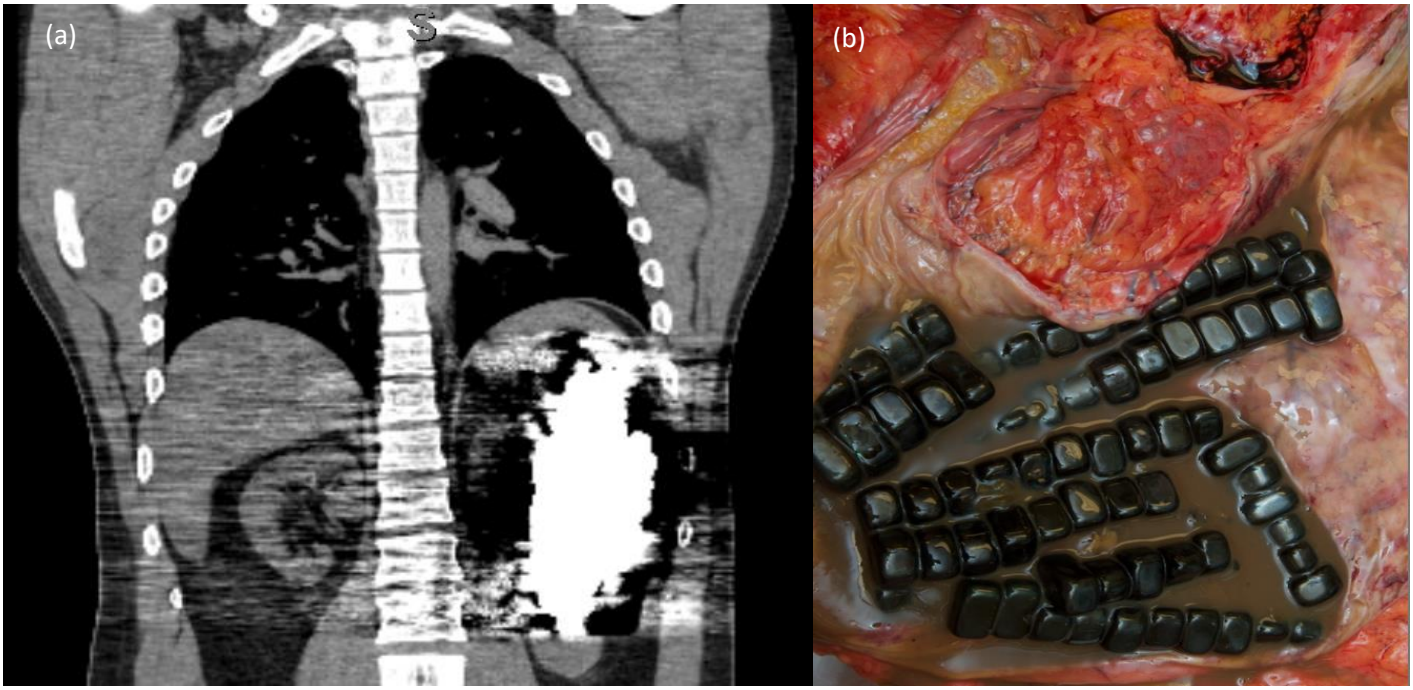

(a) PMCT: High density material within the stomach causing significant streak artifact, suggestive of metallic content. (b) Autopsy: Magnets were discovered in the stomach.

Pathology Findings: Magnet ingestion with multiple clumped magnets found in the stomach during internal examination. However, the cause of death was determined to be acute methanol toxicity. There were no signs of trauma or significant natural disease at autopsy.

Comments: There are several CT artifacts that cause image degradation, potentially obscuring or mimicking true pathologies and hampering accurate interpretation. In this case, unlike the definitive findings in autopsy, the high density seen on PMCT was consistent with metallic material but not confirmative of the type of material causing the streak artifacts, i.e., linear bands of high and low density. Concentrated barium and iodinated contrast used in clinical imaging investigations can also be highly attenuating; hence correlation with history is pivotal in strengthening differentiation. Techniques for reducing metal artifact include increasing the tube voltage or using metal artifact reduction algorithms if available.

Further reading:

1. Barrett JF, Keat N. Artifacts in CT: recognition and avoidance. Radiographics. 2004 Nov-Dec;24(6):1679-91. doi: 10.1148/rg.246045065. PMID: 15537976.

2. Triche BL, Nelson Jr JT, McGill NS, Porter KK, Sanyal R, Tessler FN, McConathy JE, Gauntt DM, Yester MV, Singh SP. Recognizing and minimizing artifacts at CT, MRI, US, and molecular imaging. RadioGraphics. 2019 Jul;39(4):1017-8.

Contributors: Grace Yi-Li Wong, Kethery Haber, Roberto Maselli, and Natalie L. Adolphi

NMDID 130715

Hyoid and thyroid cartilage fractures, often subtle and easily missed on PMCT

Case description: A 37-year-old male was found deceased and nude, except for a sock, in the backyard of an abandoned house. He had bruising and abrasions at different stages of healing all over his body.

Imaging Findings: PMCT demonstrated a hyoid (right cornu) fracture, thyroid (right cornu) cartilage fractures, rib fractures, a hepatic laceration, and hemoperitoneum.

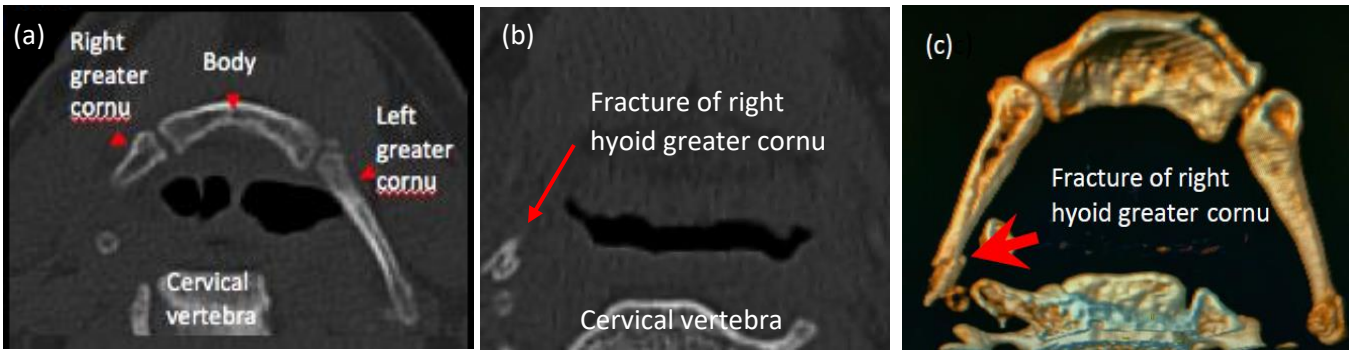

Fig 1: PMCT hyoid (bone window) (a) a more superior and (b) more inferior CT axial slice: Because the head was tilted, the hyoid bone was visualized in different thin (1 mm) axial slices. (c) Three dimensional PMCT volume rendering allowed reconstruction of the hyoid bone, demonstrating the fracture more clearly.

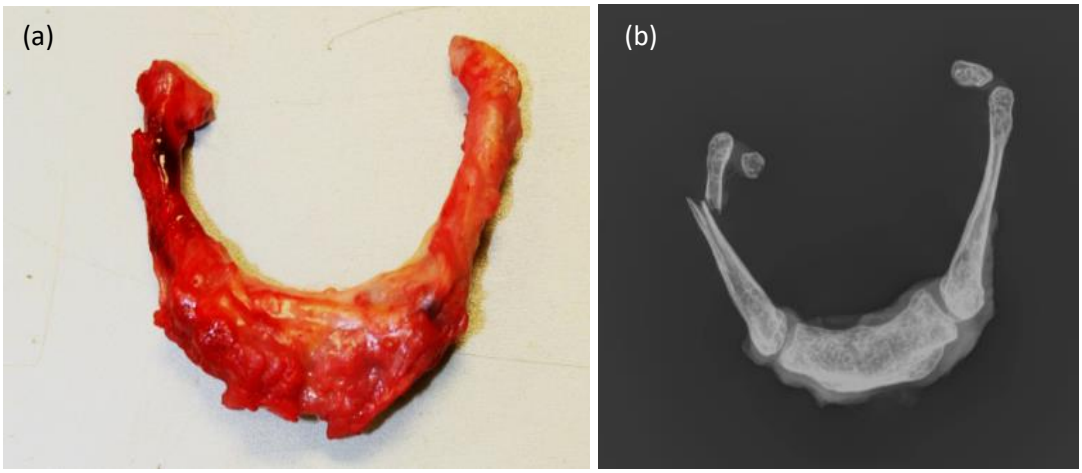

Fig 2: (a) Autopsy & (b) Radiograph demonstrating clear delineation of the right hyoid cornu fracture.

Pathologist Findings: Autopsy revealed evidence of blunt force trauma of the head and neck, trunk, and extremities; multiple abrasions and contusions on body surfaces; and scalp and neck soft tissue hemorrhages. Autopsy confirmed PMCT findings of hyoid and thyroid cartilage injuries, rib fractures, and liver lacerations causing hemoperitoneum. There was periosteal and soft tissue hemorrhage surrounding the right side of the hyoid bone and fracture of the right greater cornu of the hyoid. The right superior thyroid cornu was deformed and showed pericartilagenous hemorrhage. Postmortem toxicology revealed the presence of ethanol in femoral blood. The cause of death was attributed to blunt trauma, and the manner of death was certified as homicide.

Comments: In this case, the scene investigation and the manner of discovery raised suspicion for homicide. Without this salient history, it could have been easy to overlook the subtle hyoid and thyroid cartilage injuries when viewing whole body postmortem PMCT in a "blinded" fashion. Hyoid and thyroid fractures are more often found in cases of hanging or manual strangulation. Due to their small size, it is recommended to view thin slices of the head & neck, i.e. 0.5 - 1.0 mm, reconstructed using a bone algorithm, as these injuries may not be seen using thicker slices or a smoother (e.g., soft tissue)

reconstruction. Complimentary radiographs also provide a more focused and high-resolution overview of the fracture patterns of these small, ossified cartilages. Another challenge when assessing for small cartilage fractures includes differentiating them from normal incomplete cartilage ossifications that vary in timing and pattern. In this case, the thyroid cartilage was not completely and asymmetrically ossified. Cartilaginous soft tissue injuries can easily be missed while stippled cartilage ossifications may mimic fractures. The disadvantage of PMCT is also difficulty visualizing small muscle or pericartilagenous hemorrhages as indirect imaging signs of injury, which were observed during autopsy in this case.

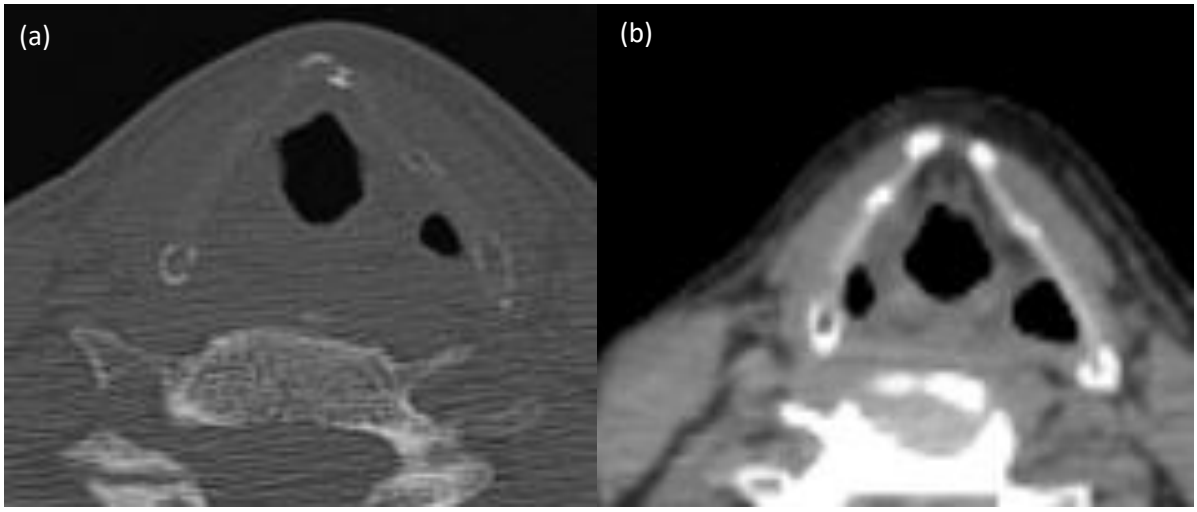

Fig 3: PMCT axial images of the incompletely ossified thyroid cartilage in (a) Bone window: Asymmetrical stippled ossification patterns may be mistaken as fractures and in (b) Soft tissue window: Injuries at the non-ossified segments of the thyroid cartilage are easily missed on PMCT.

Further Reading

1. Jehng YM, Lee FT, Pai YC, Choi WM. Hyoid bone fracture caused by blunt neck trauma. Journal of Acute Medicine. 2012 Sep 1;2(3):83-4.
2. Reed MH. Ossification of the hyoid bone during childhood. Can Assoc Radiol J. 1993 Aug;44(4):273-6. PMID: 8348355.
3. Mupparapu M, Vuppalapati A. Detection of an early ossification of thyroid cartilage in an adolescent on a lateral cephalometric radiograph. Angle Orthod. 2002 Dec;72(6):576-8. doi: 10.1043/0003-3219(2002)072<0576:DOAEOO>2.0.CO;2. PMID: 12518951.

Contributors: Yi-Li Grace Wong, Kethery Haber, and Natalie L. Adolphi

NMDID 132080

Severe cerebral edema in a case of iatrogenic viscus perforation and septic shock

Case description: A 20-year-old female, suspected of ectopic pregnancy, underwent diagnostic laparoscopy, which was converted to minimal laparotomy with salpingostomy. Pathology confirmed a tubal pregnancy with associated hemorrhage. Two days after surgery, she developed intractable nausea and vomiting coffee ground emesis. She was septic, in shock, and suspected of gastrointestinal hemorrhage given a distended, tender, rigid abdomen with foul smelling discharge from her umbilical port wound. She underwent emergency laparotomy and was found to have extensive peritonitis and a 1 cm perforation of the small intestine and an edematous right fallopian tube with oozing, resulting in total salpingectomy. Post-surgery, she required inotropes and mechanical ventilation but suffered neurologic decline with massive cerebral edema observed on antemortem imaging. Clinical tests were consistent with brain death and her family requested withdrawal of care.

Imaging Findings: A midline abdominal scar was seen in keeping with surgery. There were ascites, generalized mesenteric and abdominal fat stranding, either edema or inflammation, and high intraluminal densities in her small and large bowel, suggestive of blood product correlating with her history. Bilateral lungs were hepatized and consolidated with bilateral pleural and pericardial effusions. There was generalized subcutaneous fat stranding, i.e., anasarca, representing sepsis, multiorgan failure, and/or fluid overload. The brain was severely edematous with loss of grey/white matter differentiation, generalized hypoattenuation, sulci effacement, and tonsillar herniation.

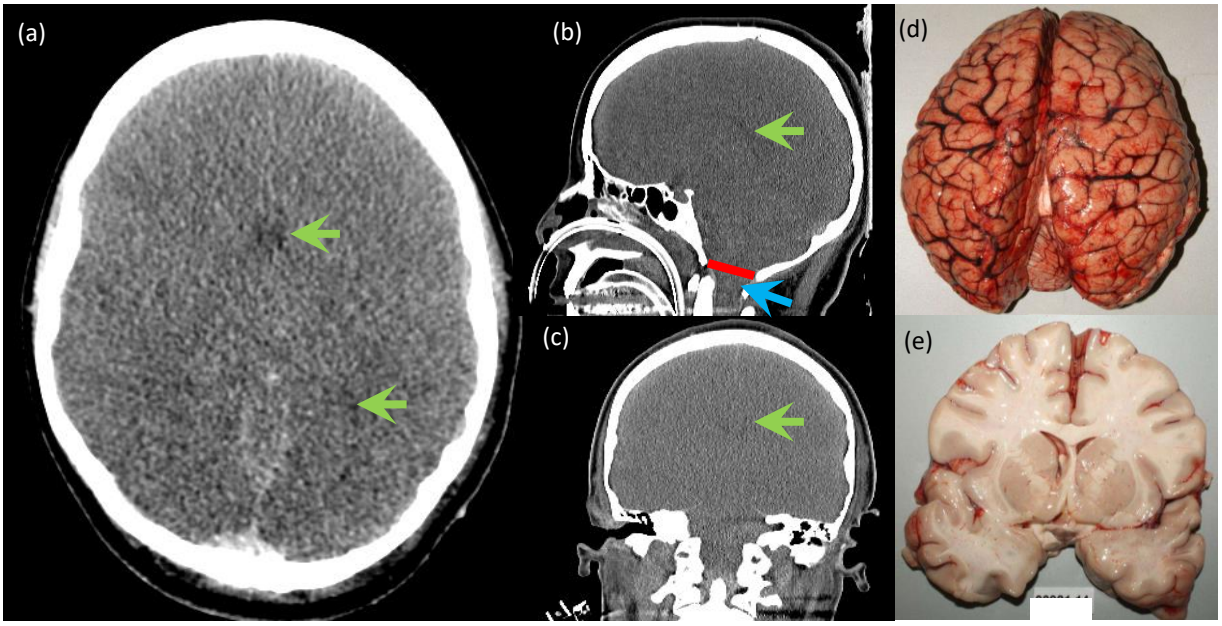

Fig 1: PMCT Brain in (a) Axial, (b) Sagittal and (c) Coronal views demonstrated loss of grey white matter differentiation, generalized hypoattenuation of brain parenchyma, effacement of sulci and slit like ventricles (green arrows). There was also tonsillar herniation (blue arrow) inferior to the foramen magnum (red line), which indicated severe cerebral edema (d & e). Autopsy images of the brain also showed flattening of sulci and effaced ventricles.

Pathology Findings: Autopsy revealed an open midline laparotomy incision with a right salpingectomy and an incompletely closed small intestinal defect with surrounding purulent mucosal exudate. There was widespread peritonitis. The brain was edematous with flattening of sulci and ventricles. Histology revealed acute damage to the lungs, liver, kidneys, and heart. Abdominal cultures during the emergency exploratory laparotomy revealed Clostridium and mixed bacteria. Postmortem blood culture revealed no growth. Postmortem culture from the abdominal cavity was positive for mixed

flora. The cause of death was peritonitis following bowel perforation during diagnostic laparoscopy for the ectopic pregnancy, and the manner of death was classified as natural.

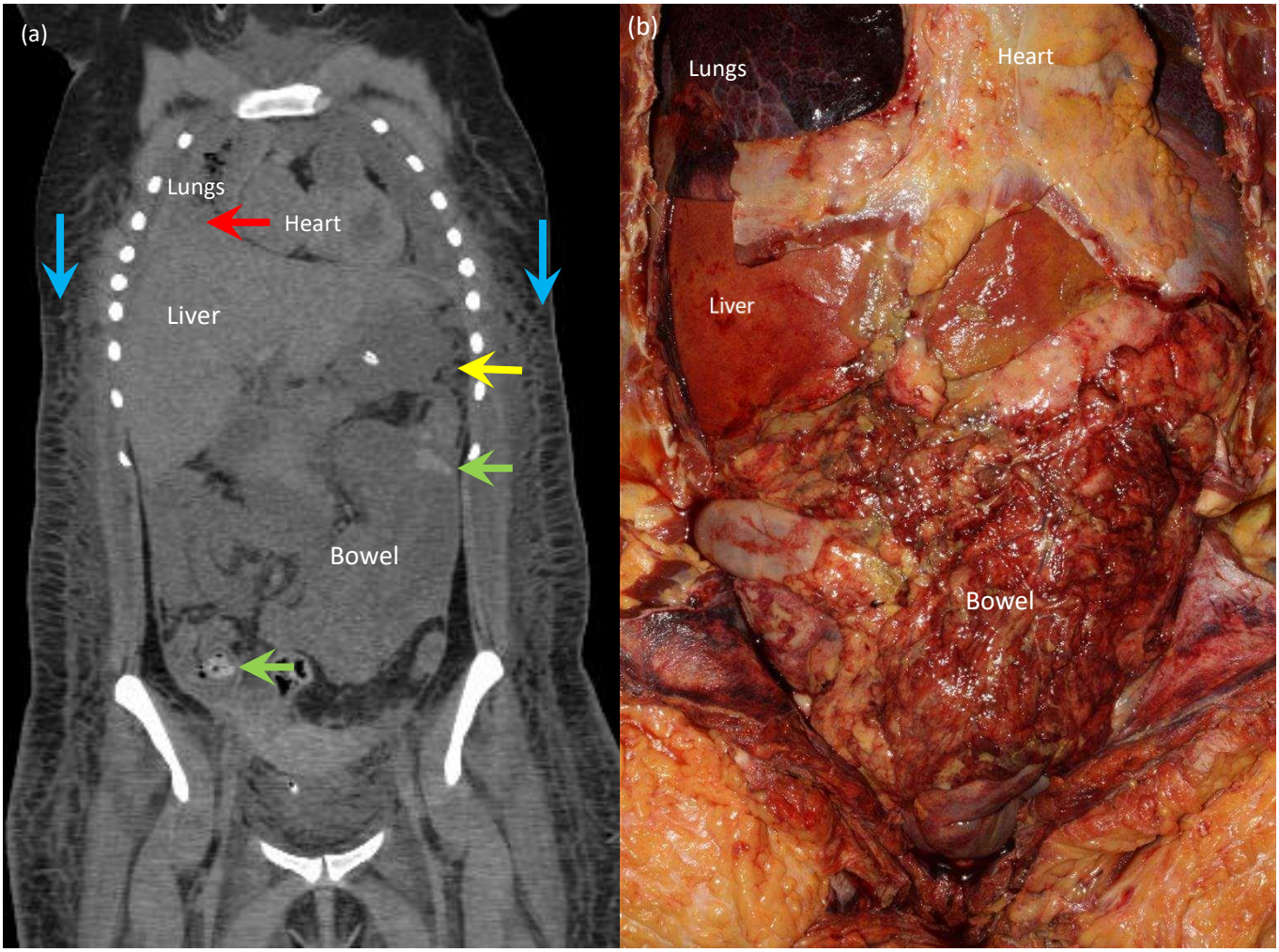

Fig 2: (a) PMCT Thorax and Abdomen (Coronal view) showed consolidated lungs (red arrow), mesenteric fat stranding (yellow arrow), bowel intraluminal high densities suspicious of blood (green arrows) and generalized subcutaneous fat stranding (blue arrows) representing anasarca. (b) Autopsy images showed extensive yellow tan, fibrinous adhesions of the peritoneal cavity, on rectum, bowel loops, spleen, diaphragmatic surfaces of bilateral lungs and bilateral subdiaphragmatic recesses.

Comments: Mild postmortem cerebral edema is a common, normal postmortem CT finding, characterized by loss of grey/ white matter differentiation and relative hypoattenuation of the brain. This is a result of hypoxia due to reduced circulation and oxygenation during agony [1]. Studies have also confirmed that there is an increase in brain volume due to postmortem edema[2]. Differentiation from antemortem cerebral edema can thus be difficult. However, in this case, PMCT was performed 16 hours after death, and the severe degree of cerebral edema with evidence of tonsillar herniation, effaced sulci, and ventricles were not expected of a "normal" postmortem cerebral edema. The history and clinical presentation of septic shock were highly suggestive that these findings were due to antemortem pathology, and PMCT findings were subsequently confirmed during autopsy examination.

Further reading and references:

1. Zech WD, Hottinger AL, Schwendener N, Schuster F, Persson A, Warntjes MJ, Jackowski C. Post-mortem 1.5 T MR quantification of regular anatomical brain structures. International journal of legal medicine. 2016 Jul;130(4):1071-80.

2. Boon BDC, Pouwels PJW, Jonkman LE, Keijzer MJ, Preziosa P, van de Berg WDJ, Geurts JJG, Scheltens P, Barkhof F, Rozemuller AJM, Bouwman FH, Steenwijk MD. Can post-mortem MRI be used as a proxy for in vivo? A case study. Brain Commun. 2019 Oct 24;1(1):fcz030. doi: 10.1093/braincomms/fcz030. PMID: 32954270; PMCID: PMC7425311.

Contributors: Grace Yi-Li Wong, Kethery Haber, Roberto Maselli, and Natalie L. Adolphi

NMDID 124687

Retained projectile: Old or new?

Case description: A 60-year old male was found unresponsive, upside down, with his seatbelt fastened, in his overturned vehicle. He was already deceased upon extraction.

Imaging Findings: PMCT showed a left nasal bone and manubrial fracture. There were healed right posterior rib fractures. There was also a metallic projectile embedded in the right sacral ala, but no surrounding acute fractures of the pelvis bone, surrounding pelvic muscle, or internal organ nor hollow viscus injuries, nor obvious entry or exit sites along the thoracic, abdomen and pelvis subcutaneous tissue.

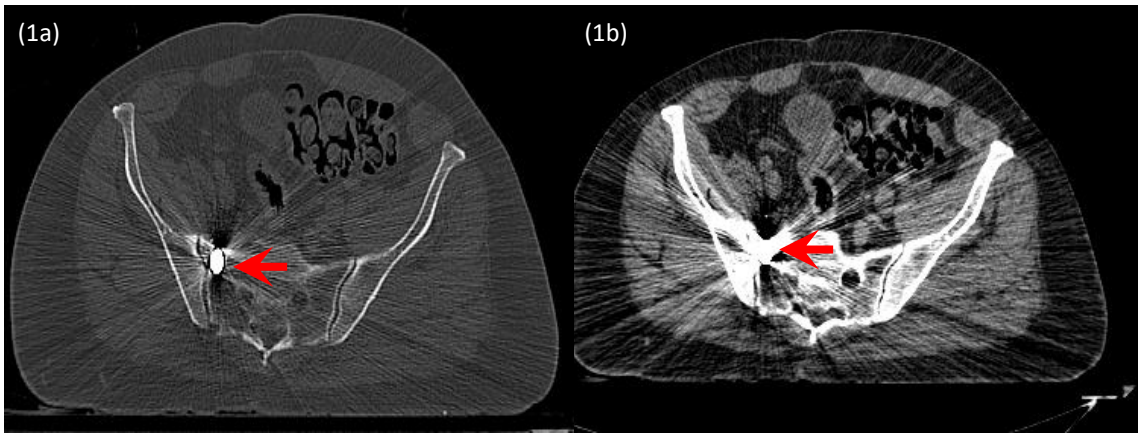

Fig 1: PMCT (axial images) of (a) Bone window and (b) Soft tissue window showing the retained projectile embedded within the right sacral ala. Metallic content caused streak artifact, causing image degradation. There was, however, no surrounding soft tissue hematoma, edema or enlargement, no obvious trajectory, cavitations, or entry or exit sites, indicating an old gunshot injury.

Pathology Findings: Autopsy examination revealed an obese man with relatively minor blunt injuries to his head, torso, and extremities, with linear bruises of the neck and across the thighs, consistent with seatbelt injuries. There was a skin tear of the scalp with underlying bleeding in the deep tissues of the scalp. There were scattered scrapes and bruises of the arms, legs, and torso, but no fresh gunshot wounds**.** Femoral blood ethanol was 0.288g/100mL indicative of acute ethanol toxicity. There was evidence of background chronic ethanol abuse with chronic active hepatitis, mild hepatic steatosis, atherosclerotic, hypertensive cardiovascular disease, obesity, and bilateral hydroceles. A remote retained silver projectile was recovered from the right pelvis. There was evidence of previous laparotomy and repair. The cause of death was mechanical asphyxia, with acute ethanol toxicity and blunt trauma as contributing conditions. The manner of death was classified accident.

Comments: PMCT is the primary imaging modality used in gunshot fatalities to identify the location of projectiles, patterns of associated bone fractures, and soft tissue injuries, which may indicate mechanism of death, bullet trajectories, and support manner of death. Incidental findings of projectiles without complete background histories may raise suspicion of foul play contributing to death. Hence, the other less described role of PMCT is to help differentiate if the projectile is from a recent or old gunshot injury, as illustrated in this case. In addition to that, if it is indeed an old gunshot injury, it is also pertinent to actively look for PMCT signs of chronic complications of prior gunshot injury, e.g., intestinal obstructions, urosepsis, spinal deformities, and decubitus ulcers. These appear like “natural” disease on imaging. However, if the old gunshot wound was inflicted by another, careful review of the previous gunshot history will be required, as chronic sequelae of remote injuries may result in classification of manner of deaths as “delayed homicide.”

Further reading:

1. Gitto L, Arunkumar P, Segovia A, Filkins JA, Formica MK, Serinelli S. Anatomical distribution and autopsy features of gunshot injuries to support the manner of death. J Forensic Leg Med. 2021 Apr;79:102135. doi: 10.1016/j.jflm.2021.102135. Epub 2021 Feb 23. PMID: 33662899.
2. Sodagari F, Katz DS, Menias CO, Moshiri M, Pellerito JS, Mustafa A, Revzin MV. Imaging Evaluation of Abdominopelvic Gunshot Trauma. Radiographics. 2020 Oct;40(6):1766-1788. doi: 10.1148/rg.2020200018. PMID: 33001782.
3. Lin P, Gill JR. Delayed homicides and the proximate cause. Am J Forensic Med Pathol. 2009 Dec;30(4):354-7. doi: 10.1097/PAF.0b013e3181c1582a. PMID: 19901806.

Contributors: Yi-Li Grace Wong, Kethery Haber, Roberto Maselli, and Natalie L. Adolphi

NMDID 133540

Lobar pneumonia vs. postmortem hypostasis; pneumoperitoneum vs. decomposition changes

Case description: A 59-year-old female, with a history of osteoarthritis, fibromyalgia, and prescription medication overuse, was found slumped over and deceased in the recliner where she usually slept. She was last seen alive the night before and had vocalized no new complaints. Emergency medical services were alerted but did not attempt resuscitation.

Imaging Findings: Preserved lung volumes with generalized patchy ground glass changes and bilateral dense lower lobe consolidations worst at gravity dependent areas with interlobular septal thickening were observed, as well as mild bronchiectasis bilaterally, worst along the left lower lobe secondary and tertiary bronchi with peribronchial thickening. A few sub-centimeter mediastinal lymph nodes were visualized. Other natural diseases found included coronary artery wall calcification, cardiomegaly, uterine leiomyomas, mild hepatomegaly, and calcified diverticulosis. In the abdomen, there was some free air anterior to the liver and mild dilatation of the esophagus above the gastroesophageal junction. Right humerus orthopedic hardware and cholecystectomy clips were also seen.

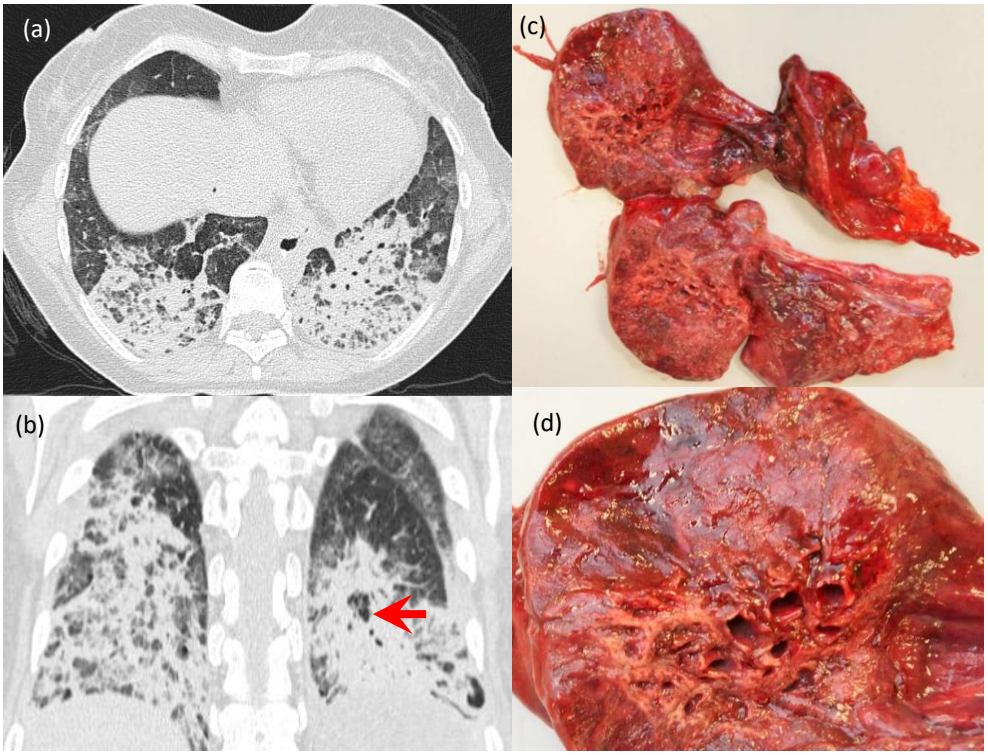

Fig 1: PMCT Thorax (Lung windows) in (a) Axial and (b) Coronal views demonstrating bilateral lower lobe asymmetric dense consolidations and interlobular septal thickening with left lower lobe bronchiectasis with peribronchial thickening (red arrow) (c) Gross macroscopic examination of the lungs shows autolysis and patchy consolidations at bilateral lower lobes with (d) Focal bronchiectasis of left lower lobe.

Pathology Findings: Bilateral lower lobe pneumonia was observed with combined lung weights of 1090g. Patchy consolidations with focal bronchiectasis were visualized. There were also bilateral pleural adhesions. Microscopic examination revealed extensive infiltration of the airspaces of the lower lobes of the lungs by neutrophils with some destruction of underlying lung architecture (pneumonia). The esophagus, stomach, small intestine, and colon were unremarkable with appropriate caliber without interruption of luminal continuity. Other natural disease included atherosclerotic and hypertensive cardiovascular disease with 30% stenosis of mid left anterior descending coronary artery, arteriolar nephrosclerosis, uterine fibroid (4.5 cm), endometrial polyp, post remote appendectomy, and cholecystectomy.

Toxicology studies revealed morphine, metabolites of hydrocodone and oxycodone (hydromorphone and oxymorphone, respectively), metabolite of alprazolam, and the antidepressant sertraline (Zoloft) and its metabolite. None of the individual substances were present in particularly elevated levels and, although their side effects would be additive, are unlikely to have caused significant, life-threatening impairment in a chronic user of opiate and benzodiazepine sedatives. As such, these results are considered non-contributory to death. The final cause of death was classified as pneumonia, and the manner of death classified as natural.

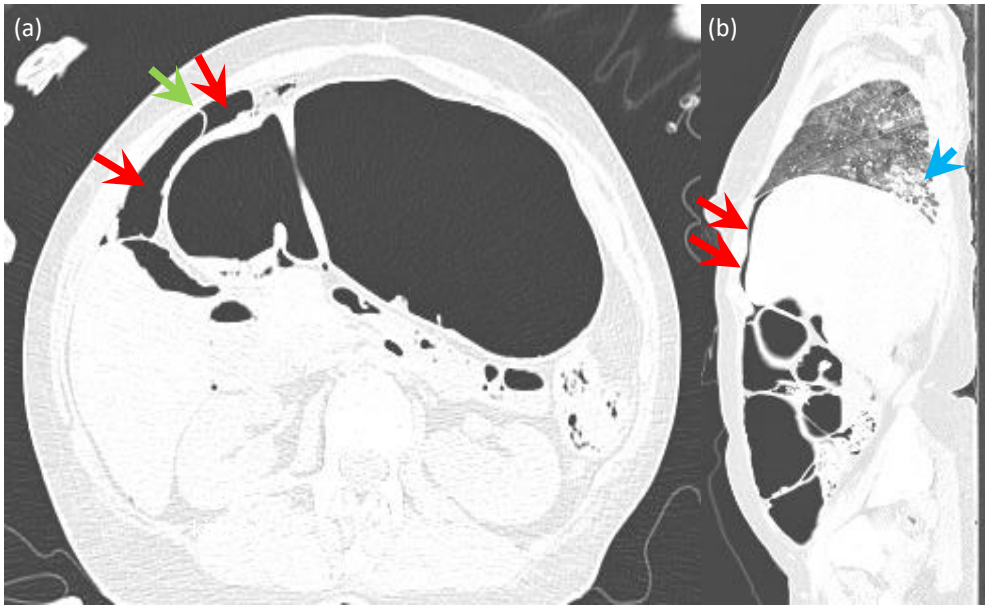

Fig 2: (a) PMCT abdomen in (a) Axial and (b) Sagittal views demonstrated intraperitoneal air anterior to the liver and stomach (red arrow) with thin septation (green arrow). The right lower lobe consolidation is also seen on sagittal view (blue arrow).

Comments:

Bilateral air space opacities in gravity dependent locations can be confusing in postmortem cases when trying to differentiate antemortem community acquired bronchopneumonia or aspiration pneumonias from postmortem livor and fluid accumulation. Aspiration pneumonias tend to occur when decedents have a history of being in a supine position (e.g., bed bound) during the event as either posterior upper lobes, superior or basal lower lobes[1]. There was also insufficient history to gauge if the decedent had been septic or had lower respiratory tract infections prior to her death. In this cause, autopsy had the advantage of discovering bilateral pleural adhesions, significantly increased lung weights, and airspace infiltrations by neutrophils suggestive of double pneumonia.

Intraperitoneal air in postmortem cases can be confusing on PMCT with the dilemma of deciding between antemortem viscus perforation, iatrogenic causes, or normal post mortem change with overlapping imaging features. Hussein et al reported that estimated gas volumes in deaths associated with intestinal perforation were 3-4 times greater than in the control group with sudden release of trapped gas from previously distended intestines, before autolysis effect of putrefactive bacteria and decomposition gas. Intraperitoneal gas due to decomposition changes presented with RAI values of more than 50 in their case samples. However, they acknowledged that small collections of intraperitoneal gas may still pose a diagnostic challenge for differentiation of these entities, and, to date, no single postmortem imaging modality or combinations are reliable imaging tools for determination of its nature. In this case, autopsy confirmed that there was no hollow viscus perforation. The dates of cholecystectomy and appendicectomy were not available and would have been suspected as a cause for minimal free air if recently performed. As for postmortem changes, putrefaction usually enters all vascular structures and slowly accumulates in potential anatomic spaces in advanced stages. In this case, there was no typical putrefactive distribution of air along the bowel walls, liver, or heart, where putrefaction is first seen. The exact

post mortem interval is unknown, but the interval between the discovery of the body and PMCT was approximately 23 hours.

Further Reading & References:

1. Mandell LA, Niederman MS. Aspiration pneumonia. New England Journal of Medicine. 2019 Feb 14;380(7):651-63.
2. Hussein MN, Heinemann A, Shokry DA, Elgebely M, Pueschel K, Hassan FM. Postmortem computed tomography differentiation between intraperitoneal decomposition gas and pneumoperitoneum. Int J Legal Med. 2022 Jan;136(1):229-235. doi: 10.1007/s00414-021-02732-7. Epub 2021 Oct 27. PMID: 34708283.
3. Egger C, Vaucher P, Doenz F, Palmiere C, Mangin P, Grabherr S. Development and validation of a postmortem radiological alteration index: the RA-Index. Int J Legal Med. 2012 Jul;126(4):559-66. doi: 10.1007/s00414-012-0686-6. Epub 2012 Mar 9. PMID: 22402872.

Contributors: Yi-Li Grace Wong, Kethery Haber, Roberto Maselli, and Natalie L. Adolphi

NMDID 134377

Unstable Type III odontoid fracture

Case description: A 60-year-old male with past medical history of traumatic brain injury, seizures, PTSD, and chronic alcohol abuse fell from a top bunk bed and was found unresponsive. Several days prior to his death, he had reportedly fallen from a roof, and broken his arm and some ribs. In the emergency room, he was diagnosed with hypoxic brain injury. He passed away that same evening.

Imaging Findings: PMCT revealed a posteriorly displaced odontoid fracture through the lateral masses of the C2 vertebra, encroaching into the upper cervical canal with high suspicion of cervical cord impingement. No additional bone fragments were seen in the spinal canal. Other than non-specific generalized cerebral edema, no intracranial hemorrhage or segmental infarcts were detected. There were also several rib and sternal fractures. There were background emphysematous changes with sub-segmental lower lobe collapse, small left pleural effusion, and upper lobe ground glass opacities, which could be due to neurogenic pulmonary edema. There was an old healed left humeral fracture but no acute extremity fractures. Toxicology testing of the blood detected no ethanol, illicit drugs, or commonly abused prescription or over-the-counter drugs.

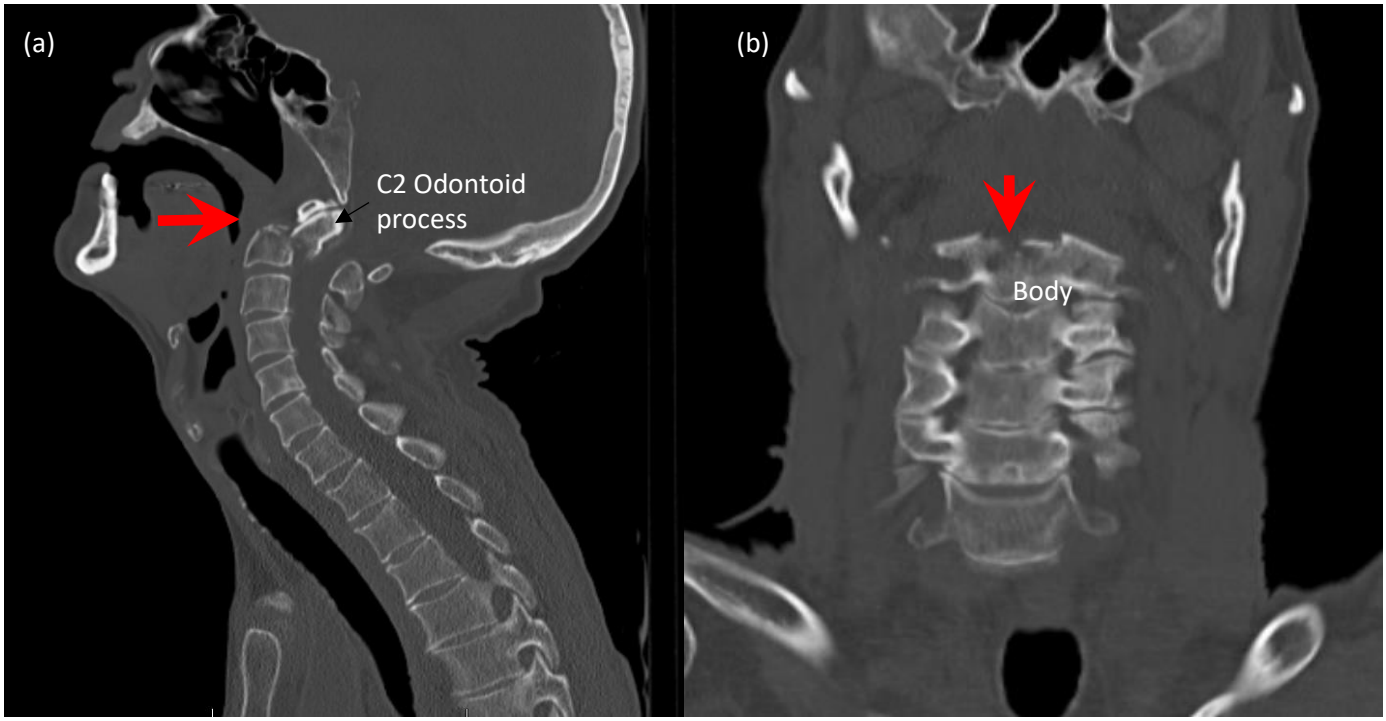

PMCT images in (a) sagittal and (b) coronal bone windows demonstrated a fracture (red arrows) at the base of the C2 vertebral odontoid process extending into the body. The fracture was unstable due to the significant posterior retropulsion into the spinal canal, likely causing cervical cord compression.

Pathology Findings: Externally, there were bruises on the nose, chest, entire left arm, left knee, and lower leg. A Type III odontoid fracture with posterior displacement causing spinal canal narrowing and surrounding hemorrhage was confirmed. Other fractures included a nasal fracture, non-displaced bilateral anterolateral and lateral rib fractures, and a manubrial fracture. No head or other spinal injury was detected. The cause of death was blunt neck trauma.

Comments: Odontoid fractures are caused either by hyperextension or hyperflexion injuries. They are the most common cervical spine fractures in the elderly, commonly missed, and have high mortality rates with delayed diagnosis. In this case, the spinal cord injury would have been immediately incapacitating and would have interfered with respiration leading to hypoxia and death. The Anderson and D'Alonzo classification divides odontoid fractures into three subtypes: (i) Type 1: Avulsion at tip of odontoid (due to alar and apical ligament avulsion); (ii) Type II: Odontoid base fracture; (iii) Type III: Base of odontoid fracture extending into C2 body, typically involving the superior C2 facet joints, and used as a differentiator

between type II and III fractures. One disadvantage of PMCT compared to PMMR is spinal cord and nerve root assessment, but it is still possible to raise the suspicion of cervical cord injury based on the direction and degree of bony displacement into the spinal canal and whether there is presence of comminuted bone fragments within the spinal canal where the cord lies.

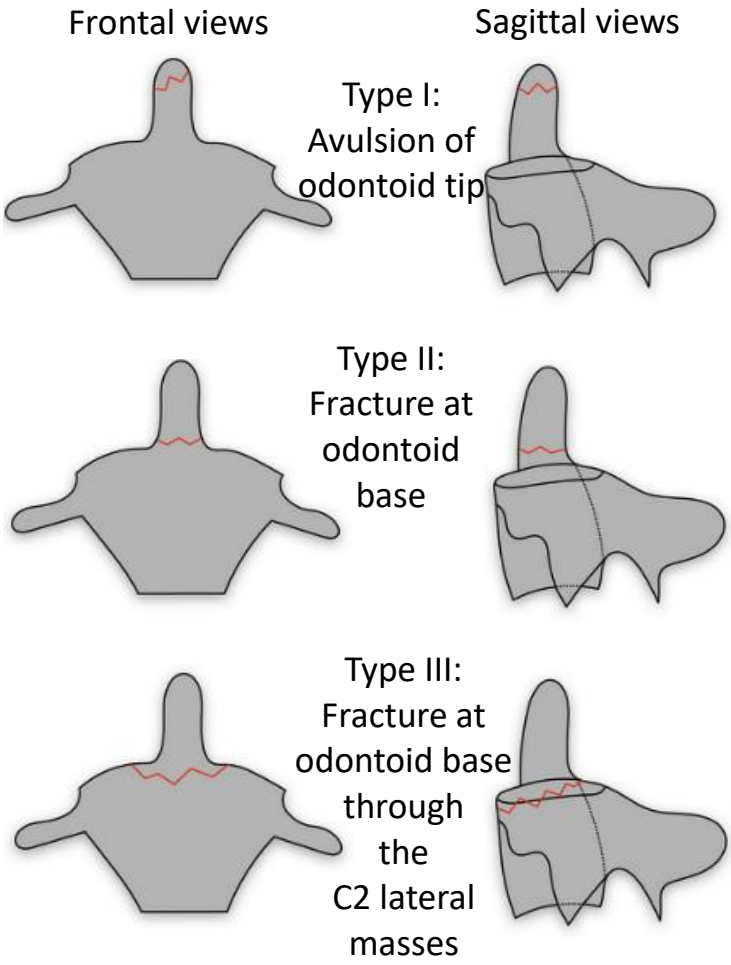

Anderson and D'Alonzo Classification of C2 Odontoid fractures

Image Reference: https://radiopaedia.org/articles/anderson-and-dalonzo-classification-of-odontoid-process-fracture?lang=us

Further Reading:

1. Huybregts JG, Jacobs WC, Vleggeert-Lankamp CL. The optimal treatment of type II and III odontoid fractures in the elderly: a systematic review. Eur Spine J. 2013 Jan;22(1):1-13. doi: 10.1007/s00586-012-2452-3. Epub 2012 Sep 2. PMID: 22941218; PMCID: PMC3540294.
2. Iyer S, Hurlbert RJ, Albert TJ. Management of Odontoid Fractures in the Elderly: A Review of the Literature and an Evidence-Based Treatment Algorithm. Neurosurgery. 2018 Apr 1;82(4):419-430. doi: 10.1093/neuros/nyx546. PMID: 29165688.

Contributors: Yi-Li Grace Wong, Kethery Haber, Roberto Maselli, and Natalie L. Adolphi

NMDID 146971

Brain tumors: Meningiomas

Case description: A 74-year old malnourished male, with a history of dementia, anemia, episodes of bradycardia, and hypertensive and atherosclerotic cardiovascular disease, was found unresponsive by his wife. The cause of death was due to sepsis with polymicrobial bacteremia secondary to urinary tract infection, bronchopneumonia, and multiple decubitus ulcers of the extremities and trunk. The manner of death was undetermined. He also had a history of meningioma that was surgically removed 8 years prior but subsequently recurred, which is the focus of this study guide.

Imaging Findings: PMCT Brain findings demonstrated (1) Evidence of left frontotemporal and sphenoid wing surgery with adjacent white matter hypoattenuation and adjacent ex-vacuo dilatation of the left ventricle temporal horn, representing encephalomalacic changes and edema; (2) A relatively homogeneous, hyperdense mass with epicenter at the left sphenoid wing (size: 2.3 x 1.7 x 3.4 cm – anteroposterior x width x craniocaudal lengths, Mean attenuation value: 40.6 HU) encroaching into the left orbital apex, compressing the left optic nerve and also extending into the left temporal fossa, compressing the left temporal lobe; (3) Left frontal scalp focal soft tissue swelling (size: 0.9 x 3.8 x 5.0 cm – depth x width x craniocaudal length; mean attenuation value of 44 HU) with adjacent bone hyperostosis and remodeling; and (4) Generalized brain atrophy with prominent ventricles, sulci, and CSF spaces.

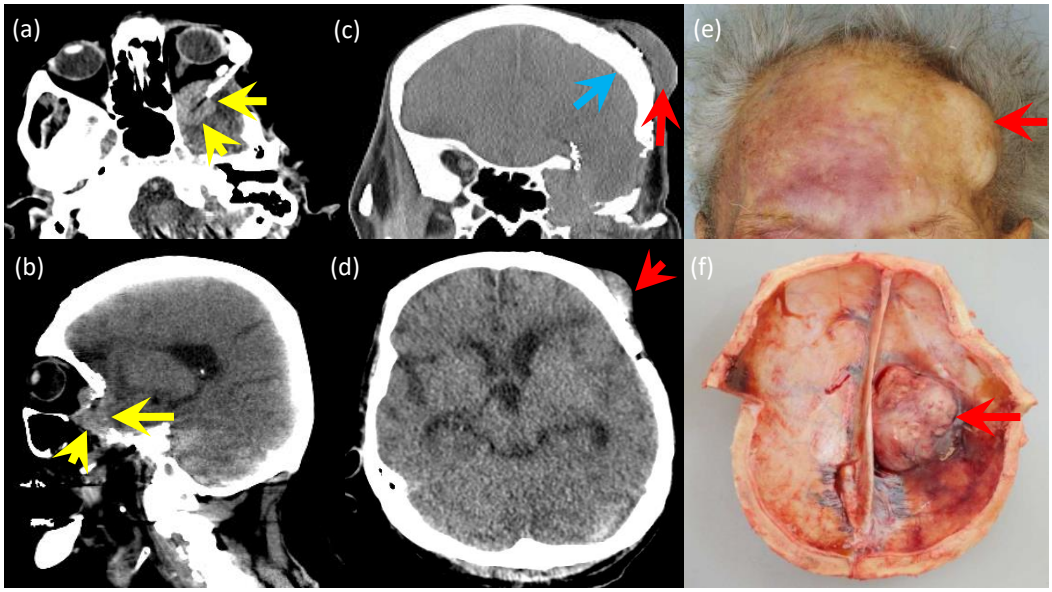

(a & b) PMCT Brain axial & sagittal views demonstrate a hyperdense mass (yellow arrows) at the left sphenoid wing encroaching into the left orbital apex and compressing the left temporal lobe; (c & d) PMCT Brain coronal & axial views show a frontal scalp soft tissue lesion (red arrows) with adjacent calvarial periosteal reaction, thickening and irregularity (blue arrow). The intracranial extraaxial extension of this mass if not well delineated on PMCT due to poor soft tissue contrast; (e) External examination showing the left frontal scalp swelling; (f) Upon dissection, the left frontal mass is seen from the inner calvarium.

Pathology Findings: Neuropathologic diagnoses of the brain were (1) Solid friable neoplasm attached to the left frontal dura mater measuring 2.5 x 4.2 x 4.8 cm. Atypical meningioma with rhabdoid and focal clear cell features involving dura mater and compressing the underlying brain; (2) Microscopic and histopathologic evidence of Lewy Body disease and Alzheimer's disease; and (3) Vascular brain injury with remote cerebellar infarct, atherosclerosis, and arteriolosclerosis.

Comments: Meningiomas are common extra-axial tumors of the meninges that are typically benign. Most tumors demonstrate hyperdense solid attenuation with well-defined margins on non-contrasted PMCTs, as observed with the left sphenoid wing tumor [figures a & b] [1-2]. In clinical contrasted CT or MRI studies, the margins of these tumors are more

easily defined, as they enhance avidly. The intracranial, extra-axial portion of the left frontal [figures c & d] was less clearly delineated due to poor soft tissue contrast between the tumor and compressed frontal brain matter. Differentiation of benign, low grade, and high grade meningiomas is difficult on non-contrast PMCT. There was trans-osseous involvement, i.e., left frontal bone hyperostosis and thickening, but this feature can also be seen in benign meningiomas due to osteoblastic activity associated with rapid growth and has been found to be the only significant CT feature predicting low-grade meningioma[2]. Predictors of high-grade meningioma (better appreciated on contrasted MRI) are large tumor size and volume, heterogeneous enhancement, intratumoral necrosis, ill-defined margins, and dural sinus and brain invasion, as well as higher rate of recurrence[2].

Further Reading & References:

1. Mathew, Rishi Philip & Muthukumar, Kumar & Natesan, Praveen & Karunakaran, Muthukalathi. (2018). Morphological spectrum of intracranial meningiomas on computed tomography (CT) and magnetic resonance imaging (MRI). Panacea Journal of Medical Sciences. 8. 70-78. 10.18231/2348-7682.2018.0017.
2. Salah F, Tabbarah A, ALArab Y N, Asmar K, Tamim H, Makki M, Sibahi A, Hourani R. Can CT and MRI features differentiate benign from malignant meningiomas? Clin Radiol. 2019 Nov;74(11):898.e15-898.e23. doi: 10.1016/j.crad.2019.07.020. Epub 2019 Aug 29. PMID: 31474303.

Contributors: Yi-Li Grace Wong, Kethery Haber, Roberto Maselli, and Natalie L. Adolphi

NMDID 169628

Distended urinary bladder in accidental fatal drug overdose

Case description: A 53-year-old female was found dead in bed. She had a prior history of feeling weak. She had a past medical history of congestive heart failure, chronic pain syndrome, depression, and prescription medication misuse.

Imaging Findings: No acute traumatic injuries were visualized. Natural disease findings included coronary artery and atherosclerotic arterial wall calcifications. The urinary bladder was grossly distended with homogeneous low-density fluid (mean attenuation value 5.1 HU, i.e., non-complicated). In this case, no prominent pill-shaped high densities were visualized in the stomach or bowel on PMCT.

Pathology Findings: Corresponding to PMCT findings, 830 ml of clear urine was collected. Toxic effects of tramadol and methadone including cerebral edema and pills in her stomach were found. Postmortem femoral blood toxicology demonstrated toxic concentrations of tramadol and methadone as well as their metabolites. Hypertensive and atherosclerotic cardiovascular disease was confirmed in autopsy with additional findings of gastritis and thyroid nodules.

Comments: The theory for the cause of urinary bladder distension includes opioid influence on the urinary bladder sphincter causing retention of urine. However, false positives (e.g., also found in intracranial bleed, pneumonia, hypothermia) and false negatives (e.g., antemortem seizure-induced evacuation or postmortem evacuation during transfer) also need to be considered during imaging interpretation. In addition to a suggestive history, the PMCTs should be interpreted holistically with (a) Combination of other suspicious findings such as cerebral edema, pulmonary edema with lack of pleural effusions and (b) exclusion of other co-morbidities or injuries which may contribute to death. The type and quantity of intoxicant obviously cannot be determined with PMCT and still requires toxicology investigations.

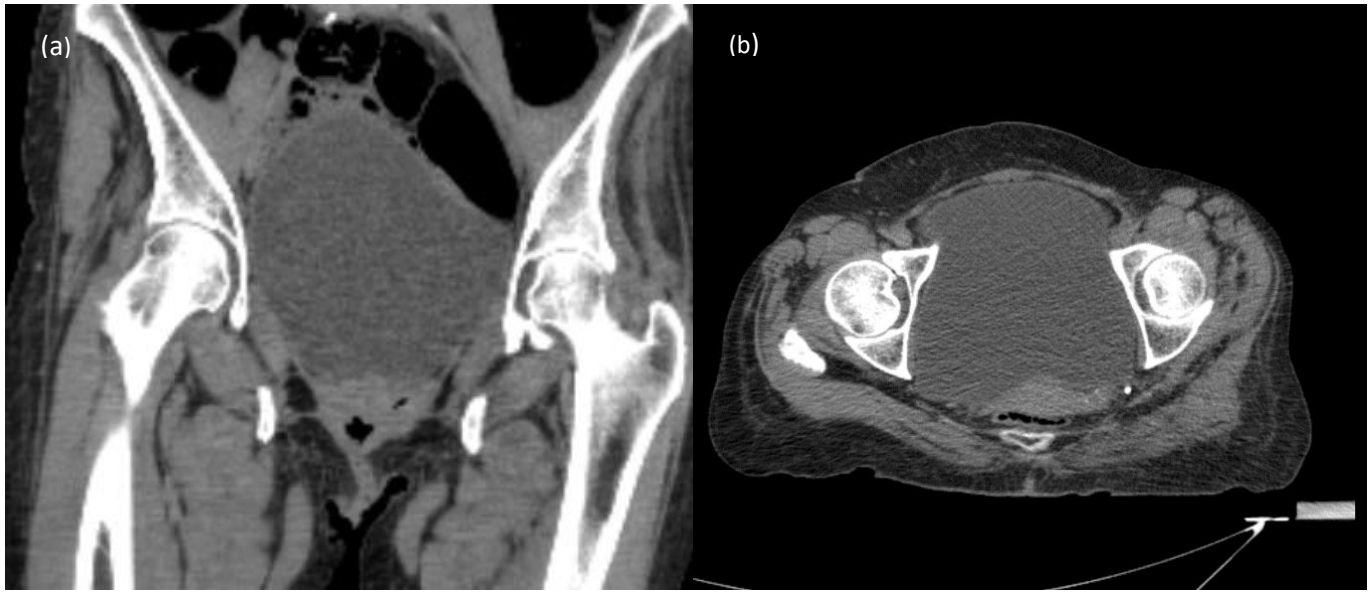

PMCT images in (a) coronal and (b) axial soft tissue windows demonstrating a fully distended urinary bladder.

Further Reading:

1. Rohner C, Franckenberg S, Schwendener N, Oestreich A, Kraemer T, Thali MJ, Hatch GM, Ruder TD. New evidence for old lore--urinary bladder distension on post-mortem computed tomography is related to intoxication. Forensic Sci Int. 2013 Feb 10;225(1-3):48-52. doi: 10.1016/j.forsciint.2012.03.029. Epub 2012 May 5. PMID: 22565114.
2. Lahaye MJ, van Kan R, Haest II, Bakers FC, Kroll J, Jacobi-Postma L, Hofman PA. 2.9. CT imaging as a valuable additional tool to establish drug abuse as cause of death. Journal of Forensic Radiology and Imaging. 2014 Apr 1;2(2):101.

Contributors: Yi-Li Grace Wong, Kethery Haber, Roberto Maselli, and Natalie L. Adolphi

NMDID 148595

Incidental findings of a large retroperitoneal mass in a case of hypothermia

Case description: A 72-year-old male with a history of hypertension and alcohol consumption was heard moaning outside his house in the early morning. The temperature that morning had been 7 ^{0}C. He was found with trash around him with contusions on his forehead, wrist, and chest wall and a scraped knuckle.

Imaging Findings: There were bilateral, remote rib fractures without evidence of acute injury. He had evidence of multiple natural comorbidities with PMCT findings of cerebral atrophy, cardiomegaly with coronary artery calcifications, an aortic valve replacement, a liver cyst, an enlarged prostate, and renal atrophy. Incidentally, a large retroperitoneal mass was also found to be encasing the abdominal aorta

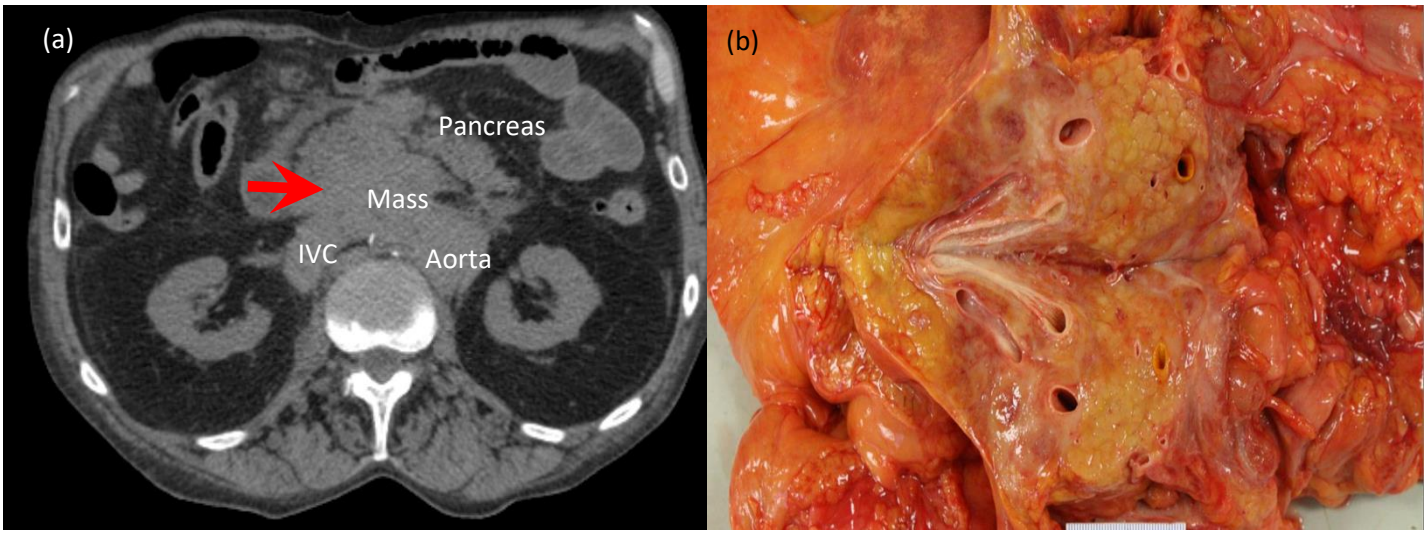

(a) PMCT: Large retroperitoneal mass (red arrow) with no clear fat plane with the inferior vena cava, and abdominal aorta. The mass also encases and displaces the pancreas anteriorly; (b) Autopsy: A large infiltrative retroperitoneal mass was seen encasing the pancreas and infiltrating mesenteric fat.

Pathology Findings: There were contusions and abrasions of the head, trunk, and extremities and remote rib fractures consistent with accidental fall on ice and the failure to get up, resulting in him remaining outdoors and exposed to the cold. There were signs of hypothermia such as Wischnewsky ulcers in the stomach and pink livor mortis suggestive of hypothermia as the cause of death. Corresponding to the mass seen on PMCT, a 20 cm, firm, tan mass was found encasing the common iliac vessels, abdominal aorta, and inferior vena cava, infiltrating the mesenteric roots, left para-adrenal tissue, and soft tissue surrounding the body of the pancreas. Cervical and mediastinal adenopathy were also apparent, measuring up to 5 cm. On microscopic examination, abnormal lymphocyte proliferation infiltrated the peripancreatic and intrapancreatic tissue. The final diagnosis was malignant lymphoma (low grade follicular variant). Other natural findings (hypertensive and atherosclerotic aortic and cardiovascular disease, coronary artery stenosis, cerebral atrophy with intracranial arterial atheromas, solitary segment VIII biliary cyst in the background of hepatic steatosis, and benign prostatic hyperplasia) corresponded to PMCT findings.

Comments: The origins of large intraabdominal or retroperitoneal masses can be inferred on cross sectional imaging by evaluating morphology of the mass, directions and patterns of mass effect, and infiltration. More often than not it is difficult to ascertain the origin of masses that have have no clear fat planes with surrounding organs and vascular systems, more so without the aid of intravenous contrast, which will help characterize the enhancement pattern of these lesions and accentuate the margins of the tumors. In addition to detecting the mass, PMCT was also valuable as a screening tool for other natural diseases present in the decedent. It is important to note PMCT limitations in establishing cause of death for certain natural disease such as acute myocardial infarction, pulmonary embolism and thromboembolic disease, as well as non-natural causes such as burns, asphyxiation, intoxication, and cervical cord injuries.

On imaging features of hypothermia, Agjayev et al. proposed that back muscles may show signs of hemorrhage on PMMR in hypothermic deaths. Other non-specific and variable signs of hypothermia that may be seen during autopsy include Wischnewsky (hemorrhagic gastric spots), frost erythema, and blood extravasation and loss of muscle striations on microscopy and WPA staining, all of which are not visualized on both PMCT and PMMR.

References:

1. Aghayev E, Thali MJ, Jackowski C, Sonnenschein M, Dirnhofer R, Yen K. MRI detects hemorrhages in the muscles of the back in hypothermia. Forensic Sci Int. 2008 Apr 7;176(2-3):183-6. doi: 10.1016/j.forsciint.2007.08.008. Epub 2008 Feb 4. PMID: 18249515.
2. Kasahara S, Makino Y, Hayakawa M, Yajima D, Ito H, Iwase H. Diagnosable and non-diagnosable causes of death by postmortem computed tomography: a review of 339 forensic cases. Leg Med (Tokyo). 2012 Sep;14(5):239-45. doi: 10.1016/j.legalmed.2012.03.007. Epub 2012 Apr 28. PMID: 22542337.

Contributors: Yi-Li Grace Wong, Kethery Haber, Roberto Maselli, and Natalie L. Adolphi

NMDID 149786

Multiple gunshot wounds with no retained projectiles

Case description: A 28-year-old male was shot multiple times by assailant(s) outside his home and was already deceased when paramedics and law enforcement arrived.

Imaging Findings: Left scapula, left posterolateral 3rd and 4th rib fractures. Some of the left 3rd and 4th rib comminuted fracture fragments were angled internally towards the thoracic cavity indicating that the direction of injury was posterior to anterior. A right medial clavicle fracture (posterior margin) was also visualized. There was emphysema surrounding the left scapula extending to neck subcutaneous tissue. Subcutaneous emphysema was also seen at the right anterior chest wall and bilateral posterior paraspinal regions. An air tract with overlying skin defect was seen at the right anterior chest wall and a small skin defect was seen at the right anterior lower thoracic-upper abdominal junction. No retained metallic projectile fragments were seen in this study. Bilateral hemothoraces, pneumothoraces, right upper lobe lung lacerations were visualized. A small localized intraperitoneal air pocket and hemoperitoneum was seen anterior to the left liver lobe.

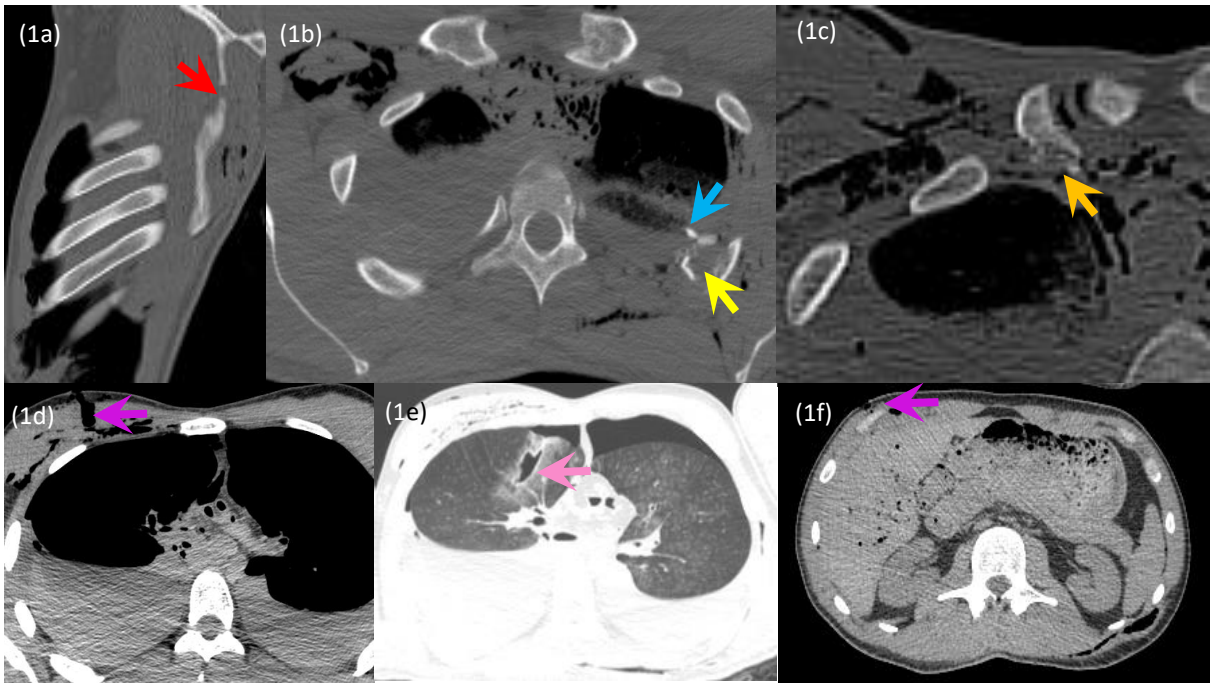

Fig 1: PMCT Thorax(a) Sagittal view (bone window) showed left scapula fracture (red arrow) with overlying deep subcutaneous emphysema. (b) Axial view (bone window) showed left posterolateral 3rd (yellow arrow) and 4th rib fractures. The fractured rib bone fragments were angled internally towards the thoracic cavity (blue arrow) indicating the direction of trauma was posterior to anterior; (c) Right medial clavicular fractures (posterior cortex) (orange arrow); (d) Axial view (soft tissue window) showed bilateral hemothoraces and a right anterior chest wall air tract perpendicular to the skin (purple arrow) corresponding with the exit wound of GSW 1 with surrounding subcutaneous emphysema. (e) Bilateral pneumothoraces and right upper lobe lung pseudocyst representing laceration (pink arrow); (f) Upper abdomen (axial view, soft tissue window) showed a small skin defect at right abdominal wall (purple arrow) corresponding to the exit wound of GSW 2 seen in autopsy (See Fig 2b). More inferiorly a small pocket of air and blood product were seen anterior to the liver (not shown)

Pathology Findings (Fig 2): Five perforating gunshot wounds (GSWs) were revealed, four at the trunk and one at the right arm. Three of the trunk GSW trajectories were back to front and left to right with entry sites at right mid back (GSW 1), right lower back (GSW 2), and left posterior shoulder (GSW 3), respectively and exit sites at the right anterior chest wall for all three cases. The 4th trunk GSW (GSW 4) entry site was also at the right back but perforated skeletal muscle and exited through the right flank with a left to right, slightly upwards trajectory. The 5th GSW (GSW 5) entry site was at right

lateral forearm with right to left, downward trajectory before exiting right distal posterior forearm. No bullets or projectile fragments were recovered in the body. Internal organs that were injured were the left lung upper lobe, esophagus, trachea, anterior mediastinum, and right subclavian artery from GSW 3 and right liver lobe with hemoperitoneum (100 ml) from GSW 2. The range of gunfire was deemed indeterminate due to the presence of thick clothing that obscured soot or stippling. Cause of death was gunshot wounds and the manner of death classified as homicide.

Fig 2: External findings (a) Posterior entry wounds of GSW 1, 2 & 4. GSW 3 entry site at left posterior shoulder is not shown; (b) Right anterior exit wounds of GSW 1, 2 & 3. GSW 4 exit site at the right flank is not shown; (C) Left forearm entry and exit sites of GSW 5.

Comments: PMCT is the first line imaging modality in ballistic deaths[1] given its sensitivity in detecting bone fractures, localizing projectiles, and even deducing some trajectories, especially in gunshot wounds of the cranium (surrounded by bone). It has been reported in a case of abdominal gunshot injury that PMCT combined with PMMR could even show signs of muzzle imprints, i.e., a hyperdense ring noted at the entrance site suggestive of combustion residue, and gas cavities surrounding the bullet [2]. However, as seen in this case, not all of the superficial entry and exit wounds could be appreciated on PMCT. Only two skin defects were seen in the right anterior chest wall and right lower chest and upper abdominal wall junction. A trajectory was assumed to be posterior to anterior, left to right because of clues from patterns of left scapula, left posterior ribs, and right clavicle fractures. However, the entrance sites were not well visualized, and an accurate number of gunshot wounds could not be identified on PMCT alone. Needless to say, PMCT cannot replace external examination and important assessments, e.g., stippling or muzzle imprints, that will help determine range of fire. Most of the gunshot wounds had also managed to evade bone, perforating intercostal muscles, and thoracic and abdominal soft tissue. The internal organ parenchymal injuries were suspected due to indirect signs of penetrating trauma such as bilateral hemothoraces, pneumothoraces, lung lacerations, a free air pocket, and blood product anterior to the liver, but were not directly visualized due to the inherent PMCT disadvantage of low soft tissue contrast.

Further reading and references:

1. Ditkofsky NG, Maresky H, Mathur S. Imaging Ballistic Injuries. Can Assoc Radiol J. 2020 Aug;71(3):335-343. doi: 10.1177/0846537120902107. Epub 2020 Feb 27. PMID: 32103684.
2. Gascho D, Bolliger SA, Thali MJ, Tappero C. Postmortem Computed Tomography and Magnetic Resonance Imaging of an Abdominal Gunshot Wound. Am J Forensic Med Pathol. 2020 Jun;41(2):119-123. doi: 10.1097/PAF.0000000000000547. PMID: 32379075.

Contributors: Yi-Li Grace Wong, Kethery Haber, Roberto Maselli, and Natalie L. Adolphi

NMDID 151841

When postmortem decomposition changes overlap with antemortem pathology on imaging

Case description: A 33-year-old male, with a past history of threatening suicide, was found lying face down next to a tower over 100-feet high. There was an impact site several feet away from him where fragments of bone were lodged several inches into the ground.

Imaging Findings: Generalized decomposition changes were noted on PMCT. There was evidence of skull base, mandible, and multiple rib fractures; a C1 cervical Jefferson fracture and L3/L4 significant listhesis; as well as sacral, pelvic, left humeral and comminuted lower limb fractures bilaterally.

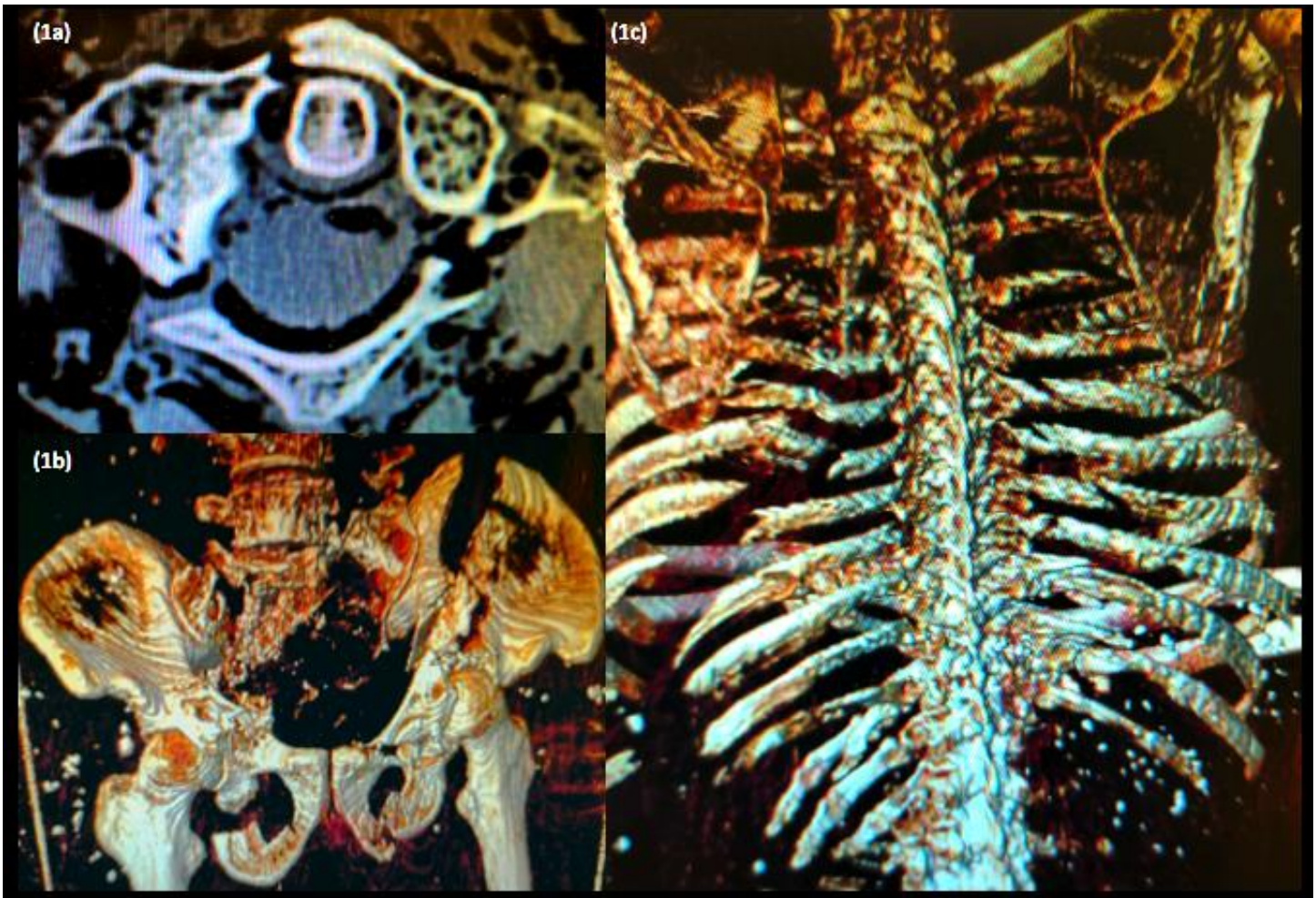

Fig 1: PMCT imaging demonstrating (a) C1 vertebra (axial view, bone window): Burst fracture with anterior and posterior arch involvement; (b) Extensive sacral and Pelvic fractures (3D volume rendering) ; (c) Multiple rib fractures (3D volume rendering)

Pathology Findings: Enhanced blue-green discoloration of the bilateral upper and lower eyelids, and of the anterior neck is present in relation to background postmortem decomposition. Multiple fractures of the head, mandible, neck, ribs, spine (including a C1 non-displaced fracture which was unstable by palpation), pelvis, and extremities. Additionally, the neck muscles were hemorrhagic, the lungs were bruised, the liver was lacerated with mesenteric hemorrhage, and there was bleeding around the aorta and left kidney. Clotted blood was found in the pelvis, likely secondary to the pelvic fractures. The pelvic floor and organs were intact. Microscopy revealed extensive postmortem changes including coagulative necrosis and bacterial colony formation in sections from all organs sampled. All in all, extensive injuries were consistent with jumping from a height and landing on the feet.

Comments: PMCT is an invaluable adjunct to autopsy in providing an overview of multiple bone fractures as demonstrated in this case. The pattern and extent of fractures may point to the mechanism of injury and aid reconstruction of events

that led to death. The disadvantage of non-contrast PMCT in characterizing soft tissue and organ injuries, however, was further accentuated in this case by generalized decomposition changes, i.e. diffuse subcutaneous edema, putrefactive gas within vessels, liver, and heart, and changes in size of the internal organs. These postmortem changes can overlap with and/or obscure antemortem injuries and pathologies. It is therefore essential to be aware of and consider "normal" postmortem changes when interpreting images with moderate to advanced decomposition changes.

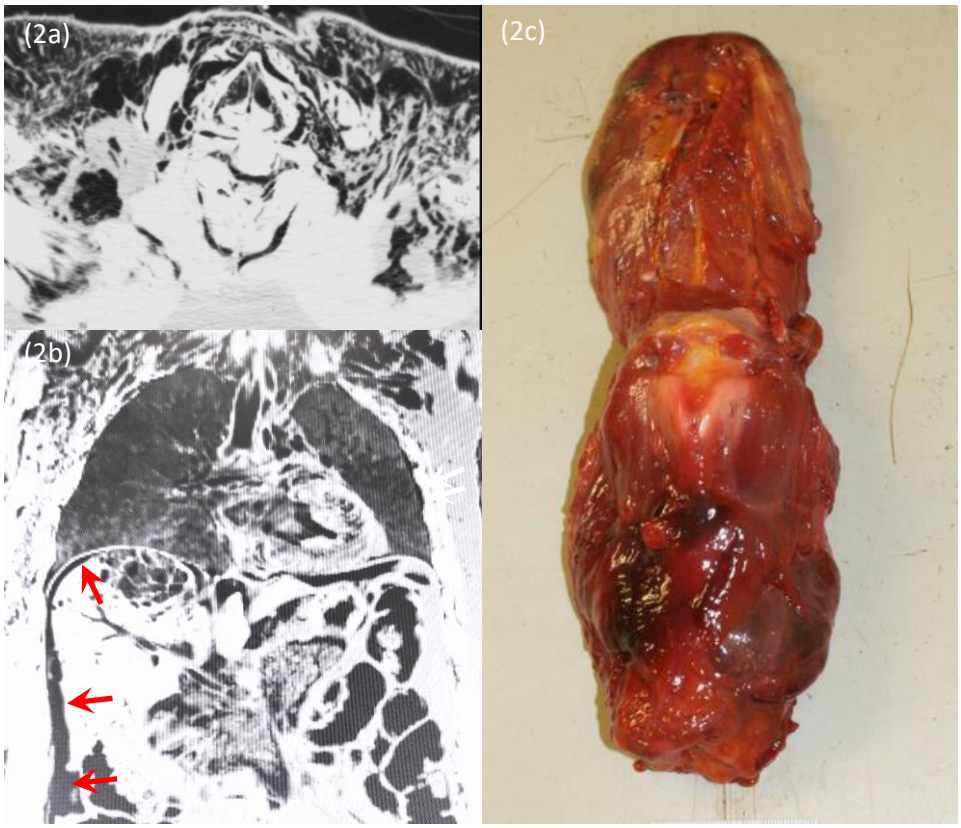

Fig 2: PMCT features of decomposition showing the (a) Neck (thyroid cartilage level, axial slice) and (b) Thorax (coronal view) demonstrating significant postmortem changes, notably diffuse subcutaneous air and putrefactive gas within the vessels and heart chambers. It is not possible to ascertain if the free intrathoracic air and free intraperitoneal air (red arrow) were due to antemortem trauma given significant rib fractures, postmortem changes, or a combination of both. (c) Autopsy: The autopsy photo of the thyrocricoid cartilage and larynx demonstrates better soft tissue delineation and hemorrhage at this level.

Further reading:

1. Schmitt-Sody M, Kurz S, Reiser M, Kanz KG, Kirchhoff C, Peschel O, Kirchhoff S. Analysis of death in major trauma: value of prompt post mortem computed tomography (pmCT) in comparison to office hour autopsy. Scand J Trauma Resusc Emerg Med. 2016 Mar 29;24:38. doi: 10.1186/s13049-016-0231-6. PMID: 27025705; PMCID: PMC4812637.
2. Ishida M, Gonoi W, Okuma H, Shirota G, Shintani Y, Abe H, Takazawa Y, Fukayama M, Ohtomo K. Common Postmortem Computed Tomography Findings Following Atraumatic Death: Differentiation between Normal Postmortem Changes and Pathologic Lesions. Korean J Radiol. 2015 Jul-Aug;16(4):798-809. doi: 10.3348/kjr.2015.16.4.798. Epub 2015 Jul 1. PMID: 26175579; PMCID: PMC4499544.

Contributors: Yi-Li Grace Wong, Kethery Haber, and Natalie L. Adolphi

NMDID 151981

Lung tumor, lung consolidations, pleural effusions, and emphysema in a death caused by hypothermia

Case description: A 58-year old, homeless male, who was a chronic tobacco smoker with unknown medical history, was found prone and unresponsive next to a street and taken to a hospital where he was found to have abnormally low body temperature. During warming in the hospital, he developed arrythmia, which progressed to asystole. Cardiopulmonary resuscitation was initiated but failed.

Imaging Findings: Bilateral dense lung consolidations with pleural effusions were seen in the background of lung emphysema and giant bullae (up to 12 cm) causing compressive atelectasis of adjacent lung parenchyma. Calcific specks were seen in the right hilar region with round like configuration causing irregular periosteal reaction of the ribs posteriorly, suspicious of mass, however was not well differentiated from the surrounding lung consolidation. There was evidence of pulmonary arterial hypertension with enlarged pulmonary trunk and main arteries. There were a few scanty mediastinal nodes that were partially obscured by mediastinal fat stranding likely representing edema. There was also signs of cardiopulmonary resuscitation with anterolateral rib and sternal fractures as well as healing left rib fractures with callus formation, likely from a prior fall. Other natural finding included cerebral atrophy, cardiomegaly with pericardial fluid, atherosclerotic calcified plaques along the aorta and branches and perinephric fat stranding representing chronic renal parenchymal disease or acute kidney injury.

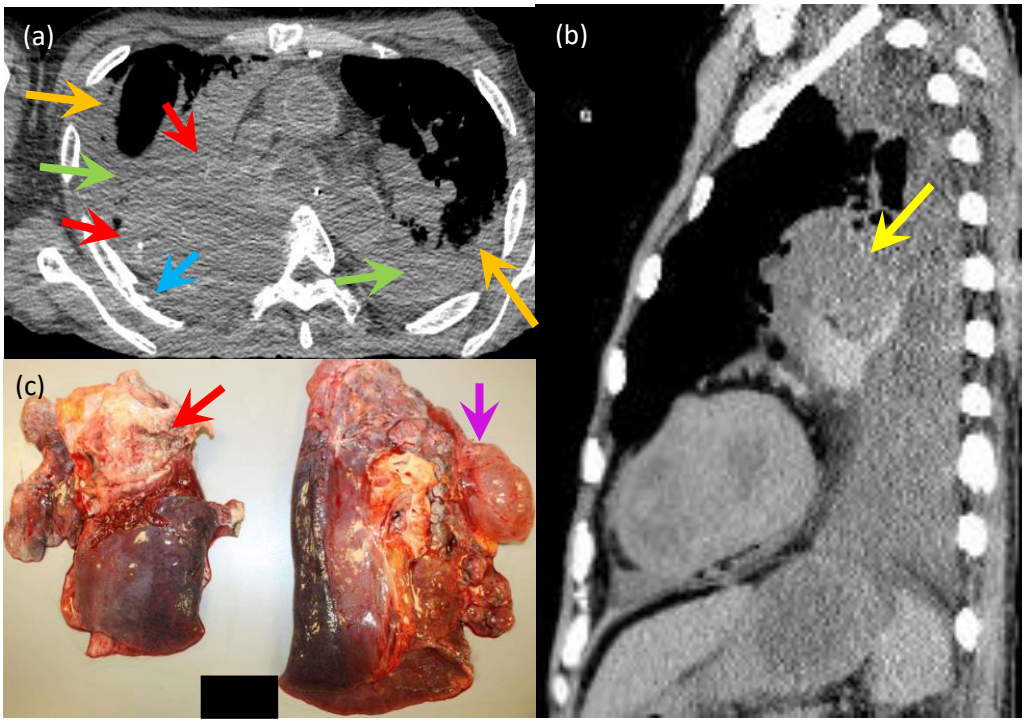

(a) PMCT Lung (Soft tissue window). Bilateral lung consolidations (green arrows) and pleural effusions with meniscal sign (orange arrows). A thin rim of calcification is seen at the right perihilar region extending posteriorly (red arrows). There was erosion into the right posterior rib causing irregular periosteal reaction (blue arrow). Left perihilar region also demonstrated enlarged left pulmonary artery (yellow arrow) mimicking hilar mass or lymphadenopathy on PMCT. (C) Autopsy image of a yellow tan right hilar necrotic mass (red arrow) with compression of bronchi. Left lung shows a large bulla (purple arrow).

Pathology Findings: Externally, the decedent was thin with scrapes of the chest from cardiopulmonary resuscitation attempts. Rib fractures and sternal fractures concurred with PMCT findings. The right lung weighed 610 g and the left lung 835 g. There were multiple bullae bilaterally, measuring up to 15 cm, larger and more numerous on the right. A right

hilar yellow-tan, focally necrotic mass with widest dimension of approximately 6 cm was found compressing bronchi and extending to the posterior right parietal pleural and soft tissues. Microscopy revealed prominent macrophages and eosinophilic, granular fluid within the lower lung lobes; anthracosis; infiltrating, predominantly discohesive tumor comprised of cells with enlarged, "bubbly" nuclei, prominent nucleoli and frequent, multiple nucleoli; and tumor-associated reactive fibrosis and necrosis. Bilateral pleural effusions and pericardial fluid were serosanguineous (right pleural cavity 80 ml, left pleural cavity 100 ml, pericardial fluid 200 ml). There was mild cardiomegaly, atherosclerosis along the aorta, and chronic hypertensive renal changes. Blood and right lung cultures yielded Streptococcus pneumoniae and other bacteria likely caused by specimen contamination during collection. Vitreous fluid tests were normal. Blood toxicology detected cotinine (breakdown product of nicotine) and ketamine (given in hospital) and its breakdown product, norketamine. There was no evidence of drug use or traumatic injuries. Based on the clinical history and presentation, the final cause of death was hypothermia given that he had been found outdoors in an overnight low temperature of -6 ^{0}C and had been transported to hospital with core temperature of 27.9 ^{0}C on arrival. The manner of death was classified as accident.

Comments: Clinical signs of hypothermia are variable and non-specific e.g., Wischnewsky (hemorrhagic gastric) spots, and frost erythema, which were not observed in this decedent. The diagnosis relied heavily on antemortem and perimortem history. There are no known specific signs of hypothermia on PMCT; however, Aghayev et al suggested that PMMR signs of back muscle hemorrhage may be a relatively specific vital sign[1].

Emphysema is an independent risk for lung carcinoma, but both are associated with chronic tobacco smoking. Exposure to tobacco smoke causes a situation of oxidative stress, with production of various mediators (TGF-β, EGRF, IL-1-IL-8 and G-CSF) that bring about a state of chronic inflammation and peripheral airway obstruction[2]. This alteration gives rise to the phenomena of epithelial lesion and irreversible DNA damage, increasing the risk of lung carcinoma[2]. On non-contrast PMCT, poor soft tissue contrast made it difficult to differentiate and delineate the tumor, the infective consolidations, and the pleural effusions. Clues to look for were aggressive invasion seen along the right posterior rib, the morphologic pattern of the calcifications along the presumed tumor margins, and in some cases the presence of regional and distant nodal and bone metastases. Without contrast, internal organ metastases, e.g., liver metastases, would be difficult to appreciate as well. Hence, autopsy confirmed the presence of concurrent tumor, community acquired pneumonia, and emphysema.

Further Reading:

1. Aghayev E, Thali MJ, Jackowski C, Sonnenschein M, Dirnhofer R, Yen K. MRI detects hemorrhages in the muscles of the back in hypothermia. Forensic Sci Int. 2008 Apr 7;176(2-3):183-6. doi: 10.1016/j.forsciint.2007.08.008. Epub 2008 Feb 4. PMID: 18249515.
2. Tubío-Pérez RA, Torres-Durán M, Pérez-Ríos M, Fernández-Villar A, Ruano-Raviña A. Lung emphysema and lung cancer: what do we know about it? Ann Transl Med. 2020 Nov;8(21):1471. doi: 10.21037/atm-20-1180. PMID: 33313216; PMCID: PMC7723574.

Contributors: Yi-Li Grace Wong, Kethery Haber, Roberto Maselli, and Natalie L. Adolphi

NMDID 152372

Acute hemorrhagic necrotizing pancreatitis

Case description: A 42-year-old male, with a history of chronic alcohol use, and complaints of weakness, vomiting and feeling ill, was found unresponsive in the bathroom of his residence.

Imaging Findings: The pancreas was mildly enlarged. No low attenuating foci were seen, i.e., necrosis or microabscesses. No air pockets or high-density hemorrhagic foci were found in this case. There was significant peripancreatic fat stranding, indicative of either edema or inflammation, extending to the perisplenic area, but no extrapancreatic fluid collections. No calculi or duct dilatations were seen along the biliary tree and pancreatic duct. There was no obvious mass effect, infiltrative features, or enlarged nodes. The liver demonstrated mild diffuse hypoattenuation indicative of hepatic steatosis. Mild putrefactive changes were seen along the liver vasculature. There were no PMCT signs of trauma.

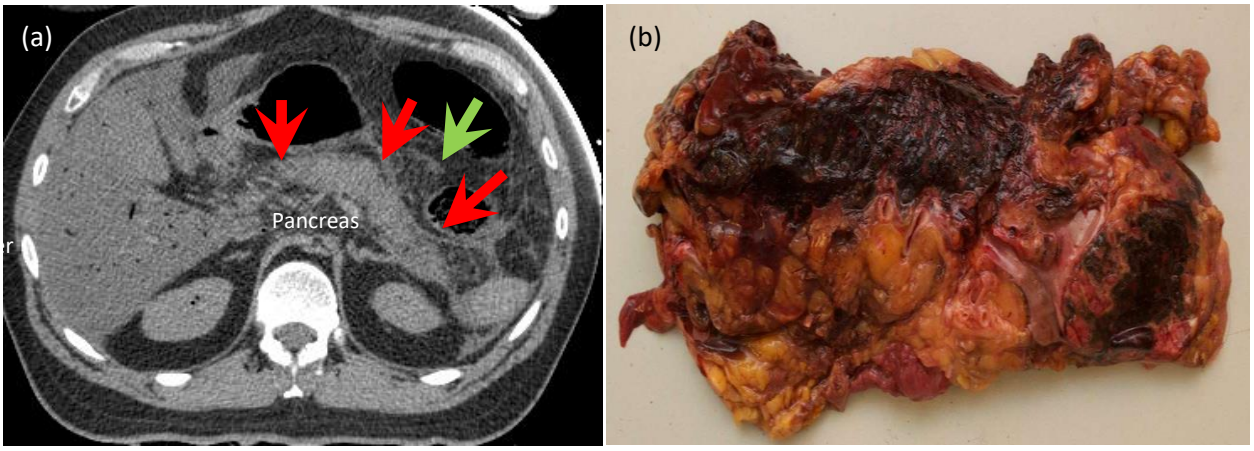

(a) PMCT: The pancreas is diffusely enlarged (red arrows) with peripancreatic fat stranding (green arrow) representing edema or inflammation; (b) Autopsy: Diffuse pancreatic hemorrhage and necrosis with severe fat necrosis involving the adjacent adipose.

Pathology Findings: Autopsy revealed severe pancreatitis with hemorrhage and abundant necrosis, fatty liver, and severe dehydration, evident from postmortem vitreous (eye) fluid electrolytes. There were no gallstones, and the intrahepatic and extrahepatic biliary tree were unremarkable. On microscopy, the pancreas showed extensive hemorrhage and necrotic foci with aggregates of polymorphonuclear cells. The liver showed severe macro- and micro-vesicular steatosis but no increase in fibrosis or portal inflammation. The cause of death was acute hemorrhagic necrotizing pancreatitis, and the manner of death was classified as natural.

Comments: The PMCT findings of the pancreas suggested interstitial edematous pancreatitis with mildly enlarged size and peripancreatic fat stranding. However, specific features for necrosis and hemorrhage were not visualised unlike on gross macroscopic and microscopic examinations. Parenchymal foci of gas, highly suggestive of superimposed infection/ emphysematous pancreatitis were also not seen in this case. Imaging features of acute pancreatitis can be subtle on non-contrasted PMCT and limits evaluation, particularly for the visualization of complications such as low attenuation microabscesses, biliary inflammation, splenic venous thrombosis, and arterial pseudoaneurysms[1]. Kashara et al. found no suggestive PMCT findings of pancreatitis in their case samples[2]. It has also been reported that in contrast-enhanced scans performed in living patients, pancreatic necrosis alone can be seen in fewer than 5% of patients[1]. Early stages of acute pancreatitis can appear unremarkable on imaging. Needless to say, it is essential to be aware of the possibility of false negatives on PMCT and have a high index of clinical suspicion when the history and risk factors are suggestive.

Further reading:

1. Thoeni RF. The revised Atlanta classification of acute pancreatitis: its importance for the radiologist and its effect on treatment. Radiology. 2012 Mar;262(3):751-64.

2. Kasahara S, Makino Y, Hayakawa M, Yajima D, Ito H, Iwase H. Diagnosable and non-diagnosable causes of death by postmortem computed tomography: a review of 339 forensic cases. Leg Med (Tokyo). 2012 Sep;14(5):239-45. doi: 10.1016/j.legalmed.2012.03.007. Epub 2012 Apr 28. PMID: 22542337.

Contributors: Yi-Li Grace Wong, Kethery Haber, Roberto Maselli, and Natalie L. Adolphi

NMDID 153141

Pulmonary edema: Antemortem or postmortem changes?

Case description: A 37-year-old male, with a history of schizophrenia and lower back pain, was found dead on the floor by a relative. He was prescribed 120 pills of hydrocodone for pain, filled 3 days prior to death. Only 48 pills were left. He was known to abuse his and his wife's medications.

Imaging Findings: Bilateral anterior buckle fractures of the ribs are observed, likely due to cardiopulmonary resuscitation efforts, as well as a healed left 9th posterior rib fracture with callus. No other fractures were observed. Other observations include diffuse cerebral and pulmonary edema, no pleural effusions, mild cardiomegaly, hepatomegaly with putrefactive changes, and high density sediments in the stomach.

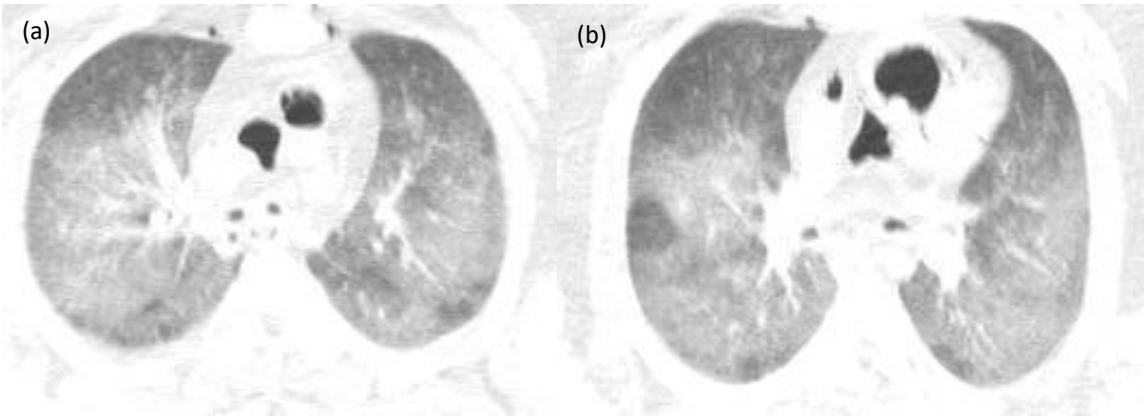

(a) PMCT lung (a) Axial view: Diffuse ground glass changes at gravity dependent lung. There are no segmental consolidations, pleural effusions, nor pneumothorax.

Pathology Findings: Findings at autopsy included bilateral pulmonary edema (right lung 750 g, left lung 1380 g), moderate blood and froth in the airways, an enlarged, fatty liver, morbid obesity (body mass index 43.23 kg/m^2), mild hypertensive and atherosclerotic cardiovascular disease, moderate (50%) atherosclerosis of the left anterior descending coronary artery, cardiomegaly (425 g), bilateral ventricular hypertrophy, and moderate three vessel coronary atherosclerosis. Microscopy revealed (1) Heart: Patchy myocyte hypertrophy, patchy interstitial and perivascular fibrosis; (2) Lungs: Patchy intraalveolar and peribronchial accumulation of neutrophils and pink granular material as well as erythrocytes; and (3) Liver: Moderate macro-and microvesicular steatosis and foci of increased portal lymphocytic inflammation. Postmortem blood toxicology screen showed a lethal concentration of hydrocodone, therapeutic concentrations of alprazolam (Xanax), acetaminophen (Tylenol), dihydrocodeine (metabolite of hydrocodone), quetiapine, and its metabolite, norquetiapine. There was no ethanol (alcohol) detected in the blood. The cause of death is toxic effects of multiple drugs. The autopsy findings and investigative reports of the circumstances surrounding death indicate the manner of death to be accident.

Comments: Hypostasis in the lungs is a known time-dependent "normal" postmortem change with gravity dependent predisposition. It is due to pressure gradient between pulmonary vasculature and alveolar spaces and an alteration of capillary permeability[1]. On PMCT, it presents early as ground glass changes at dependent areas, which gradually increase in volume and density with time, sometimes masking or mimicking antemortem pathology, e.g., pneumonic consolidations. In terms of patterns and distributions, these changes may be seen in a posterior location if the decedent was supine, or in an anterior location if the decedent was found prone. There are also no specific PMCT signs of drug overdose, but it has been suggested that pulmonary congestion without pleural effusion, bronchus fluid-level, high densities within the stomach, and/or a distended urinary bladder (due to opioid influence on the urinary bladder sphincter) may be clues to a drug overdose-related death. In this case, the pulmonary edema was confirmed during autopsy but appears relatively similar in density and location to hypostasis and could have been a mixture of both entities.

Further Reading & References:

1. Shiotani S, Kobayashi T, Hayakawa H, Kikuchi K, Kohno M. Postmortem pulmonary edema: a comparison between immediate and delayed postmortem computed tomography. Leg Med (Tokyo). 2011 May;13(3):151-5. doi: 10.1016/j.legalmed.2010.12.008. PMID: 21315646.
2. Lahaye MJ, van Kan R, Haest II, Bakers FC, Kroll J, Jacobi-Postma L, Hofman PA. 2.9. CT imaging as a valuable additional tool to establish drug abuse as cause of death. Journal of Forensic Radiology and Imaging. 2014 Apr 1;2(2):101.
3. Rohner C, Franckenberg S, Schwendener N, Oestreich A, Kraemer T, Thali MJ, Hatch GM, Ruder TD. New evidence for old lore--urinary bladder distension on post-mortem computed tomography is related to intoxication. Forensic Sci Int. 2013 Feb 10;225(1-3):48-52. doi: 10.1016/j.forsciint.2012.03.029. Epub 2012 May 5. PMID: 22565114.

Contributors: Yi-Li Grace Wong, Kethery Haber, Roberto Maselli, and Natalie L. Adolphi

NMDID 155040

Infrarenal abdominal aortic aneurysm rupture causing large left retroperitoneal hematoma

Case description: A 64-year-old male staying at a hotel was witnessed to be sitting on the bed, clutching his chest with labored breathing. According to reports, security from the hotel helped him to the floor but he became unresponsive. EMS responded but he failed to be resuscitated.

Imaging Findings: Fusiform infrarenal abdominal aortic aneurysm with widest CT dimension of 9.2 cm and disruption of wall calcifications were suggestive of rupture in the presence of a large left retroperitoneal hematoma.

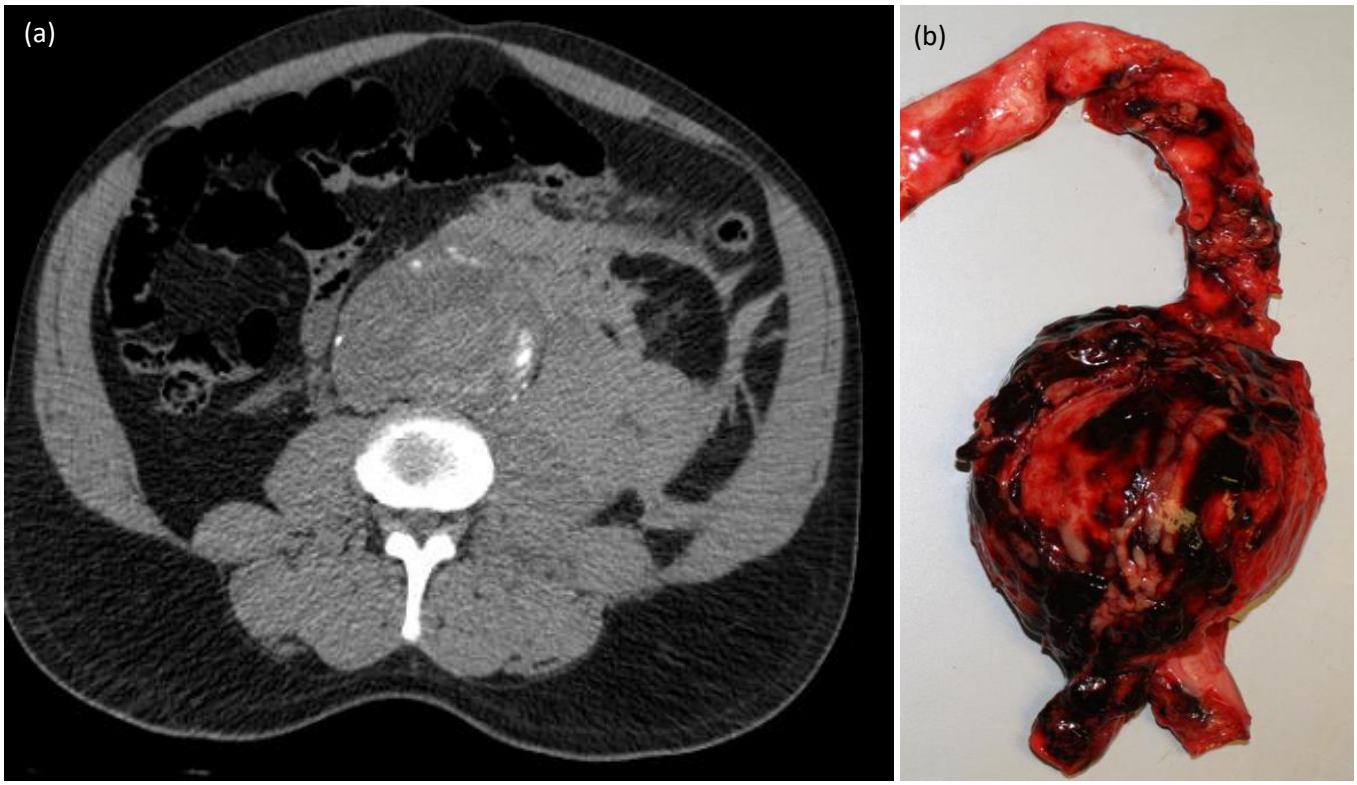

(a) PMCT (axial view, soft tissue window): Fusiform dilatation of infrarenal abdominal aorta and surrounding left periaortic hematoma; (b) Autopsy: Ruptured infrarenal aortic aneurysm

Pathology Findings: Infrarenal abdominal aneurysm measuring 10.5 cm in diameter, distal to renal arteries, confirmed PMCT findings. Microscopic findings were media necrosis, with adherent fibrin on the intimal surface, and focal disruption with hemorrhage. The rupture caused massive hemorrhage into the surrounding abdominal mesentery and perirenal adipose tissue leading to death. Additional findings included moderate to severe coronary artery atherosclerosis, cardiomegaly (655 g) and left ventricular hypertrophy.

Comments: PMCT is typically performed without intravascular contrast, which is used in clinical imaging to opacify vessels and demonstrate active extravasation of blood. The technical challenges of using intravascular contrast in postmortem studies are due to cessation of vascular circulation, hemostasis, intravascular clotting and gas, as well as increased vascular permeability causing contrast leak into surrounding soft tissues, which overlaps with antemortem findings of true active hemorrhage. The presence of extraluminal signs as seen in this case, i.e., intermediate to high density retroperitoneal hematoma and periaortic fat stranding, in addition to aortic aneurysmal dilatation, imply complete rupture.

Further Reading:

1. Grabherr S, Grimm J, Baumann P, Mangin P. Application of contrast media in post-mortem imaging (CT and MRI). Radiol Med. 2015 Sep;120(9):824-34. doi: 10.1007/s11547-015-0532-2. Epub 2015 Apr 5. PMID: 25841652.

2. Vu KN, Kaitoukov Y, Morin-Roy F, Kauffmann C, Giroux MF, Thérasse E, Soulez G, Tang A. Rupture signs on computed tomography, treatment, and outcome of abdominal aortic aneurysms. Insights Imaging. 2014 Jun;5(3):281-93. doi: 10.1007/s13244-014-0327-3. Epub 2014 May 1. PMID: 24789068; PMCID: PMC4035490.

Contributors: Yi-Li Grace Wong, Kethery Haber, Roberto Maselli, and Natalie L. Adolphi

NMDID 158501

Gunshot wound of the neck

Case description: A 20-year-old male was found deceased outside of his residence, lying face down in a pool of blood. Prior to this, occupants of the residence had called 911 after witnessing a confrontation between the decedent and other occupant(s).

Imaging Findings: A left anterior lower neck focal subcutaneous defect was seen, associated with generalized neck space emphysema extending to right infraclavicular soft tissue. The cervical spine was preserved. There were no retained projectiles seen in the neck. A small metallic foreign body was seen external to the right hand. There were also fractures of the right distal humerus and fibula.

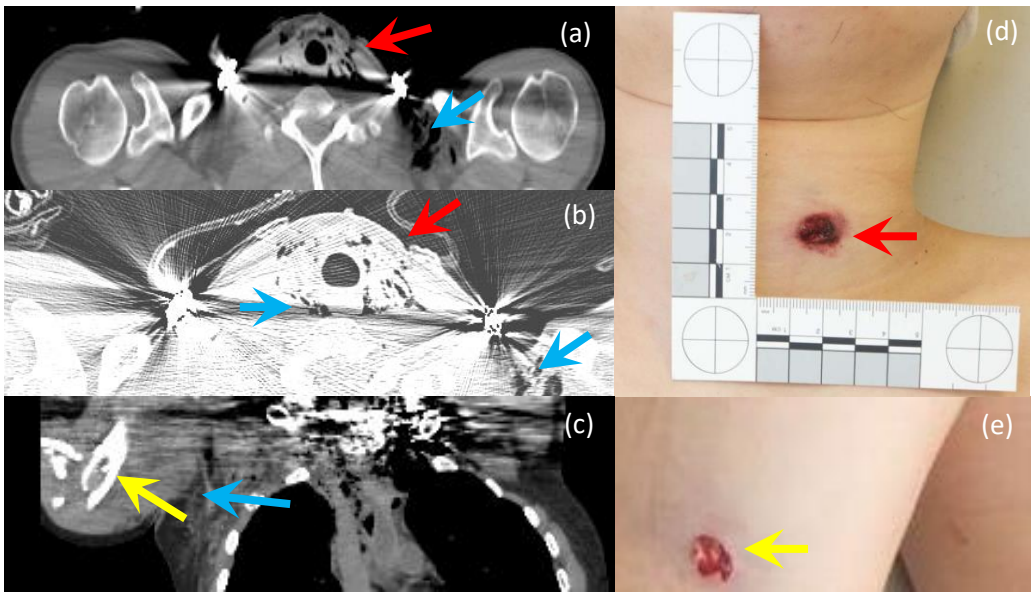

(a) PMCT Neck (soft tissue window, axial slice) demonstrated a left lower neck subcutaneous defect with a linear subcutaneous air tract (red arrows) and deep neck space and soft tissue emphysema (blue arrows), better seen in (b) lung window. However, no high-density projectiles were seen in the neck. (c) PMCT of the upper thorax (soft tissue window, coronal slice) shows right distal humerus comminuted fractures with no projectile fragments. Note the necklace causes significant streak artifact leading to image degradation. External examinations of the (a) Left anterior neck entrance wound and (b) Right lateral arm exit wound.

Pathology Findings: A fatal gunshot wound (indeterminate range of fire) penetrated the left side of the neck and perforated the airway and major vessels of the neck before exiting the side of the right arm. A copper-jacketed, moderately deformed missile was recovered, free-floating in the inside of the sealed body bag. Given the absence of defects corresponding to the exit wound in the jacket, sweater, and shirts, it is most likely that this missile originated from the wound track involving the neck and right upper arm, was initially retained inside the clothing, and subsequently dislodged during transport of the decedent. Postmortem toxicological testing performed on the femoral blood revealed the presence of morphine. Another gunshot wound of the right lower leg fractured the bones of the lower leg. The cause of death was multiple gunshot wounds of the neck. The manner of death was classified as homicide.

Comments: Gunshot injuries to the neck are associated with high mortality due to the presence of vital structures in this region[1-2]. A common imaging presentation for gunshot wounds of the neck is generalized superficial and deep neck space subcutaneous emphysema, as seen in this case. However, if there are no projectile fragments, obvious entrance/exit skin defects, bone fractures, or wound channels in the neck spaces, the trajectory of the bullets can be difficult to decipher, particularly if the pathway is atypical. Fatal injuries to look out for include vascular and cervical spine injuries. Cervical

spine fractures were excluded, but soft tissue and vascular injuries were not appreciated on PMCT, as there were no indirect signs of fatal hemorrhage, e.g., high-density hematoma or muscle asymmetry. As most PMCTs are non-contrasted, extravasation of contrast used in clinical cases (as a sign of vascular disruption) cannot be demonstrated. The presence of metallic artifact from the necklace also impeded interpretation. Without witness accounts, scene investigations, and background history, differentiation from other penetrating injuries, e.g., stab wounds or iatrogenic injuries would have been challenging on imaging alone.

Further Reading & References:

1. Godhi S, Mittal GS, Kukreja P. Gunshot injury in the neck with an atypical bullet trajectory. J Maxillofac Oral Surg. 2011 Mar;10(1):80-4. doi: 10.1007/s12663-010-0124-6. Epub 2010 Nov 27. PMID: 22379328; PMCID: PMC3177495.
2. Gascho D, Marosi M, Thali MJ, Deininger-Czermak E. Postmortem Computed Tomography and Magnetic Resonance Imaging of Gunshot Wounds to the Neck. J Forensic Sci. 2020 Jul;65(4):1360-1364. doi: 10.1111/1556-4029.14311. Epub 2020 Feb 27. PMID: 32105348.

Contributors: Yi-Li Grace Wong, Kethery Haber, Roberto Maselli, and Natalie L. Adolphi

NMDID 164164

Hepatocellular carcinoma in the background of liver cirrhosis and hepatic steatosis

Case description: A 43-year-old male with history of chronic alcohol abuse, hepatitis C, and previously repaired bleeding esophageal varices was admitted for abdominal pain, nausea, vomiting, dyspnea, and signs of sepsis. Laboratory tests detected blood changes indicating liver and kidney damage.

Imaging Findings (Fig. 1): A heterogenous area of liver hyper-attenuation was seen measuring approximately 8.4 x 10.1 cm. A smaller hyperattenuating lesion was also seen at the right liver lobe tip measuring 2.2 x 2.9 cm. There was diffuse low density of the liver with mean attenuation value of 30-39 HU. The liver margins were nodular, and there was surrounding high density perihepatic hematoma suspicious of tumor rupture or bleeding.

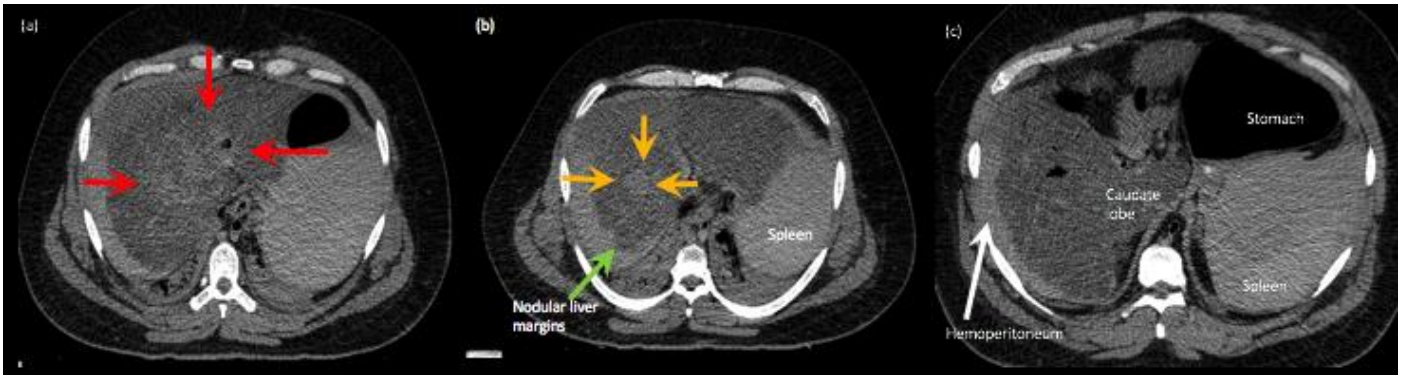

Fig 1: Axial slices of PMCT upper abdomen demonstrate (a) Ill-defined right liver lobe mass-like heterogeneity (red arrows); (b) A round focal high density liver lesion (Yellow arrow) and nodular liver margins (green arrow) in the background of a diffusely hypoattenuating hepatic steatosis. (c) The caudate lobe appears enlarged. Additionally, there is high density hemoperitoneum (white arrow) surrounding the right liver lobe. Constellation of findings are suspicious of a hepatoma (HCC) in the background of cirrhosis and diffuse hepatic steatosis.

Pathology Findings (Fig. 2): Macronodular cirrhosis and fatty liver change with two liver tumors respectively measuring 1.5 x 1.2 x 1 cm and 2.5 x 1.8 x 1.7 cm, one of which appeared to have been bleeding causing hemoperitoneum. Microscopy confirmed that these tumors were hepatocellular carcinomas with background cirrhosis. Cause of death was hepatic cirrhosis with hepatocellular carcinoma due to chronic ethanol abuse and hepatitis C infection.

Fig 2: Autopsy shows (a) Fatty changes and macronodular cirrhosis; (b) One of the liver nodules with yellow tan to hemorrhagic cut surface; (c) 2100 ml hemoperitoneum

Comments: Hepatocellular carcinomas (HCC) typically enhance avidly in arterial phases of clinical multiphasic contrast-enhanced CT scans, deriving blood predominantly from the hepatic artery. Not all HCCs may be seen on uncontrasted PMCT and have a wide range of appearances. Small HCCs and satellite lesions may be similar in density to the rest of the liver. In this case, the large area of mixed heterogenous parenchymal density on uncontrasted PMCT had similar high density compared with the smaller round focal inferior tumor, mimicking a larger tumor. The heterogeneous appearance may be attributed to fatty metamorphosis, necrosis, calcifications, and bleeding around the tumor. There are also other

hepatic lesions that may mimic HCCS such as hemangiomas, focal fat infiltration, and regenerating or dysplastic nodules, which are difficult to differentiate on imaging alone. In this case, index of suspicion of HCC was high because of the presence of cirrhosis with a diffusely hypodense fatty liver, history of Hepatitis C, and chronic alcohol abuse.

Further reading:

1. Attwa MH, El-Etreby SA. Guide for diagnosis and treatment of hepatocellular carcinoma. World J Hepatol. 2015 Jun 28;7(12):1632-51. doi: 10.4254/wjh.v7.i12.1632. PMID: 26140083; PMCID: PMC4483545..
2. Bialecki ES, Di Bisceglie AM. Diagnosis of hepatocellular carcinoma. HPB (Oxford). 2005;7(1):26-34. doi: 10.1080/13651820410024049. PMID: 18333158; PMCID: PMC2023919.

Contributors: Yi-Li Grace Wong, Kethery Haber, Roberto Maselli, Natalie L. Adolphi

NMDID 176154

High densities within the stomach in a case of drug overdose

Case description: A 15-year-old female with a history of illicit drug use, bipolar disorder, schizophrenia, depression, anxiety, previous attempted suicide, and self-harm was found lying face down and deceased in a wooded area. Her medication bag contained multiple, empty prescription bottles.

Imaging Findings: High density material (mean attenuation value of 380 HU), not causing streak artifacts, were seen mixed with the stomach contents. There was no PMCT evidence of acute, traumatic injury.

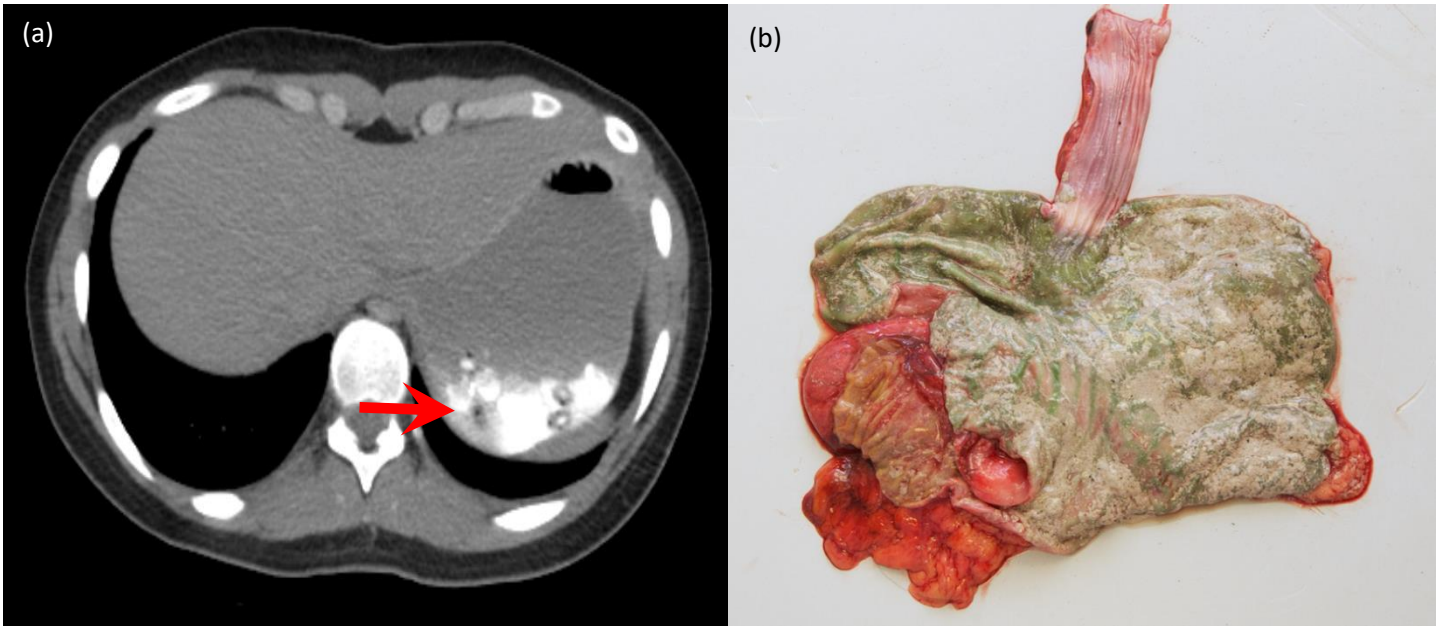

(a) PMCT: High density was seen within the stomach (red arrows); (b) Autopsy: Pills, pill fragments and partially digested pills were found during autopsy.

Pathology Findings: Externally, numerous scrapes and bruises were found throughout the body. There were healed, linear scars in her left upper and lower extremities but no internal injuries overall. Multiple pills and pill fragments within the stomach, as well as granular material consistent with partially digested pills, were present in the stomach. There were no signs of natural disease. Based on toxicology results, the cause of death was toxic effects of multiple drugs (bupropion, lamotrigine, naltrexone, prazosin, propranolol, ziprasidone) based on toxicology results.

Comments: In this case, the high-densities were of mixed discrete round and "fluid-like" CT morphology, correlating with pathology findings. Given the history, her young age and lack of natural disease, suspicion of drug or medication overdose was raised. However, contents could not be confirmed without direct internal inspection of stomach contents. It is also important to note that high intraluminal densities found within the gastrointestinal tract on CT have a wide range of differential diagnoses. It can be challenging at times to differentiate acute gastrointestinal hemorrhage and/or drug overdoses from ingested foods, e.g., pinto beans, barium oral contrast used in antemortem medical imaging investigations, and a wide range of common medications or supplements, e.g. calcium carbonate, calcium resonium, potassium chloride, glycerine suppository, aluminium hydroxide, and iron sulphate.

Further Reading:

1. Sin FN, Tsang JP, Siu KL, Ma JK, Yung AW. Medications as causes of intraluminal hyperdensities: what radiologists need to know. Eur J Radiol. 2012 Jul;81(7):1652-6. doi: 10.1016/j.ejrad.2011.03.010. Epub 2011 Apr 3. PMID: 21459531.
2. Coelho MP, Goel A, Klumpp M, Mincolla M. Intraluminal hyperdense appearance of the small bowel on high resolution computed tomography of the abdomen and pelvis secondary to use of Calcium Carbonate tablets

(Tums) mimicking a small bowel fistula. Radiol Case Rep. 2020 Aug 12;15(10):1875-1878. doi: 10.1016/j.radcr.2020.07.044. PMID: 32884604; PMCID: PMC7453116.

Contributors: Yi-Li Grace Wong, Kethery Haber, Roberto Maselli, and Natalie L. Adolphi

NMDID 181912

Thoracic aortic rupture and hemothorax

Case description: A 58-year-old female complained of constipation and heartburn after methadone treatment, developed shortness of breath and collapsed to her death.

Imaging Findings: A large right hemothorax with maximum depth of 10.4 cm causing right lung compressive atelectasis and left mediastinal shift was observed. Other findings include an enlarged thoracic aorta (in widest dimensions (anteroposterior x width): ascending: 3.3 x1.7 cm – partially collapsed, arch: 1.6 cm- partially collapsed, descending 4.6 x 4.6 cm); discontinuity of wall calcifications at the level of the proximal arch with surrounding periaortic soft tissue density suspicious of paraaortic hematoma (maximum depth 1.2 cm) along the descending aorta; and no obvious double lumen. The infrarenal abdominal aorta was also ectasic (widest dimension: 3.3 cm) with irregular wall and discontinuity of coarse wall calcifications, but no periaortic hematoma was seen. There were cardiopulmonary resuscitation induced bilateral rib fractures, left more than right. Natural disease included dense coronary artery calcifications in RCA, LAD, and circumflex arteries, as well as iliac and lower limb peripheral arteries.

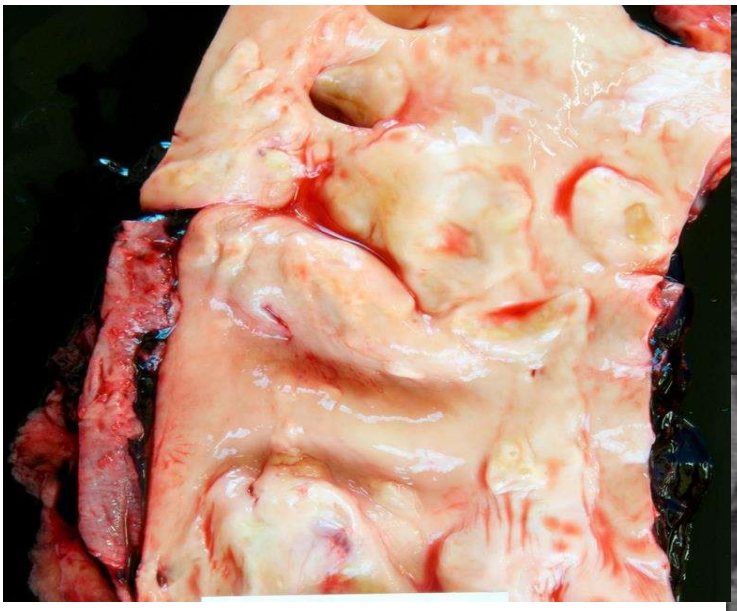

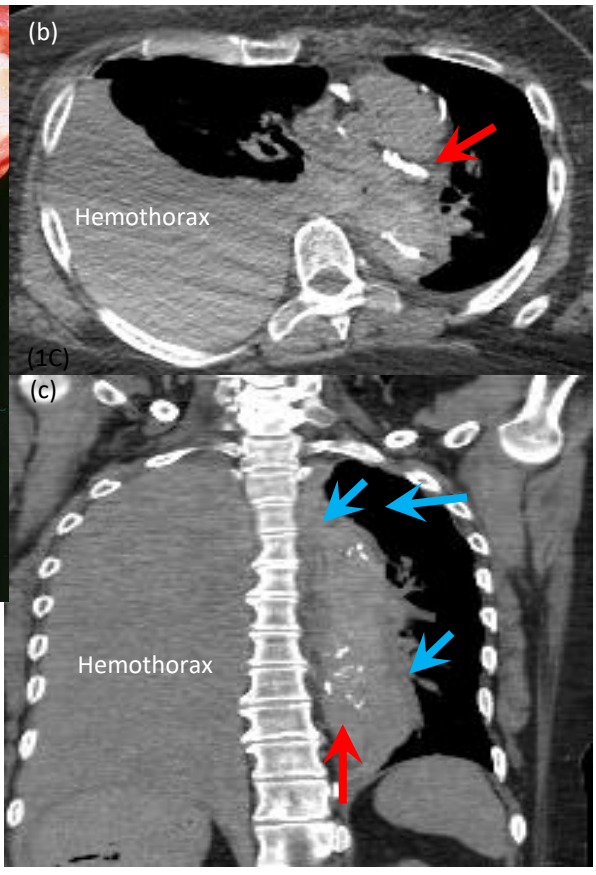

(a) Autopsy: Severely atheromatous aorta with evidence of dissection; PMCT: Thorax (soft tissue window) in (b) Axial and (c) Coronal views showed a large right hemothorax with intermediate to high density. The thoracic aorta is enlarged with irregular margins, discontinuity in calcification (red arrows) and periaortic blood suspicious of dissection and rupture.

Pathology Findings: A 5 mm rent was seen along the posterior aspect of the ascending aorta, proximal to the origin of the brachiocephalic trunk. Surrounding this rent was a dissection of the aortic wall over a segment of ascending aorta approximately 15 cm long. The rent also extended through the entire thickness of the aorta, in continuity with the right pleural cavity with 2 liters of hemothorax. Other natural findings included cardiomegaly (weight 410 g), cardiac hypertrophy, severe coronary artery stenosis, and renal scarring with nephrosclerosis. Postmortem blood toxicology revealed methamphetamine, which could have exacerbated the hypertension and contributed to the aortic dissection. Methadone and morphine were also identified. As no morphine was prescribed to the decedent, it is likely that it was a breakdown product from heroin. The cause of death was aortic dissection and rupture due to hypertensive cardiovascular disease, exacerbated by toxic effects of methamphetamine. The manner of death was classified as accident.

Comments: PMCT can identify almost all cases of sudden death caused by aortic rupture[1]. Typical findings include aortic dilatation, extensive hemorrhages, and unusual locations of intravascular gas at dependent areas suggestive of overlapping layers or secondary collapse of the aorta[2]. Aortic dissection may be more challenging to detect without intravascular contrast, but indirect signs are inwardly displaced intimal calcifications or flaps within the aortic lumen, with or without calcification, and the double lumen sign. However, it is important to be aware that atypical sedimentation and postmortem clotting can have overlapping features with the double lumen sign.

References & Further Reading:

1. Kaneko T, Hibi M, Ishibashi M, Nakatsuka A, Omori Y, Ishikura K, Hatada T, Takeda T, Takei Y, Takeda K. Postmortem computed tomography is an informative approach for prevention of sudden unexpected natural death in the elderly. Risk Management and Healthcare Policy. 2010;3:13-20 https://doi.org/10.2147/RMHP.S10260.
2. S Kluschke F, Ross S, Flach PM, Schweitzer W, Ampanozi G, Gascho D, Vonlanthen B, Thali MJ, Ruder TD. To see or not to see–Ambiguous findings on post-mortem cross-sectional imaging in a case of ruptured abdominal aortic aneurysm. Legal medicine. 2013 Sep 1;15(5):256-9.

Contributors: Yi-Li Grace Wong, Kethery Haber, Roberto Maselli, and Natalie L. Adolphi

NMDID 185843

Incidental findings of lytic and sclerotic vertebral metastasis in a case of motor vehicle accident

Case description: A 69-year-old male was witnessed to lose control of his vehicle, which overturned and resulted in him being ejected from the vehicle and pronounced dead on the scene.

Imaging Findings: There were multiple fractures of the skull (with pneumocranium and intracranial hemorrhages), fracture of the facial bones, thoracic cage, vertebrae (including a dislocation at T9-T10 vertebral level), pelvis, and lower extremities, with associated intracranial and intrathoracic soft tissue injuries. Incidentally, a C7 lytic destructive bone lesion with expansile soft tissue component was seen, suspicious of tumor replacement. There were also patchy irregular sclerotic cervical and thoracic spine lesions, also suspicious of bone metastasis. The prostate was irregular, nodular and enlarged measuring 5.0 x 4.8 x 5.2 cm (anteroposterior x width x craniocaudal length). No other obvious mass was seen on PMCT. There were also calcifications along the medium and large arteries.

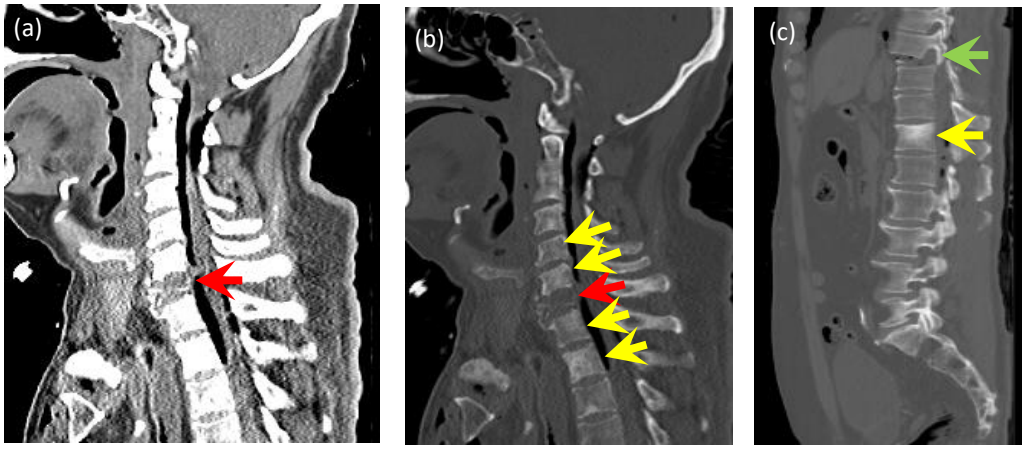

Fig. 1: (a) Soft tissue window and (b) bone window of the cervical spine shows destruction of C7 vertebral body with soft tissue component within, which appears lytic on bone window (red arrows). There is irregular patchy sclerosis of the cervical, T1, and T2 vertebrae (yellow arrows), most obvious at T1 vertebral body. (c) Lumbar spine (bone window, sagittal view) shows T12 vertebral body patchy sclerosis (yellow arrow) as well as a traumatic T9-T10 dislocation (green arrow) that likely caused spinal cord transection at this level.

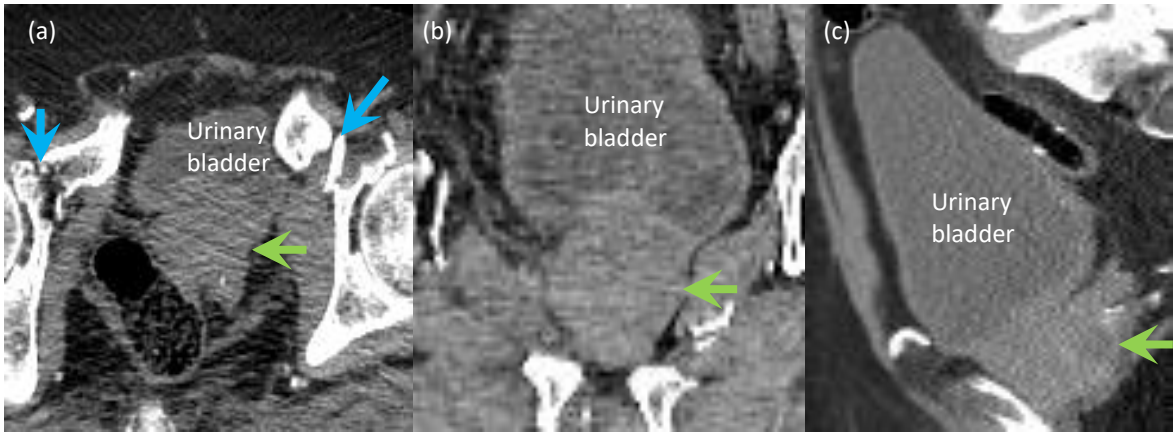

Fig. 2: (a) Axial, (b) Coronal and (c) Sagittal views of an irregular, enlarged, nodular prostate (green arrows) causing urinary bladder distension. Bilateral traumatic pubic bone and acetabular fractures are also shown (blue arrows).

Pathology Findings: External examination revealed a well-nourished male with abrasions and contusions of the face, trunk, and extremities, and palpable rib cage fractures. Postmortem toxicology showed no alcohol or common drugs of abuse. The cause of death was blunt trauma. The combination of external examination and investigative reports indicated the manner of death to be accidental.

Comments: PMCT was not only useful for demonstrating the extent of traumatic injuries in this case, but also identified natural disease, such as the previously undiagnosed bone metastases and atherosclerotic disease. In this case, the primary malignancy is suspected to be from the prostate gland given its irregular, enlarged and nodular morphology, the decedent's age, and that prostate cancers are the most common primary malignant tumor in men. Prostate primaries commonly have sclerotic (blastic) spinal metastases, but 15% may present with mixed lytic and sclerotic metastases. Other primary tumors which may demonstrate mixed lytic and sclerotic bone lesions include lung, breast, cervix, and testicular carcinomas[1-2]. On PMCT, metastatic lesions with no bone involvement may be difficult to detect, e.g., in soft tissues such as the liver, and in certain cases, the primary may not be obvious on imaging. It is also important to be aware of spinal metastasis mimics, such as benign hemangioma, discogenic endplate changes, and discitis-osteomyelitis.

Further Reading and References:

1. Shah LM, Salzman KL. Imaging of spinal metastatic disease. Int J Surg Oncol. 2011;2011:769753. doi: 10.1155/2011/769753. Epub 2011 Nov 3. PMID: 22312523; PMCID: PMC3263660.
2. Chapman S, Nakielny R. 2019. Aids to radiological differential diagnosis (7th Ed.). United States.

Contributors: Yi-Li Grace Wong, Kethery Haber, Roberto Maselli, and Natalie L. Adolphi

NMDID 188757

Traumatic diaphragmatic rupture, rib fractures, pneumothorax, hemothorax, long bone fractures

Case description: The decedent was the 21-year-old driver of a motor vehicle that struck a semi-truck, head on, in bad weather. He was pronounced dead at the scene of the accident.

Imaging Findings: There were rib fractures with bilateral pneumothoraces (left > right), bilateral hemothoraces (left > right), and a left raised hemidiaphragm suggestive of rupture, with stomach and bowel herniation into the left thoracic cavity, causing right mediastinal shift and compressive atelectasis of adjacent lung. There were also minimal perihepatic and perinephric hematoma, subarachnoid hemorrhage, and left radius and bilateral femur fractures.

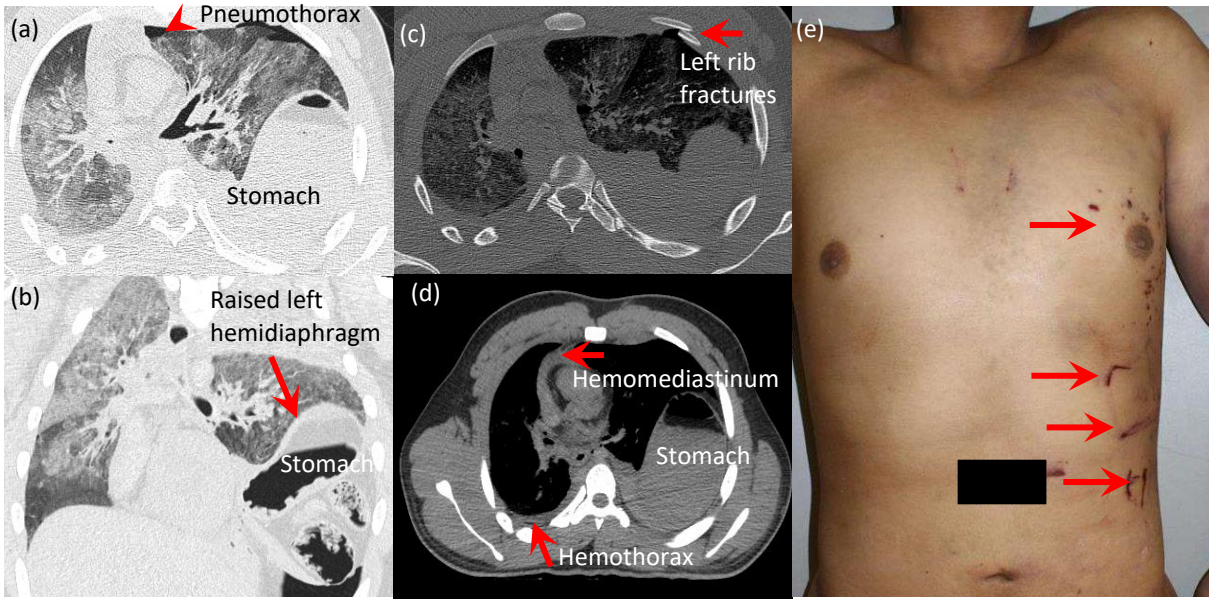

PMCT Thorax in (a) Axial view (lung window) showed a left pneumothorax; (b) Coronal view demonstrated a raised hemidiaphragm with stomach herniating superiorly into the left intrathoracic cavity; (c) Axial view (bone window): Left anterior rib fracture; (d) Axial view (soft tissue window) showed the stomach in the left intrathoracic cavity and hemomediastinum; (e) External examination shows multiple superficial abrasions of the left anterior and lateral chest, and left flank.

Pathology Findings: External examination revealed numerous abrasions of the face, left chest wall, left flank, and extremities. There were palpable fractures felt at the left forearm and bilateral thighs, corresponding to PMCT findings. The cause of death was blunt chest trauma, and the manner of death was classified as accident.

Comments: Blunt traumatic diaphragmatic rupture is associated with high rates of morbidity and mortality[1]. In a study by Lim et al, 74.5% of traumatic diaphragmatic ruptures were associated with blunt trauma, 84.2% of which the main cause was traffic accidents, and the most common location was at the posterolateral part of left diaphragm (derived from the pleuroperitoneal membrane, its weakest part structurally)[1]. CT scans have a sensitivity of 61-87% and specificity of 72-100% in detecting diaphragmatic ruptures, and these injuries are often associated with internal organ, and to lesser extent, hollow viscus perforation[1].

Several studies have suggested PMCT to be an alternative to autopsy with percentage of agreement on cause of death ranging between 46-100% and body region specific injuries between 53-100%[2]. PMCT has several advantages in traumatic settings in identifying bone fractures and air, e.g., pneumothorax, pneumopericardium and pneumomediastinum. In this case, external examination complements PMCT, as among the most frequently missed injuries on PMCT are superficial injuries (e.g., abrasions, contusions) and vessel injuries (e.g., dissection, transections). Despite these limitations, PMCT

can be used as an alternative for conventional autopsy in situations where the cause(s) of death are clearly represented on imaging, and the death is not suspicious.

Further Reading and References:

1. Lim KH, Park J. Blunt traumatic diaphragmatic rupture: Single-center experience with 38 patients. Medicine (Baltimore). 2018 Oct;97(41):e12849. doi: 10.1097/MD.0000000000012849. PMID: 30313123; PMCID: PMC6203559.
2. Scholing M, Saltzherr TP, Fung Kon Jin PH, Ponsen KJ, Reitsma JB, Lameris JS, Goslings JC. The value of postmortem computed tomography as an alternative for autopsy in trauma victims: a systematic review. Eur Radiol. 2009 Oct;19(10):2333-41. doi: 10.1007/s00330-009-1440-4. Epub 2009 May 21. PMID: 19458952; PMCID: PMC2758189..

Contributors: Yi-Li Grace Wong, Kethery Haber, Roberto Maselli, and Natalie L. Adolphi

NMDID 188922

Organ procurement, intrathoracic and retroperitoneal hematomas in a case of gunshot wounds to the chest

Case description: A 25-year-old male was found supine, gasping at the kitchen entrance, after gunshots had been fired at a party. He was pronounced dead at the hospital approximately 3 hours after the incident.

Imaging Findings: PMCT showed evidence of procurement with open defects of the anterolateral thoracic cage and anterior abdominal walls, absent spleen, left kidney and left adrenal glands. Perihepatic and bilateral retroperitoneal hematomas, right more than left, surrounding the right kidney, posterior ascending, and descending colon were visualized. Left lateral rib non-displaced fractures were seen. Multiple high-density foreign bodies causing streak artifact were visualized at the left anterior chest-abdominal wall junction (T12/L1 level), left retroperitoneum, and perihepatic regions. In the chest, there was significant intrathoracic free air and bilateral hemothoraces with adjacent lung collapse. At the right occipital base, a round high-density metallic object (not shown) was seen embedded in the scalp muscle. However, other than diffuse cerebral edema, no underlying occipital bone fractures or intracranial hemorrhage were seen.

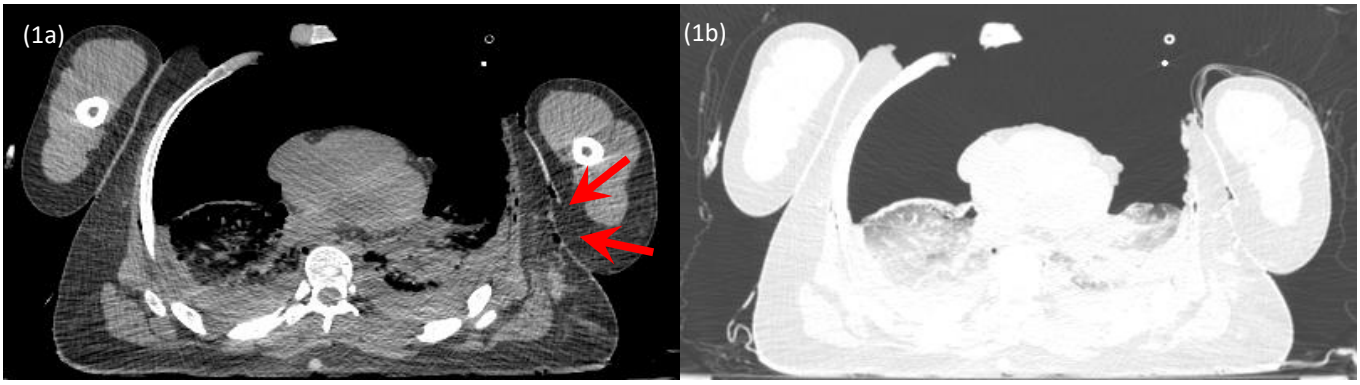

Fig 1: PMCT Thorax (axial views) in (a) Soft tissue and (b) Lung windows showed anterolateral chest wall open defects (due to bilateral thoracotomies and organ procurement), bilateral intrathoracic air, hemothoraces with adjacent lung collapses. Left lateral chest wall skin irregularity and linear air pockets represented the left lateral chest wall entry site (red arrows). However, the right chest wall entry site was not well visualized on PMCT due to the iatrogenic right anterolateral chest wall open defect.

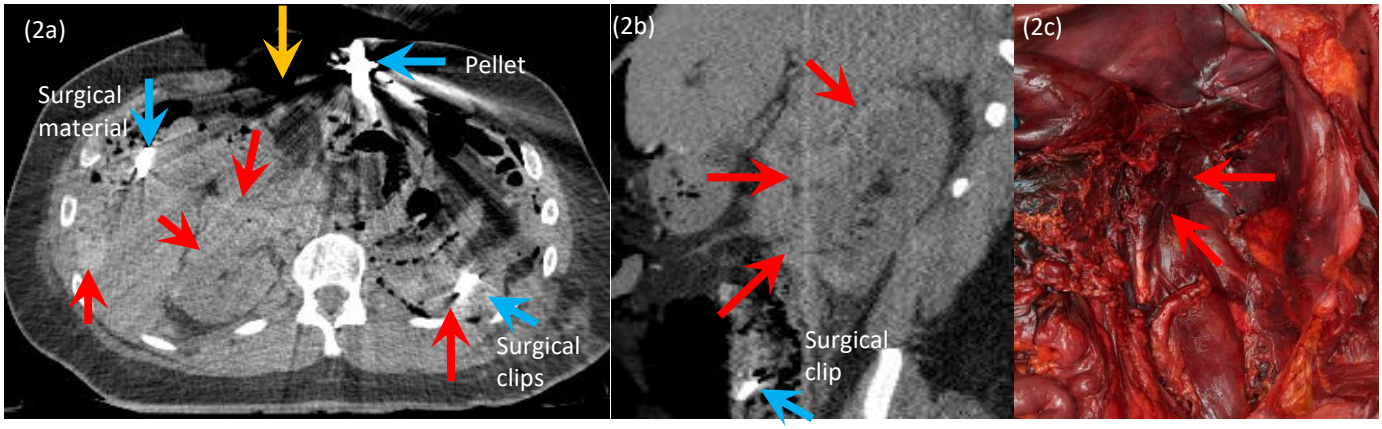

Fig 2: PMCT Abdomen in (a) Axial view: High density retroperitoneal hemorrhages surrounded the right kidney and posterior to the ascending and descending colon (red arrows). The left adrenal, left kidney and spleen were absent. Anterior abdominal wall defect was due to organ procurement (yellow arrow). High density foreign bodies were seen causing streak artifact (blue arrows); (b) Sagittal view: Hematoma anterior to the right kidney, right perinephric retroperitoneal space (red arrows); (c) Autopsy image showed absent left retroperitoneal organs with residual retroperitoneal hematoma (red arrows)

Pathology Findings: Autopsy examination revealed evidence of bilateral anterior thoracotomy and open laparotomy incision without closure, a total of three gunshot wounds, all of which were of an indeterminate range of fire. One gunshot wound entered the right lateral chest, one entered the left lateral chest, and one perforated the left elbow and forearm and reentered the body at the left lateral chest. The gunshot wound of the right lateral chest caused severe lacerations of the liver and right adrenal gland and lacerated the right kidney. The gunshot wound of the left lateral chest perforated the rib cage and left hemidiaphragm and entered the left side of the abdominal cavity, where the wound could no longer be tracked. The gunshot wound of the left elbow perforated the forearm muscles, exited at the left anterior forearm and re-entered the left lateral chest wall, where it perforated the soft tissue of the body wall; the wound path tapered off at an angle and was no longer traceable. Of the foreign bodies seen on PMCT, grey metal pellets were retrieved from the left anterior chest-abdominal wall and right occipital subscapsular tissue. The other foreign bodies seen within the intrabdominal and retroperitoneal spaces were surgical staple lines and sutures. The cause of death was multiple gunshot wounds of the torso, and the manner of death classified as homicide.

Comments:

One of the major strengths of PMCT in ballistic related death is localization of lodged projectiles and identification of associated bone fractures[1-2]. The entrance wound on the left side of the thorax was inferred from a lateral chest wall skin irregularity with underlying a short air track and rib fractures. The high-density foreign body seen at the left anterior chest-abdominal wall was presumed to be a bullet pellet and was indeed proven in autopsy to be an intact yellow jacketed missile. These PMCT findings inferred an anterior, inferior, and leftward bullet trajectory prior to autopsy.

However, the right chest wall entry site was obscured on imaging with no obvious skin defects other than that of the thoracotomy defect. This case demonstrates that surgical intervention, such as postmortem organ procurement, may distort the normal appearance of anatomical structures and obscure injuries and pathologies. Diaphragm, liver, right adrenal, and kidney injuries seen on autopsy were not well visualized on imaging due to poor soft tissue contrast, and no definite trajectory could be identified. Nevertheless, injuries were suspected given helpful indirect signs such as the perihepatic and retroperitoneal hematomas (Fig 2).

To note, the other intraabdominal high-density foreign bodies causing streak artifact at perihepatic and bilateral retroperitoneal spaces were not bullet fragments but surgical sutures from the organ procurement and could potentially cause confusion and misinterpretation if not viewed carefully. There has also been a rare care report of a renal bullets mimicking a large renal stone[3]. Hence, it is important to be aware that not all metallic appearing objects are retained projectile fragments, and not all retained projectiles necessarily need to have a metallic appearance.

Further reading and references:

1. Gascho D, Bolliger SA, Thali MJ, Tappero C. Postmortem Computed Tomography and Magnetic Resonance Imaging of an Abdominal Gunshot Wound. Am J Forensic Med Pathol. 2020 Jun;41(2):119-123. doi:10.1097/PAF.0000000000000547. PMID: 32379075..
2. Ditkofsky, N., Elbanna, K.Y., Robins, J. et al. Ballistic Injury Imaging: The Basics. Curr Radiol Rep 6, 45 (2018). https://doi.org/10.1007/s40134-018-0304-6.
3. Khan SR, Pearle MS, Robertson WG, Gambaro G, Canales BK, Doizi S, Traxer O, Tiselius HG. Kidney stones. Nat Rev Dis Primers. 2016 Feb 25;2:16008. doi: 10.1038/nrdp.2016.8. PMID: 27188687; PMCID: PMC5685519.

Contributors: Yi-Li Grace Wong, Kethery Haber, Roberto Maselli, and Natalie L. Adolphi

NMDID 193393

Gunshot wound of the head demonstrating skull vault, base and facial bone fractures with pneumocephalus, pneumoventricle, and intracranial hemorrhages

Case description: A 21-year old male with history of depression was found deceased in his car with a pistol and gunshot wound to his head.

Imaging Findings: Relevant imaging findings are summarized in Figures 1-3

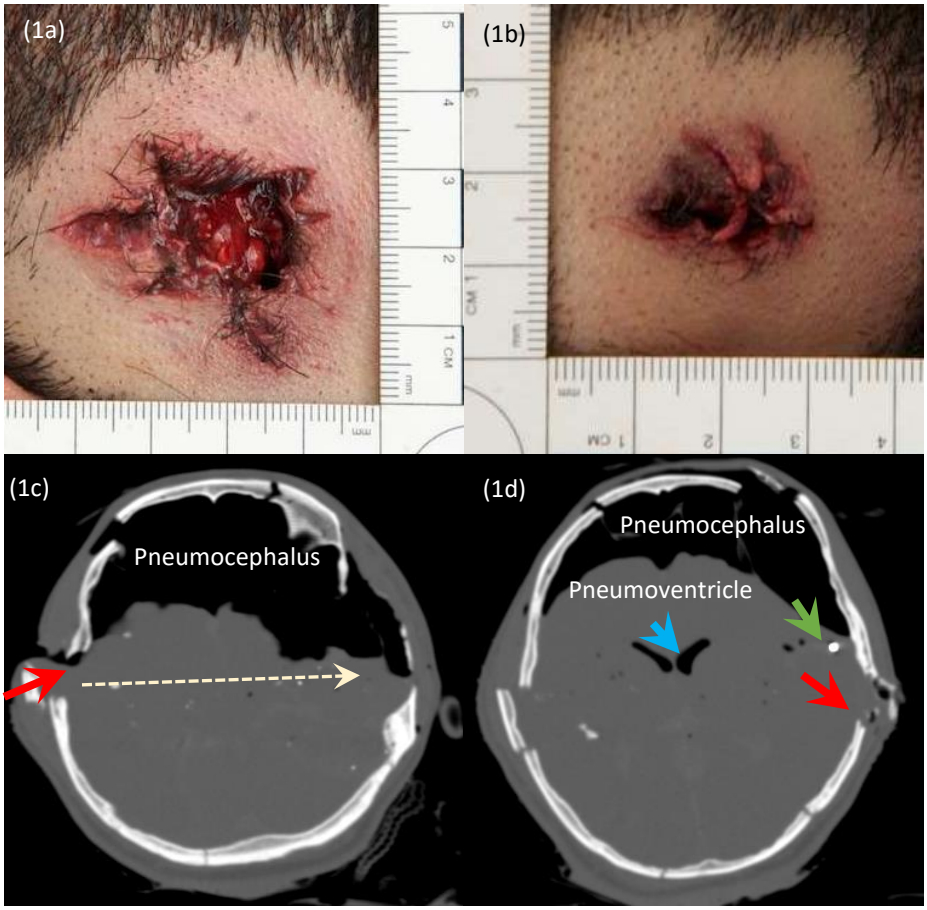

Fig 1: External examination showed the (a) Entrance wound on the right temple consisting of a 1.5 x 1.5 cm round defect with 0.2 cm wide circumferential marginal abrasion and multiple radiating lacerations. Soot and stippling were not visible at the surrounding skin. (b) Exit wound at the left temple consisting of a 2 x 1.5 cm stellate laceration without marginal abrasion. Soot and stippling were not visible at the surrounding skin. (c) PMCT of the entrance site with internal beveling of the frontotemporal bone (red arrow). Bone fragments were also seen traversing across these sites with right to left trajectory (dotted arrows). (d) Exit site with external beveling of the left temporal bone and bony projection into the scalp (red arrow). A round high-density bullet fragment (green arrow), pneumocephalus, and pneumoventricle were also noted.

Pathology Findings: Entrance wound was at the right temple and the exit wound as at the left temple. A muzzle imprint was seen adjacent to the wound with lack of gunpowder residue/stippling around the entrance, consistent with contact range of fire. There were no other significant injuries. The cause of death was gunshot wound of the head, and the manner of death classified as suicide.

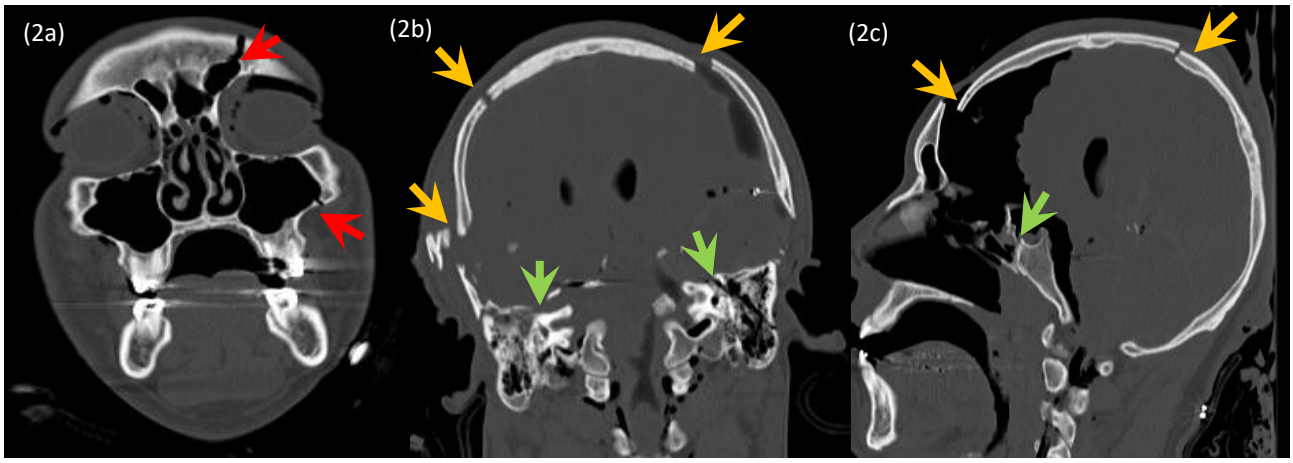

Fig 2: PMCT Brain in bone windows in (a) Coronal view at the level of facial bones showed left frontal bone fracture extending to the left frontal paranasal sinuses and left maxillary sinus lateral wall fractures (red arrows), (b) Coronal view at the level of mastoid bone showed bilateral mastoid fractures extending to bilateral middle cranial fossae (skull base, green arrows) and displaced skull vault fractures of the right temporal and left parietal bone (orange arrows); (c) Sagittal view showed depressed frontal bone fractures (orange arrows), anterior and middle cranial fossae fractures involving the sella turcica and sphenoid sinuses (middle cranial fossae structures, green arrow). In summary there were facial (red arrows), skull vault (orange arrows) and skull base (green arrows) fractures.

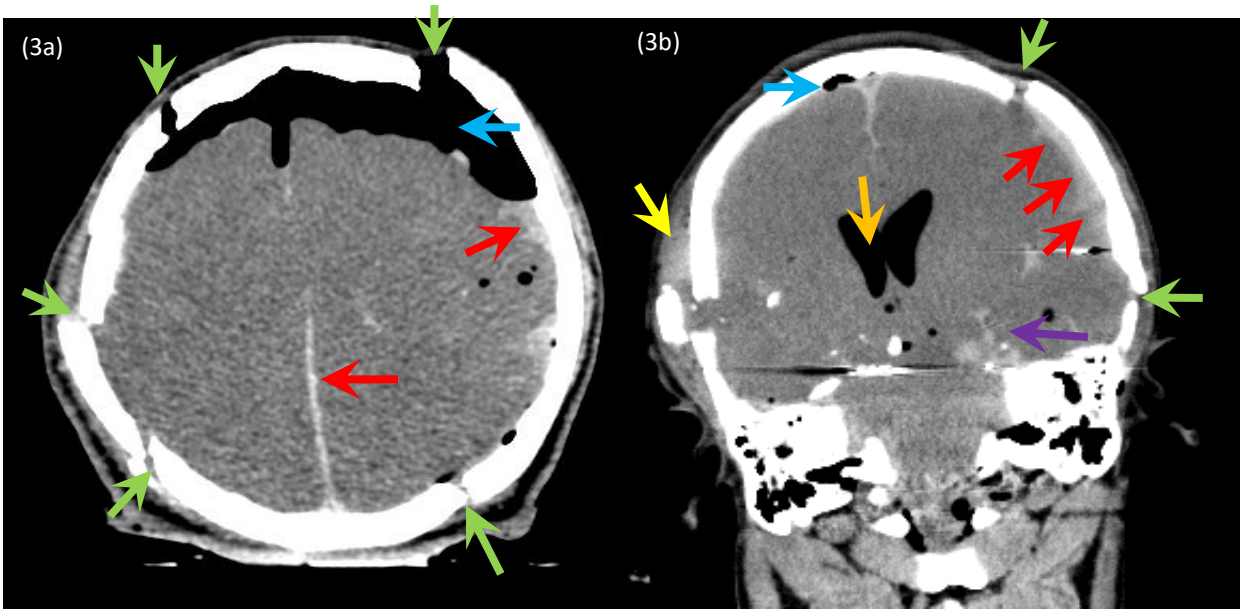

Fig 3: PMCT Brain in (a) Axial and (b) Coronal views demonstrated evidence of severe head trauma with bilateral frontal and parietal skull vault fractures (green arrows), pneumocranium (blue arrows), pneumoventricles (orange arrow), left frontal (crescenteric shaped) and posterior interhemispheric subdural hemorrhages (red arrows) with subarachnoid hemorrhages along sulci (purple arrow).

Comments: PMCT generally has low sensitivity for abrasions, contusions, and subcutaneous hemorrhages but has shown promising results in identifying intracranial entrance and exit wounds by means of internal and external beveling of calvarial fractures respectively[1] (Fig 1c-d). Bone fragments also tend to project externally as subcutaneous bone chips at the exit wound sites (Fig 1d). Imaging reconstruction of bullet trajectories can be done by means of linear tissue defects, bone/bullet fragments along the path, bone and parenchymal injuries, most readily in the head, face and neck[1] (Fig 1d). In addition to attempting to identify the entrance site, exit site, and bullet trajectory, an additional role of PMCT is to describe associated bone and parenchymal injuries resulting from the high velocity penetrating injuries, as illustrated in

this case (Fig 2-3). Commonly seen head gunshot wound injuries noted on PMCT are intracranial hemorrhages, pneumocephalus, and skull base, vault, and facial fractures. However, direct vascular injuries that are associated with high mortality, e.g., arterial or venous transection, dissection, and occlusions, cannot generally be observed without contrast/angiographic studies[3].

Further Reading & References:

1. Ampanozi G, Halbheer D, Ebert LC, Thali MJ, Held U. Postmortem imaging findings and cause of death determination compared with autopsy: a systematic review of diagnostic test accuracy and meta-analysis. Int J Legal Med. 2020 Jan;134(1):321-337. doi: 10.1007/s00414-019-02140-y. Epub 2019 Aug 27. PMID: 31455980.
2. Cascini F, Polacco M, Cittadini F, Paliani GB, Oliva A, Rossi R. Post-mortem computed tomography for forensic applications: A systematic review of gunshot deaths. Med Sci Law. 2020 Jan;60(1):54-62. doi: 10.1177/0025802419883164. Epub 2019 Nov 19. PMID: 31739723.
3. Dawoud FM, Feldman MJ, Yengo-Kahn AM, Roth SG, Wolfson DI, Ahluwalia R, Kelly PD, Chitale RV. Traumatic Cerebrovascular Injuries Associated with Gunshot Wounds to the Head: A Single-Institution Ten-Year Experience. World Neurosurg. 2021 Feb;146:e1031-e1044. doi: 10.1016/j.wneu.2020.11.078. Epub 2020 Nov 21. PMID: 33227526; PMCID: PMC8054034.

Contributors: Yi-Li Grace Wong, Kethery Haber, Roberto Maselli, and Natalie L. Adolphi

NMDID 198518

Fall from cliff with basilar skull, cervical odontoid, and thoracic spine fractures

Case description: A 24-year-old female with history of drug induced psychosis was last seen alive, but distressed, on a hiking trail. She had no known previous suicidal ideations or attempts. She was later found deceased at the bottom of a cliff.

Imaging Findings: Significant findings included blunt head, cervical and thoracic spine injuries with subarachnoid intracranial hemorrhages, pneumocephalus, and fractures of the base of skull, C2 (Type II odontoid-unstable), and T12 vertebral body.

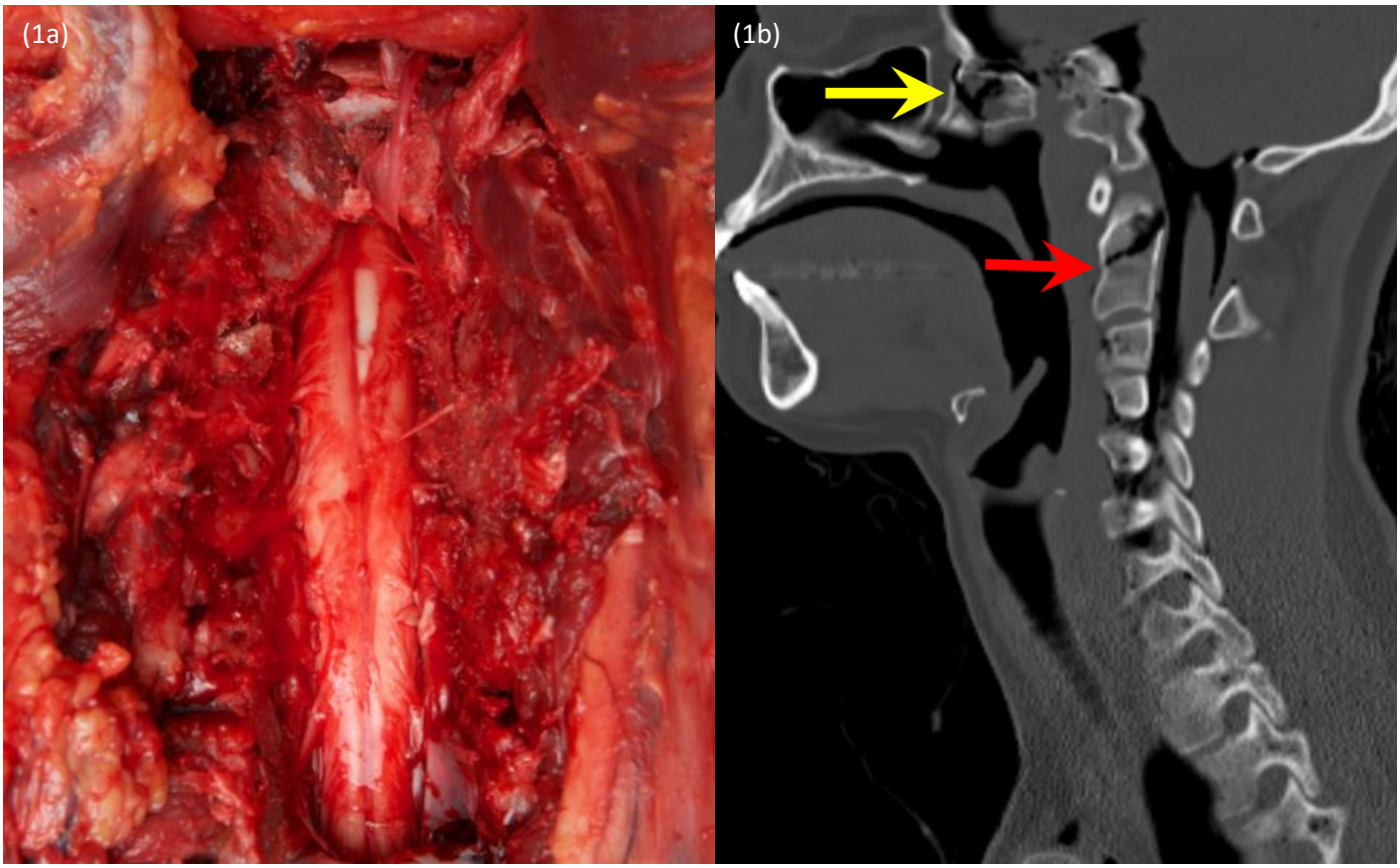

Fig 1: (a) Autopsy: Visualization of the cervical cord with minimal subarachnoid hemorrhage not visualised on PMCT; (b) PMCT (sagittal view, bone window): Base of skull (yellow arrow) and unstable C2 odontoid (red arrow) fracture, raising the suspicion for cord injury.

Pathology Findings: Multiple superficial contusions and abrasions were seen throughout the body, mostly of the face and extremities. There were scalp lacerations and skull fractures. There were also subarachnoid hemorrhages and focal brain contusions. Paraspinal muscle hemorrhage was seen at the level of the cervical and thoracic fractures. There was a thin film of subarachnoid blood at the cervical spinal cord but no other injuries to the cord. Toxicology studies were negative for alcohol and common drugs of abuse.

Comments: This case demonstrates the adjunctive role of PMCT as a pre-autopsy guide in identifying subtle bone fractures, especially at areas which require more extensive dissection during autopsy such as the skull base, facial and spinal vertebrae. Autopsy has the advantage over PMCT in delineating soft tissue injuries or hemorrhages such as the paraspinal muscles. The thin film of subarachnoid hemorrhage around the cervical cord was also not visualized on PMCT. There have been numerous studies on whether PMCT alone can replace autopsy. However, it is more likely that the combination of both complimentary techniques is likely to increase detection and diagnostic yield of death investigations.

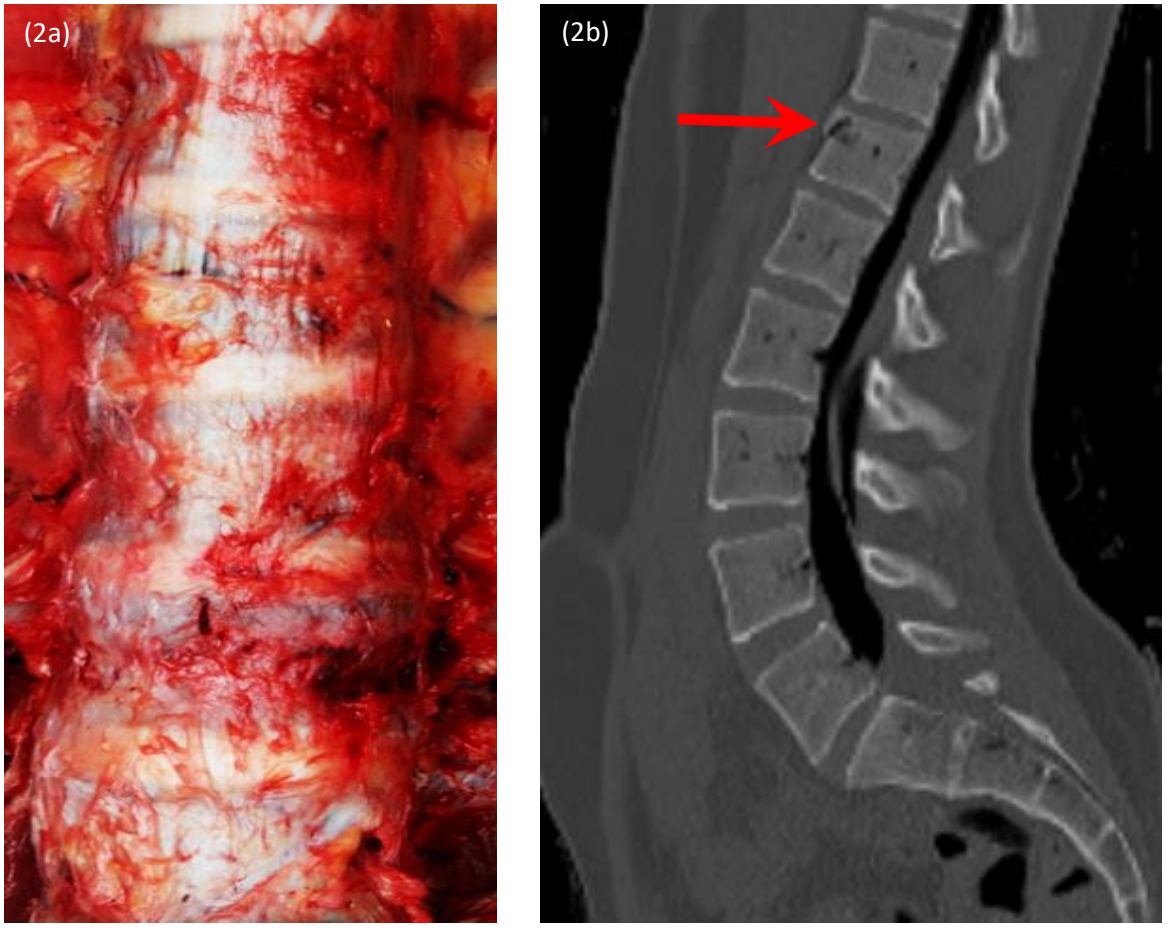

Fig 2: (a) Autopsy: Advantage over PMCT in visualizing soft tissue injury and hemorrhages surrounding the T12 vertebral body fracture (b) PMCT (sagittal view, bone window): Stable T12 anterior column compression fracture with no posterior retropulsion into spinal canal (red arrow)

Further Reading:

1. Panda A, Kumar A, Gamanagatti S, Mishra B. Virtopsy computed tomography in trauma: normal postmortem changes and pathologic spectrum of findings. Current problems in diagnostic radiology. 2015 Sep 1;44(5):391-406.
2. Legrand L, Delabarde T, Souillard-Scemama R, Sec I, Plu I, Laborie JM, Delannoy Y, Hamza L, Taccoen M, de Jong L, Benzakoun J, Edjlali M, Méder JF, Oppenheim C, Ludes B. Comparison between postmortem computed tomography and autopsy in the detection of traumatic head injuries. J Neuroradiol. 2020 Feb;47(1):5-12. doi: 10.1016/j.neurad.2019.03.008. Epub 2019 Apr 4. PMID: 30954548.

Contributors: Yi-Li Grace Wong, Kethery Haber, Roberto Maselli, and Natalie L. Adolphi

NMDID 199470

Evidence of gunshot wounds: Old or recent?

Case description A 54-year-old male, with a history of diabetes, gunshot wound to the abdomen the prior year, and reported "overdose" 2 months prior, was dropped off unresponsive at the emergency department door by another male who had picked him up for a ride and stated he needed help. Resuscitation efforts were initiated but unsuccessful.

Imaging Findings: High density discrete round structures causing streak artifact, indicative of metallic foreign bodies, were embedded in the left lumbar retroperitoneal and subcutaneous fat. Natural disease findings, including multiple bilateral lung cysts and bullae, aortic calcified plaques and coronary artery calcifications, were also seen. Bilateral acute anterior rib fractures were likely due to resuscitative efforts. There were no other bony fractures on PMCT.

Pathology Findings: The retained bullet from the previous gunshot wound was recovered from the soft tissue of the back during autopsy. There was evidence of previous surgical intervention for the remote gunshot wound; surgically-repaired bowel appeared well-healed and healthy. Aside from scar tissue within his heart, there were no other significant traumatic injuries or natural diseases that contributed to his death. Blood toxicology demonstrated the presence of methamphetamine (and its breakdown product) and THC (the active component of marijuana).

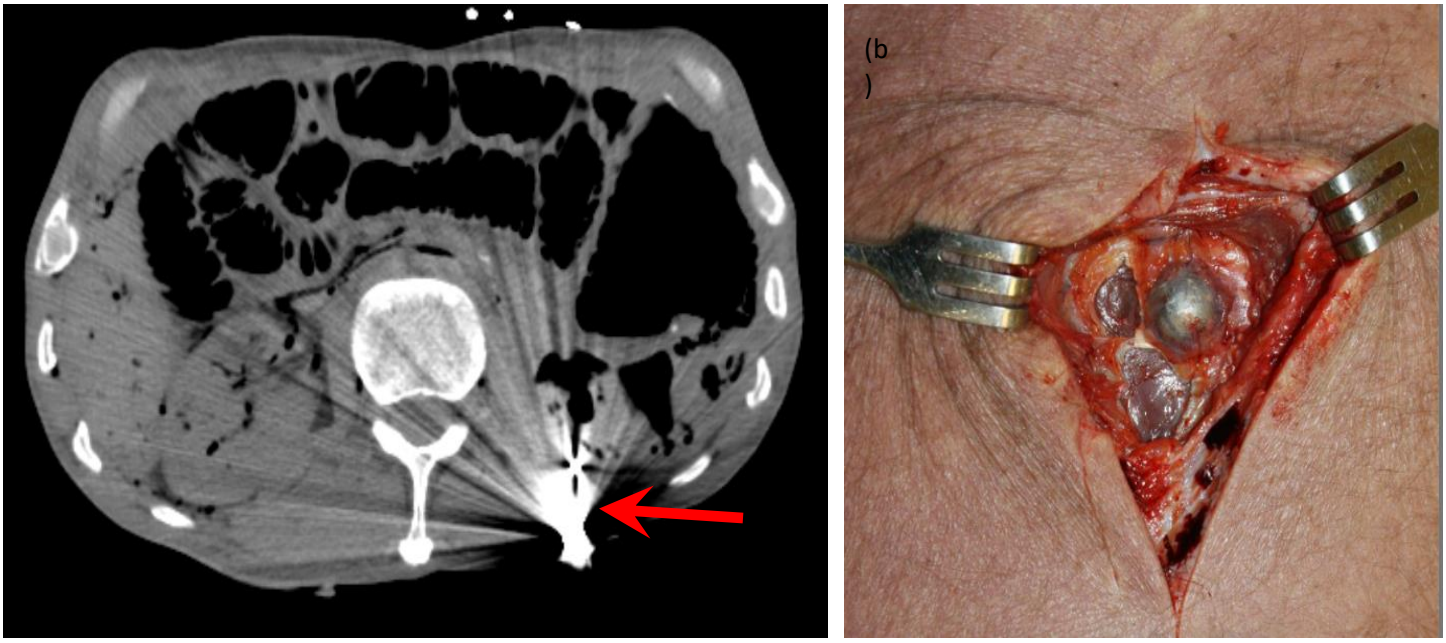

(a) PMCT: High densities causing streak artifact are seen embedded within the left lumbar soft tissue (red arrow). There was no surrounding hematoma, fat stranding, retroperitoneal air track, hemoperitoneum nor pneumoperitoneum. (b) Autopsy: Retained bullets from an old gunshot wound were retrieved during autopsy.

Comments:

The antemortem history of a treated gunshot wound was helpful, especially given the ambiguous circumstances of how the decedent was transported to the hospital without a clear perimortem history. In cases with dubious antemortem and perimortem history, PMCT findings of metallic foreign bodies suspicious of projectiles can lead to erroneous assumptions of a potential homicide as the cause of death. To reduce the risk of interpretation error, if considering imaging alone, it is useful to look for secondary signs of acute injury such as surrounding high density hemorrhages or fat stranding/edema, loss of normal surrounding soft tissue contours, a possible air track delineating bullet trajectory, and acute fractures with no signs of healing, i.e., callus, periosteal reaction. None of the secondary signs of acute injury were seen in this case, hence increasing confidence that it was an old projectile that had no significance in the cause of death. In this case, the cause of death was found to be the toxic effects of methamphetamine.

Further reading:

1. Ditkofsky N, Elbanna KY, Robins J, Ali IT, O'Keeffe M, Berger FH. Ballistic injury imaging: the basics. Current Radiology Reports. 2018 Dec;6(12):1-10. doi:101007/s40134-018-0304-6
2. Kirchhoff SM, Scaparra EF, Grimm J, Scherr M, Graw M, Reiser MF, Peschel O. Postmortem computed tomography (PMCT) and autopsy in deadly gunshot wounds--a comparative study. Int J Legal Med. 2016 May;130(3):819-26. doi: 10.1007/s00414-015-1225-z. Epub 2015 Jul 9. PMID: 26156451.

Contributors: Yi-Li Grace Wong, Kethery Haber, Roberto Maselli, and Natalie L. Adolphi